





THESIS



This is to certify that the

thesis entitled

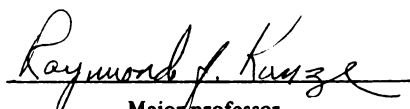
SHORT DURATION EVAPOTRANSPIRATION ESTIMATED  
BY CLASS A PAN AND METEOROLOGICAL PARAMETERS

presented by

GHASSEM ASRAR

has been accepted towards fulfillment  
of the requirements for

Ph.D. degree in Soil Science

  
Major professor

Date 2/26/81





OVERDUE FINES:

25¢ per day per item

RETURNING LIBRARY MATERIALS:

Place in book return to remove  
charge from circulation record.

K-308  
G-20 28



SHORT DURATION EVAPOTRANSPIRATION ESTIMATED BY  
CLASS A PAN AND METEOROLOGICAL PARAMETERS

By

Ghassem Asrar

A DISSERTATION

Submitted to  
Michigan State University  
in partial fulfillment of the requirements  
for the degree of

DOCTOR OF PHILOSOPHY

Department of Crop and Soil Sciences

1981

# ABSTRACT

## SHORT DURATION EVAPOTRANSPIRATION ESTIMATED BY CLASS A PAN AND METEOROLOGICAL PARAMETERS

By

Ghassem Asrar

It is generally recognized that climate is one of the most important factors determining the amount of water loss by evapotranspiration. Hence, meteorological budgeting techniques have been used for estimating soil water losses. However, monthly or weekly values of the climatic elements frequently mask daily extremes during the course of a season and thereby bias the final result. Any analysis designed for greater accuracy of determining soil moisture losses must, of necessity, be based on daily, hourly or even shorter measurement periods.

The objectives of this study were to: (1) establish a relationship for estimating potential evapotranspiration with a U.S. Class A evaporation pan and correlate these data with micrometeorological measurements taken over short time intervals, and (2) improve and test an explicit aerodynamic evaporation model based on the concept of turbulent diffusion.

A field study was conducted over a short grass covered area with a fetch to height ratio of 30:1 at the Michigan State University Soil Science Research Farm. Soil properties

9116576

measured in this study were: (1) gravimetric moisture content, (2) soil moisture potential by tensiometers, (3) bulk density, (4) soil moisture-matric potential by pressure plate, and (5) profiles of soil temperature.

A U.S. Class A pan was used in conjunction with a monitoring system based on a stress-strain concept to measure water losses from the pan over short periods.

Profiles of air temperature, wind-speed and absolute humidity were obtained by measuring and recording the values of these parameters every two minutes at five different elevations. These data were later smoothed, combined and averaged for ten-minute periods.

Gravimetrically determined soil moisture and soil moisture potentials, measured by tensiometer, indicated that the evapotranspiration under the irrigated treatments of this study was at its potential rate during the entire season. The rate of evapotranspiration under such conditions is controlled primarily by the weather conditions. However, under non-irrigated treatments and in general, in the absence of adequate soil moisture, the evaporation rate is controlled either by soil and/or weather.

Cummulative pan evaporation measured over periods of a day indicated linear, but different, increases with time for all the periods of this study. Simple correlation coefficients between the cummulative pan evaporation, pan temperature, air temperature and wind-speed were positive and highly significant at the one percent level of probability. A highly significant but negative correlation coefficient was obtained between cummulative pan evaporation and atmospheric humidity.

Air temperature profiles indicated, at some time, the presence of an unstable atmospheric condition. This usually occurred late at night or very early in the morning but changed to a more stable condition due to an increase in air temperature during the daylight hours.

Profiles of wind-speed showed the formation of turbulent boundary layers above the ground surface and an increase in their thickness with time during the day. A graphical procedure was used to obtain the aerodynamic parameters related to these profiles.

Profiles of absolute humidity usually indicated a gradual decrease in humidity with elevation above the ground. This relationship was reversed for late evening and early morning hours.

Detailed analyses of temperature, wind-speed and humidity profiles indicated that the classical equations of heat, momentum and water vapor transport should be modified to better represent these phenomena under a wide range of atmospheric conditions.

The profiles of air temperature, wind-speed and absolute humidity were used to study the effectiveness of a defined stability parameter,  $S$ , and the functions,  $f(S)$ , in adjusting for the influence of atmospheric stability upon the transport of water vapor. The results indicated that the model proposed in this study, proved to be more accurate than the original equation of Thornthwaite-Holzman in approximating evapotranspiration from a lysimeter and evaporation from a Class A pan over short periods.





To Peace and Brotherhood

## ACKNOWLEDGEMENTS

The author wishes to thank Dr. Raymond J. Kunze under whose guidance and encouragement this project was developed and carried out. I would like to express my sincere appreciation to Dr. Dale E. Linvill (Agricultural Engineering), Dr. Reinier J.B. Bouwmeester (Civil Engineering) and Dr. Maurice L. Vitosh (Crop and Soil Sciences), members of my Guidance Committee.

Thanks to Dr. Gary L. Cloud and Mr. David Kanistanaux (Metallurgy, Mechanics, and Materials Science), for their advice and use of their facilities in automating the Class A pan.

A special thanks is extended to Messer's Gary F. Connor (Agricultural Engineering) and Dallas A. Hyde (Crop and Soil Sciences) for their assistance in preparing and installing the weather station.

A final thanks to Messer's Anders G. Johanson, Mark R. Riordan and Richard Wiggins (Computer Laboratory) for their help in data manipulation and programming phases of this study.

# TABLE OF CONTENTS

	Page
LIST OF TABLES . . . . .	iv
LIST OF FIGURES . . . . .	vi
LIST OF APPENDICES . . . . .	viii
LIST OF SYMBOLS . . . . .	ix
INTRODUCTION . . . . .	1
LITERATURE REVIEW . . . . .	3
THEORETICAL MODEL DEVELOPMENT . . . . .	12
EXTENSION OF THEORETICAL MODEL DEVELOPMENT . . . . .	21
MATERIALS AND METHODS . . . . .	24
Soil Measurements . . . . .	26
Evaporation Measurements from Class A pan . . . . .	29
Micrometeorological Measurements . . . . .	36
Collecting and Analysis of Data . . . . .	40
RESULTS AND DISCUSSION . . . . .	43
I. Evapotranspiration from Soil . . . . .	43
II. Evapotranspiration from Class A pan . . . . .	49
III. Evaporation Estimated by Aerodynamic Models . . . . .	65
CONCLUSIONS . . . . .	86
APPENDICES . . . . .	88
LIST OF REFERENCES . . . . .	126



# LIST OF TABLES

Table	Page
1 Soil moisture content influenced by irrigation, rainfall and type of crop during the experimental study . . . . .	45
2 Bulk density and moisture holding capacity of Metea loamy sand at different potential levels and sampling depths . . . . .	47
3 Regression equations representing cumulative pan evaporation over short periods . . . . .	50
4 Simple correlation coefficients between cumulation pan evaporation, pan temperature and weather parameters for short duration measurements . . . . .	55
5 Pan coefficient ( $K_p$ ) for Class A pan for different ground covers, relative humidity and wind speed . . . . .	58
6 Reference evapotranspiration ( $ET_0$ ) computed from cumulative pan evaporation ( $E_{pan}$ ) and pan coefficient ( $K_p$ ) . . . . .	59
7 Cumulative actual evapotranspiration ( $ET$ ) for corn, soybeans and turfgrass computed from reference evapotranspiration ( $ET_0$ ) and crop coefficient ( $K_C$ ) . . . . .	64
8 Displacement height, roughness parameter, frictional velocity and shear stress determined from wind speed profiles . . . . .	78
9 Evaporation rates measured with an automated Class A pan and computed according to the Thornthwaite-Holzman and a modified version of this equation from atmospheric profile data over short periods . . . . .	81
10 Evapotranspiration rates measured with lysimeter (after Morgan et. al.) and computed according to the Thornthwaite-Holzman and modified Thornthwaite-Holzman equations from atmospheric profile data . . . . .	84

## LIST OF TABLES (cont'd.)

Table	Page
B-1 Smoothed weather data averaged over ten-minute periods, July 24, 1980 . . . . .	101
B-2 Smoothed weather data averaged over ten-minute periods, July 25, 1980 . . . . .	103
B-3 Smoothed weather data averaged over ten-minute periods, July 30, 1980 . . . . .	105
B-4 Smoothed weather data averaged over ten-minute periods, August 1, 1980. . . . .	107
B-5 Smoothed weather data averaged over ten-minute periods, August 4, 1980. . . . .	109
B-6 Smoothed weather data averaged over ten-minute periods, August 7, 1980. . . . .	113
B-7 Smoothed weather data averaged over ten-minute periods, August 8, 1980. . . . .	115

# LIST OF FIGURES

Figure		Page
1	Schematic diagram of the experimental site on the Michigan State University Soil Science Farm . . . . .	25
2	Soil moisture content-matric potential relationship for Metea loamy sand . . . . .	28
3	Position of strain gages (a) on an active-arm and (b) their full-bridge arrangement . . . . .	33
4	Calibration curve for pan assembly . . . . .	35
5	Tachometer 555-circuit for conditioning anemometer signals . . . . .	38
6	Cross sectional (a) and close up (b) views of a psychrometer unit . . . . .	39
7	Schematic view of all sensors and data acquisition system . . . . .	41
8	Rainfall distribution and soil moisture status during the growing season as indicated by tensiometers placed in irrigated corn and soybean plots. . . . .	44
9	Air, soil and Class A pan temperature averaged hourly, July 25, 1980 . . . . .	52
10	Air, soil and Class A pan temperature averaged hourly, August 4, 1980 . . . . .	53
11	Air, soil and Class A pan temperature averaged hourly, August 7, 1980 . . . . .	54
12	Crop coefficient as related to percent of growing season for corn in Michigan . . . . .	61
13	Crop coefficient as related to percent of growing season for soybeans in Michigan . . . . .	62
14	Crop coefficient as related to percent of growing season for turfgrass in Michigan . . . . .	63



LIST OF FIGURES (cont'd.)	Page
15 Air temperature profiles at different hours, above a short turfgrass cover, July 25, 1980 . .	66
16 Air temperature profiles at different hours, above a short turfgrass cover, August 4, 1980 . . . . .	67
17 Air temperature profiles at different hours, above a short turfgrass cover, August 7, 1980 .	68
18 Wind speed profiles at different hours, above a short turfgrass cover, July 25, 1980 . . . . .	70
19 Wind speed profiles at different hours, above a short turfgrass cover, August 4, 1980 . . . . .	71
20 Wind speed profiles at different hours, above a short turfgrass cover, August 7, 1980 . . . . .	72
21 Humidity profiles at different hours, above a short turfgrass cover, July 25, 1980 . . . . .	74
22 Humidity profiles at different hours, above a short turfgrass cover, August 4, 1980 . . . . .	75
23 Humidity profiles at different hours, above a short turfgrass cover, August 7, 1980 . . . . .	76
24 Functional relationship of stability para- meter (S) and Richardson number (Ri) under different atmospheric conditions . . . . .	80

# LIST OF APPENDICES

Appendix	Page
A. FORTRAN IV Program for Data Processing and Data Conversion . . . . .	87
B. Smoothed and Averaged Field Data . . . . .	98
C. Integration of Equation [29]. . . . .	117
D. Illustrative Examples for Computing Evaporation Rates from Equations [32] and [35] . . . . .	121

# LIST OF SYMBOLS

Symbols	Meaning
$a$	$Z(\partial T/\partial Z)$
$b$	$Z(\partial U/\partial Z)$
$B$	constant of proportionality
$CB$	centibar
$d$	displacement height
$D$	diameter
$\Delta EB$	change in bridge output
$\Delta L$	change in length
$\Delta q$	change in water vapor concentration
$\Delta R$	change in bridge resistance
$\Delta T$	change in temperature
$\Delta U$	change in wind speed
$\Delta Z$	change in elevation
$\partial T/\partial Z$	temperature gradient
$\partial U/\partial Z$	wind speed gradient
$e$	thickness
$E$	flux of water vapor
$E_{aero}$	evaporation computed from aerodynamic models
$E_B$	bridge output in milivolts
$E_{cum}$	cumulative pan evaporation
$E_1$	modulus of elasticity



Symbols	Meaning
$ET_o$	reference evapotranspiration
$ET_p$	potential evapotranspiration
$E_{pan}$	pan evaporation
$\epsilon$	strain
$g$	acceleration of gravity
$GF$	gage factor
$k$	VonKarmen constant
$K_c$	crop coefficient
$K_h$	heat transfer coefficient
$K_m$	mass transfer coefficient
$K_p$	pan coefficient
$K_w$	water vapor transfer coefficient
$K_x$	diffusion coefficient in x-direction
$K_y$	diffusion coefficient in y-direction
$K_z$	diffusion coefficient in z-direction
$l$	mixing length
$L$	length
$\ln$	natural logarithm
$n$	power coefficient
$P$	applied load
$q$	water vapor concentration
$r$	simple coefficient of correlation
$r^2$	coefficient of determination
$R$	bridge resistance
$Ri$	Richardson number
$\overline{Ri}$	average Richardson number

Symbols	Meaning
$\rho_a$	density of air
$\rho_w$	density of water
S	stability parameter
$S_o$	strain per unit load
$\Sigma$	summation of several terms
t	time
T	absolute temperature
$T_{air}$	air temperature
$T_{pan}$	pan temperature
$\tau$	shear stress
$\theta_m$	gravimetric soil moisture content
u	velocity component in x-direction
U	wind speed
$U_*$	frictional velocity
v	velocity component in y-direction
V	voltage
w	velocity component in z-direction
x	horizontal direction
y	transverse direction
z	vertical direction
Z	elevation above the ground surface
$z_o$	roughness coefficient

## INTRODUCTION

Maintaining soil moisture conditions near optimum levels for a given crop requires reliable estimates of the constantly changing water demands. Frequent soil moisture measurements are required if the status of soil moisture conditions are to be maintained near such levels. Water stored in the soil and additions of irrigation water can be managed efficiently only if the expected evapotranspiration and other water losses are known.

There is a continuing need for improving the methodology of measuring soil moisture losses. The soil moisture losses can be obtained by direct measurement or computation of the water vapor flux to the atmosphere. Generally, measurement of evapotranspiration rates are obtained as follows: (1) the direct measurement of water losses from soil and vegetated surfaces by obtaining differences in soil water content for a given time period, (2) the transformation of water loss measurements made for non-vegetated surfaces (i.e., evaporation pans and tanks), and (3) empirical formulae based on climatic data. Often because of difficulties in obtaining accurate direct measurements of soil moisture losses under field condition, the second and third approaches are preferred above the first.



It is generally recognized that climate is one of the most important factors determining the amount of water loss by evapotranspiration, particularly when crops are grown under optimum growth conditions. Hence, meteorological budgeting techniques have been used, with some degree of success, for estimating soil water losses. However, monthly values of the important climatic elements frequently mask daily extremes during the course of a season and thereby bias the final result. Any analysis designed for greater accuracy of determining soil water losses should be based on daily, hourly, or even shorter, periodical weather observations.

The objectives of this study were to establish a relationship for estimating potential evapotranspiration from a U.S. Class A evaporation pan and to correlate these data with micro-meteorological data on a short-term basis. A final objective was to modify and test an explicit aerodynamic evaporation model based on the concept of turbulent diffusion.



## LITERATURE REVIEW

Many aspects of water resource planning are not as critical in humid areas as in the more arid regions. However, pressures on the currently adequate water resources of humid areas are increasing. With greater competition for these resources, there will be greater demand for increasing the efficiency of their use, particularly as use is related to water loss. At least 90 percent of water used for irrigation in the State of Michigan is lost to the atmosphere through evapotranspiration while consumptive losses for most other water uses is less than 10 percent (1,57). Evapotranspiration rates are minimal in areas under water conservation practices and maximal in areas of wastewater disposal (81). The rates of evapotranspiration and the factors affecting them have been the subject of much work and research. Present methods of measuring or estimating evapotranspiration are in part extensions or modifications of methods for measuring evaporation since the two are similar physical processes.

The soil is the source of water for transpiring plants. Hence, soil moisture measurements are still an important supplement to evapotranspiration studies. Any soil parameter such as texture, structure, or pore space which affects the conductivity, hydraulic gradient, vapor pressure, or vapor diffusion

near the soil surface will indirectly affect the rate of evaporation from the soil surface (69).

The water potential and hydraulic conductivity of the soil influence the rate at which a plant transpires (87). If the soil potential is high, the soil can supply water to the plant roots nearly at the same rate as it is transpired by the plant. Thus, in a moist soil, the transpiration is at potential rate and is primarily determined by weather conditions (73).

The classic definition of potential evapotranspiration is "evaporation from an extended surface of a short green crop, actively growing, completely shading the ground, of uniform height and not short of water." Provided that all restrictive conditions are fulfilled, the definition suggests that potential evapotranspiration represents the maximum possible rate of water loss from a vegetative-covered surface (94,97).

VanBavel (93) redefines potential evapotranspiration for any vegetation in terms of appropriate meteorological variables and aerodynamic properties of the cover suggesting that "when the surface is wet and imposes no restriction upon the flow of water vapor, the potential value of evapotranspiration is reached." For soil moisture contents equivalent to or greater than the field capacity, the evaporation is considered as potential evapotranspiration (16,26). As the soil dries out, the hydraulic conductivity decreases and eventually the soil cannot supply sufficient water to the plant. Consequently, the actual transpiration falls below the potential one (69).

Therefore, when the soil is unable to supply sufficient water to maintain potential evapotranspiration rate under a given set of atmospheric conditions, the rate of evapotranspiration is controlled by soil properties (55,77).

The ratio between potential evapotranspiration and actual evapotranspiration for an area is related to the rate of moisture supply to the soil surface (81). Soil moisture measurements are generally adequate for long-time evapotranspiration averages, but unfortunately, technical difficulties prevent the use of soil moisture depletion measurements for short-time evapotranspiration studies (28,87).

Measured values of evapotranspiration obtained by monitoring soil moisture over a period of years also show considerable variation in standard error of determination (86). This investigation shows an average year to year variation of  $\pm 11\%$  of the average mean evapotranspiration from the same crop at the same location. Hence, the error of  $\pm 11\%$  for predicting future evapotranspiration from soil sampling appears to be about the same as the error to be expected from estimates obtained based on other empirical methods.

Tensiometers have proven to be very suitable for monitoring the soil moisture in coarse textured soils (21). This is true primarily because of the larger amount of available soil moisture that is held by the soil in the measurable tension range of these instruments.

There are two principal factors associated with the influence of cover crops on evapotranspiration (87). The

first is related to light reflection. Reflection of light from a bare soil especially when wet, is usually lower than that from a dense crop canopy. Based on the reflection alone, evapotranspiration would normally be expected to increase as the percent of cover decreased. The second factor is associated with the relative evaporation rates from a bare soil and a transpiring crop. Evaporation from moist bare soils decreases rapidly one or two days after irrigation or rainfall; however, soil water storage usually is sufficient to maintain transpiration from the soil for a considerable period of time (26,55). Consequently, evapotranspiration increases as the percent cover increases relative to evaporation from a bare soil.

Many empirical formulas relating climatological measurements and evapotranspiration have been developed. These formulae were based on the empirical relations obtained between the observed evaporation and climatic data for a specific crop and region. Therefore, in order to be able to use them in another region, they must be tested and adjusted to the conditions of the new area. Empirical methods have the greatest usefulness when correlated with potential evapotranspiration (39,85). Empirical methods can be grouped into four classes: (1) those depending primarily on the relation of evapotranspiration to radiation, (2) temperature methods, (3) humidity methods, and (4) evaporimeters.

One of the earlier writers on the subject of evapotranspiration was Dalton (14), who showed that the rate of evaporation was proportional to the difference between the water vapor pressure at the evaporating surface and in the

atmosphere. This principal, based on the vapor transfer concept, has been used in all of the evaporation and evapotranspiration methods developed since that time.

In 1942, Blaney and Morin (4) published an empirical formula for estimating monthly pan evaporation or evapotranspiration as a function of monthly mean temperatures, monthly percent of annual daytime hours, and monthly mean relative humidity. This formula was later modified by Criddle (13), by omitting the humidity factor and introducing a new constant of proportionality into the equation. This new formula also gave an estimate of the monthly mean evapotranspiration rate. However, Blaney (3) has suggested that this formula can also be used for estimating pan evaporation with the use of appropriate coefficients.

In 1956, Hargreaves (37) proposed an empirical method of estimating pan evaporation from a study of temperature, humidity and monthly daytime relations. This model was later tested by a number of his graduate students (38,63) and was considered to be fairly good for normal wind velocities under a wide range of climatic conditions. In 1968, an empirical method of estimating pan evaporation from climatic data was proposed by Christiansen (10). Later Christiansen and Hargreaves (11) developed a series of formulas for converting pan evaporation directly to potential evapotranspiration and calculating potential evapotranspiration from climatic data.

The basic deficiencies of any empirical approach are generally estimates of evapotranspiration over very short time periods (8).



Evaporimeters measure the drying ability of the air. Evaporation from a pan or free water surface is a physical process that depends on the availability of energy to evaporate the water. The rate of evaporation is, therefore, largely dependent on climatic parameters such as solar radiation, air temperature, wind velocity and relative humidity (11,44). Meteorological factors have similar influences on evaporation from free water, soil surfaces and transpiration from plant surfaces (31). The major differences between these forms of water loss are; (1) changing characteristics of the plant surfaces during growing season, (2) availability of water for evaporation, and (3) differences in energy absorption characteristics. Thus, it appears that evaporimeters could only provide an integrated measurement of complex meteorological factors affecting evapotranspiration.

Among the pans and tanks tested, the U.S. Weather Bureau Class A pan provides the best correlation with, and the most practical and economical method of estimating potential evapotranspiration (5,71,78). Class A pan evaporation data provide a useful general reference over a wide range of climatic circumstances (29). With measurements from a carefully sited Class A evaporation pan in a locality, it is possible to calculate the cumulative evapotranspiration in a simple way (41). The pan coefficient,  $K_p$ , is given by the ratio  $ET_p/E_{pan}$ , where  $ET_p$  is potential evapotranspiration and  $E_{pan}$  is pan evaporation. The coefficient is used in practices as an "adjusting factor" for pan losses to give an estimate

of potential evapotranspiration (18,31). This ratio was found to change during the course of the growing season, primarily during the following two periods: (1) from planting until 5 to 6 weeks of age, during which evapotranspiration is controlled by moisture content of the upper soil layers, and (2) from the beginning of flowering, evapotranspiration increases rapidly as the plant cover the ground, reaches a maximum at peak flowering, and then decreases until harvest (8,34). The coefficient  $K_p$  also depends on the type, size and environment of the pan (100). The use of a single ratio to estimate water requirements using Class A pan data will introduce only small errors. These generally are lower than or comparable to the uncertainties in water requirement values obtained from intensive soil moisture measurements in gravimetric methods (32). Measurements of Class A pan evaporation losses from different parts of the United States suggest a standard deviation of 10% for annual evaporative losses within regional zones (79).

One of the shortcomings of using pans for estimating evapotranspiration is the formation of surface films compressed sufficiently to reduce the evaporation rate. The rather large reduction of evaporation, up to 20%, by naturally occurring surface films indicates that their frequency of occurrence and areal extent may need to be estimated and, if possible, taken into account when evaluating the evaporation from a pan in which the surface is assumed to be contaminated (15). However, the major problem in using the Class A pan is that,

the time period for which reasonable estimates can be made is relatively long, particularly in humid regions where climate is variable (85). In spite of the limitations, Class A evaporation pans do provide fairly satisfactory indices of evapotranspiration especially where installation and operating standards are complied with (11).

Physics of evaporation is complexed by energy exchanges and transformations, some being controlled by aerodynamic factors. Both energy exchanges and aerodynamic transfers are essentially meteorological; thus, the maximum rate of evaporation is determined primarily by climatological factors (48,77). Micrometeorological methods provide a measurement of the flux density of water vapor in the boundary layer of the atmosphere. Though these methods have limitations as to where and how they can be used as well as instrumental difficulties, they have important advantages. When applicable, micrometeorological methods can measure the potential evapotranspiration over very short periods (66). Evapotranspiration correlates best with meteorological elements when the crop is transpiring at the potential rate. This rate will not be reached until the crop has attained full ground cover and is adequately supplied with water (39). Micrometeorological methods in greatest use are the energy balance method, aerodynamic method and a combination of the two. In the energy balance method the principle of conservation of energy to the surface of the ground gives some basic equation that can help us to understand evapotranspiration (74). All energy

arriving at the soil and plant surfaces must be accounted for in this approach (64). Jensen and Haise (43) developed a formula for estimating evapotranspiration using solar radiation and climatic data. This model has given fairly good results where the radiation and heat flux data are available. The upward flux of water vapor in the surface layer of the atmosphere is the resultant of turbulent diffusion carried along a mean gradient of water vapor concentration (23,81). Therefore, evaporation and hence evapotranspiration can be estimated based on the vapor flow rate from the evaporating surface. This may be done by the use of aerodynamic methods, either implicitly as a bulk aerodynamic method or explicitly as a profile method. The profile method will be presented in more detail in the following section. In the combination method, one energy balance equation and one aerodynamic equation are combined to produce an equation that can be used to estimate potential evapotranspiration. In 1948, Penman (65) was the first to develop a formula based on this concept. Although his formula is considered to give the best results, it is seldom used because of its complexity and the availability of several parameters required in the model.

## THEORETICAL MODEL DEVELOPMENT

Recent advances in understanding of boundary layer phenomena have provided potential means of monitoring evapotranspiration by measuring water vapor transfer into the atmosphere. In the case of air flow over land surface, the lower atmosphere may be divided into two layers (27). First, is the laminar layer at the surface. The thickness of this layer is of the order of several millimeters; and temperature, humidity and wind velocity vary almost linearly with height. Transfer of heat, water vapor and momentum through this layer are essentially molecular processes. Second, is the turbulent boundary layer with varying thickness depending on the level of turbulence. In this layer wind velocity, water vapor and temperature vary, approximately, linearly with logarithm of height. Transfer of heat, vapor and momentum through this layer are turbulent processes (74). The capacity for water movement in the processes of turbulent transfer are more than 100 times greater than the molecular transfer processes (81). The process of evaporation and diffusion of water vapor into the earth's turbulent air stream, above or downwind from free liquid or saturated solid surfaces is practically one of gaseous diffusion and can be represented by

$$\frac{dq}{dt} = \frac{\partial}{\partial x} \left( K_x \frac{\partial q}{\partial x} \right) + \frac{\partial}{\partial y} \left( K_y \frac{\partial q}{\partial y} \right) + \frac{\partial}{\partial z} \left( K_z \frac{\partial q}{\partial z} \right) \dots [1]$$

where  $q$  is the water vapor concentration,  $K$ 's are effective coefficients of diffusion,  $t$  the time and  $dq/dt$  denotes the change in vapor concentration with time. If  $u$ ,  $v$  and  $w$  are the components of the velocity and  $q$  is assumed to be a function of  $x$ ,  $y$ ,  $z$  and  $t$ , the total differential can be represented by

$$\frac{dq}{dt} = \frac{\partial q}{\partial t} + u \frac{\partial q}{\partial x} + v \frac{\partial q}{\partial y} + w \frac{\partial q}{\partial z} \dots [2]$$

However, according to Sutton (82), evaporation from a saturated soil or reservoir which is part of a very large homogenous area depends only on height and time. Equation [1] then reduces to

$$\frac{\partial q}{\partial t} = \frac{\partial}{\partial z} \left( K_z \frac{\partial q}{\partial z} \right) \dots [3]$$

Integrating Equation [3] from 0 to  $Z$  gives

$$\int_0^Z \frac{\partial q}{\partial t} dz = \frac{E}{\rho_a} + K_z \frac{\partial q}{\partial z} \dots [4]$$

where  $E/\rho_a$  is the integration constant proportional to water vapor flux ( $E$ ) divided by density of air ( $\rho_a$ ) at the surface (6). The quantity of  $\partial q/\partial t$  is always limited under actual conditions. Thus for sufficiently small  $Z$ , such as the one considered in micrometeorological studies, the first (integral) term in Equation [4] is negligibly small when compared with the remaining two terms in the equation. Therefore, it reduces to

$$E = -\rho_a K_z \frac{\partial q}{\partial z} \dots [5]$$

The negative sign represents the downgradient flux of water vapor. Other researchers have used a different approach to derive the equation of vertical flux of water vapor based on

the Reynold's formulation of turbulent stress. The final results are the same as Equation [5]. If eddies of transferred substances can be measured in their upward movement, an analysis of the resulting air layer can be considered. Within the limits of this layer the evaporation is exclusively determined by the value of turbulent exchange coefficient, and the vertical gradient of transferred substances (6). Therefore, the rate of evaporation could be obtained from data on the humidity profile in the surface air layer, provided that the value of turbulent exchange coefficient for water vapor is known. But, since the laws governing the turbulent motion are extremely complicated, there is no accurate, theoretical method for determining the turbulent exchange coefficient in the atmosphere. Hence, many investigators have made extensive use of approximations obtained by processing various empirical data in a variety of ways in attempts to model these meteorological phenomena. The substantial variability of the transfer coefficients with landscape and atmospheric conditions permits the use of such modeling attempts (70).

The increase in wind speed with height over an extended uniform surface can be represented by

$$U = \frac{U^*}{k} \ln \frac{Z-d}{Z_0} \quad . . . . . [6]$$

when the atmosphere is near a state of neutral stability (66). In Equation [6],  $U$  is the wind velocity at height  $Z$  above ground and  $Z_0$  is the roughness coefficient. The displacement height,  $d$ , represents the effective raising of the boundary due to

roughness,  $k$  is VonKarman constant ( $k=0.41$ ), and  $U_*$  is the friction velocity which represents the characteristic velocity in a turbulent boundary layer. The magnitude of  $U_*$  is determined by

$$U_* = \left( \frac{\tau}{\rho_a} \right)^{1/2} \dots \dots \dots [7]$$

where  $\tau$  is the shear stress, the flux of horizontal momentum transferred vertically and absorbed by the ground and assumed to be constant in the lower layer of atmosphere.  $\rho_a$  is the density of air. Based on the assumption of constancy of shear stress with height, we can define

$$\left( \frac{\tau}{\rho_a} \right) = K_m \frac{\partial u}{\partial z} \dots \dots \dots [8]$$

where  $K_m$  is the transport coefficient for the momentum and frequently known as eddy diffusivity. Combining Equations [6], [7] and [8] yields

$$K_m = kU_* (Z-d) \dots \dots \dots [9]$$

The effect of aerodynamic roughness on turbulent transfer of moisture and energy from vegetative surfaces is an important factor in evapotranspiration. In general, evapotranspiration increases with vegetation height due to increased roughness and zero-plane displacement ( $d$ ) at a given windspeed, which in turn increases the coefficient of turbulent exchange (74,84). Reducing the turbulent transfer offers some potential for increasing water use efficiency because it is the linking mechanism between crop surface and bulk atmosphere (36).

When thermal stratification prevails, the logarithmic wind profile, Equation [6], no longer holds (83). In this



case, buoyancy due to temperature gradient in the atmosphere boundary layer also plays a major role in the transport and mixing of the air and entities contained therein (74).

Therefore, since turbulence can either be generated thermally or mechanically, both temperature and wind speed play an important role in stability of air (59).

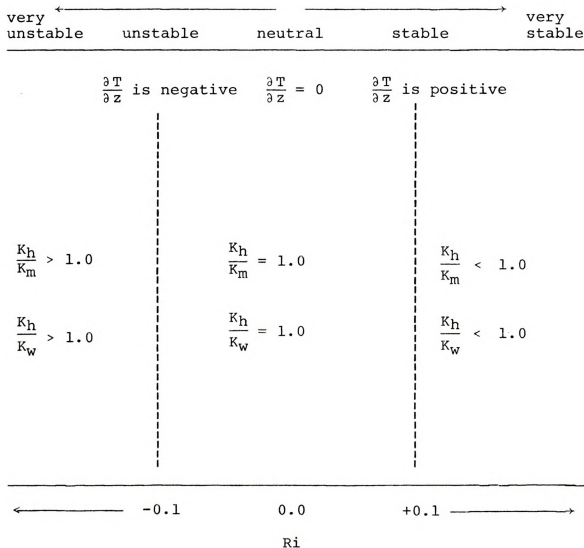
Generally, the temperature induced eddies are more efficient in transport and mixing, than mechanical eddies (61). A convenient stability parameter for use in this area is the Richardson number,  $Ri$ . It approximates the ratio between the forces producing thermal and mechanical turbulences. In gradient form it appears as

$$Ri = \frac{g}{T} \frac{\left(\frac{\partial T}{\partial z}\right)}{\left(\frac{\partial u}{\partial z}\right)^2} \dots \dots \dots [10]$$

where  $g$  is the acceleration due to gravity,  $T$ -temperature,  $\partial T/\partial Z$ -temperature gradient and  $\partial U/\partial Z$ -wind velocity gradient. Under neutral or adiabatic atmospheric conditions ( $Ri=0$ ), the transfer mechanisms for heat and water vapor are identical for freely evaporating surfaces (23,24). Therefore, the eddy diffusivities for momentum, heat and water vapor are identical ( $K_m=K_h=K_w$ ) and all could be obtained from Equation [9]. Under most conditions, however, adiabatic or near neutral conditions are seldom realized, and predictions of all three fluxes become complex. In an unstable atmospheric condition (i.e., lapse,  $\partial T/\partial Z$  negative), the profile of wind, humidity and temperature remain similar and ratio of  $K_h/K_m$ ,  $K_w/K_m$ , hence  $K_h/K_w$  remain constant (unity) for  $Ri$  ranging from 0.0 to -0.1 (99). However, for very unstable conditions,  $Ri$  is quite dependent

on the wind profile, i.e.,  $Ri$  is less than  $-0.1$  as the wind gradient diminishes, and the ratio  $K_h/K_w$  will depart smoothly from unity and becomes greater than one (12,49).

In stable atmospheric conditions (i.e., inversion,  $\partial T/\partial z$  positive), the eddy diffusion of momentum, heat and water vapor is also constant up to  $Ri$  of  $+0.1$  (47). But, at Richardson numbers greater than  $+0.1$ ,  $K_h/K_w$  will be less than unity (58, 98). The influence of atmospheric conditions represented by Richardson numbers are shown schematically below.



Under conditions of very strong stability, it has been suggested that turbulence changes character to gravity waves (49). At very strong stabilities a value of  $(Ri)_{\max}$  is reached where turbulent motion ceases entirely. Turbulence is then replaced by laminar flow governed by molecular rather than turbulent diffusion (59). Evaporation under stable condition decreases rapidly with increasing  $Ri$ . This decrease is constant throughout turbulence decay and indicates that  $Ri$  is no longer a useful stability criterion in profile equations (12). It appears that the largest departure of  $Kh/Kw$  from unity will occur when either temperature or humidity is passive additive or the temperature gradient is of opposite sign to the humidity gradient (95). Since the logarithmic law does not fit the wind profile under non-neutral conditions, various proposals have been made to modify it.

In 1935, Rossby and Montgomery (75) tried to implement Prandtl's views on the semi-empirical theory of a boundary layer problem and develop a relation for the coefficient of turbulent mixing under adiabatic conditions. They assumed that under adiabatic temperature distribution the mixing length in the lower layer of the atmosphere varied linearly with height, reaching a value proportional to the roughness of underlying surface at  $Z=0$

$$l = k (Z + Z_0) \dots \dots \dots [11]$$

where  $l$  is the mixing length,  $Z_0$  is the roughness coefficient and  $k$  is the non-dimensional VonKarman constant ( $k=0.41$ ). In the mixing length theory, it has been assumed that a discrete

mass of fluid with a given property leaves a level and retains this property for some characteristic vertical distance before mixing and becomes once again indistinguishable from its mean surrounding. Rossby and Montgomery assumed that the influence of stability on exchange is determined at a given elevation by the Richardson number and is not dependent on the Ri numbers corresponding to other elevations (75). Based on this assumption, and for stable atmospheric conditions they derived the general equation

$$K_m = kU_*Z (1+B\text{Ri})^{-\frac{1}{2}} \dots \dots \dots [12]$$

where  $K_m$  is a function of Ri and  $B=9$ . The equivalent form of this expression proposed by Holzman (40) for unstable cases is

$$K_m = kU_*Z (1-B\text{Ri})^{+\frac{1}{2}} \dots \dots \dots [13]$$

Measurements by Panofsky, Blackadar and McVehil (60) and observations of temperature fluctuations by Priestly (70) lead the way to deriving a modified equation which covered a broader range of stability. Such an equation was first suggested by Ellison (27) and is introduced in the literature under the name KEYPS (47). The KEYPS relationship for a stable atmospheric condition is

$$K_m = kU_*Z (1+B\text{Ri})^{-\frac{1}{4}} \dots \dots \dots [14]$$

The equivalent KEYPS equation for an unstable condition is

$$K_m = kU_*Z (1-B\text{Ri})^{+\frac{1}{4}} \dots \dots \dots [15]$$

where B takes the same value for both stable and unstable conditions at a given location.

Morgan et. al. (52) suggest that, for a wide range of stability, the general form of the equation should be

$$K_m = kU^*Z (1+B|Ri|)^{\pm n} \dots \dots \dots [16]$$

which offers the best mathematical representation of  $K_m(Ri)$  relationship. However, for their data obtained at the University of California at Davis, the authors suggest that the exponent  $n$  apparently needs to be 33% higher than the ( $\frac{1}{4}$ ) power proposed by Ellison as used in KEYPS profile. On the other hand, the exponent of ( $\frac{1}{4}$ ) suggested by Holzman (40) was too high for their data. The Davis data indicate one could use a  $B$  value significantly smaller than 9.0, originally proposed by Holzman, to extend the usefulness of the expression over a range of  $Ri$  from -1.0 to +1.0. However, this is at the expense of errors in  $K_m$  of up to 10% to 15% in the zones of  $Ri$  around -0.1 to +0.1 (52).

## EXTENSION OF THEORETICAL MODEL DEVELOPMENT

A modified version of Equation [5] under thermal stratification gives

$$E = -\rho_a K_m \frac{\partial q}{\partial z} \dots \dots \dots [17]$$

After rearranging the terms, Equation [17] can be presented as

$$\frac{\partial q}{\partial z} = - \frac{E}{\rho_a K_m} \dots \dots \dots [18]$$

Substituting for  $K_m$  from Equation [16] into Equation [18] gives

$$\frac{\partial q}{\partial z} = - \frac{E}{\rho_a k U_* Z (1+B|Ri|)^{\pm n}} \dots \dots \dots [19]$$

From Equations [7] and [8] we have

$$\frac{\partial u}{\partial z} = \frac{U_*}{K_m} \dots \dots \dots [20]$$

Under non-neutral conditions, we can rewrite Equation [20] as

$$\frac{\partial u}{\partial z} = \frac{U_*}{kZ (1+B|Ri|)^{\pm n}} \dots \dots \dots [21]$$

Then substituting for  $U_*$  in Equation [19], its equivalence from Equation [21], we get

$$\frac{\partial q}{\partial z} = - \frac{E}{\rho_a k^2 Z^2 (1+B|Ri|)^{\pm 2n}} \cdot \frac{1}{\frac{\partial u}{\partial z}} \dots \dots [22]$$

or by introducing the definition of  $R_i$  as given in Equation [10] we obtain

$$\frac{\partial q}{\partial z} = - \frac{1}{\rho_a k^2 z^2} \cdot \frac{E}{\left(1 + \left| \frac{Bg}{T} \cdot \left( \frac{\partial T}{\partial z} \right) \right| \right)^{\pm 2n}} \cdot \frac{1}{\frac{\partial u}{\partial z}} \quad \dots [23]$$

Equation [23] is very difficult to integrate in its present form. Therefore, in order to change this equation into a more suitable form, we assume, as Holzman (40) suggested, the logarithmic distribution of properties near the ground. Making this assumption we obtain

$$\frac{\partial T}{\partial z} = \frac{a}{z} \quad \dots \dots \dots [24]$$

and

$$\frac{\partial u}{\partial z} = \frac{b}{z} \quad \dots \dots \dots [25]$$

Substituting these relations into Equation [23] gives

$$\frac{\partial q}{\partial z} = - \frac{1}{\rho_a k^2 z^2 b} \cdot \frac{E}{\left(1 + \left| \frac{Bg}{T} \cdot \left( \frac{z}{b} \right) \right| \right)^{\pm 2n}} \quad \dots \dots [26]$$

or

$$\frac{\partial q}{\partial z} = - \frac{1}{\rho_a k^2 b} \cdot \frac{E}{z (1 + |SZ|)^{\pm 2n}} \quad \dots \dots \dots [27]$$

where

$$S = \frac{Bga}{b^2 T} \quad \dots \dots \dots [28]$$

The variable  $S$  from hereon is referred to as a stability parameter. Selecting  $\frac{1}{4}$  for  $n$  according to KEYPS, Equation [27] becomes

$$\frac{\partial q}{\partial z} = - \frac{1}{\rho_a k^2 b} \cdot \frac{E}{z (1 + |SZ|)^{\pm \frac{1}{2}}} \quad \dots \dots \dots [29]$$

Integrating Equations [24] and [25] and expressing the changes of temperature and wind-speed in finite difference notation, we obtain

$$a = \frac{T_2 - T_1}{\ln\left(\frac{Z_2}{Z_1}\right)} = \frac{\Delta T}{\ln\left(\frac{Z_2}{Z_1}\right)} \dots\dots\dots [30]$$

and

$$b = \frac{U_2 - U_1}{\ln\left(\frac{Z_2}{Z_1}\right)} = \frac{\Delta U}{\ln\left(\frac{Z_2}{Z_1}\right)} \dots\dots\dots [31]$$

Integrating Equation [29], see Appendix C for detail of the procedure, substituting for b and solving for E we have

$$E = \frac{\rho_a k^2 \Delta q \Delta U}{\ln\left(\frac{Z_2}{Z_1}\right)} \cdot f(S) \dots\dots\dots [32]$$

where

$$f(S) = \frac{1}{\ln \left| \frac{\sqrt{1+SZ_2}-1}{\sqrt{1+SZ_2}+1} \cdot \frac{\sqrt{1+SZ_1}+1}{\sqrt{1+SZ_1}-1} \right|} \dots [33]$$

for unstable atmospheric conditions (Ri and/or S negative, n positive), and

$$f(S) = \frac{1}{[2(\sqrt{1+SZ_2} - \sqrt{1+SZ_1}) + \ln \left| \frac{\sqrt{1+SZ_2}-1}{\sqrt{1+SZ_1}+1} \cdot \frac{\sqrt{1+SZ_1}+1}{\sqrt{1+SZ_1}-1} \right|]} \dots [34]$$

for stable atmospheric conditions (Ri and/or S positive, n negative). When neutral or near adiabatic conditions prevail in the atmosphere, the function f(S) becomes unity and Equation [32] becomes

$$E = \frac{\rho_a k^2 \Delta q \Delta U}{[\ln\left(\frac{Z_2}{Z_1}\right)]^2} \dots\dots\dots [35]$$

which is the original expression suggested by Thornthwaite and Holzman (88).





## MATERIALS AND METHODS

This study was conducted at the Michigan State University Soil Science Research Farm. The farm is located on the corner of South Hagadorn Road and Mt. Hope Highway, two miles southeast of the center of the campus. A small weather station was established on grass plots in the mid-section of the northern portion of the farm, Figure 1. The fetch to height ratio for the eight-meter level of measurement was approximately 30:1 in the west to southwest direction.

The soil type for this study, according to Ingham County Soil Survey Report (92) and on site inspection by Dr. D. Mokma, soil survey and classification specialist in the Department of Crop and Soil Sciences, was Metea loamy sand, hereafter referred to as MtB. Typically, the surface layer of MtB series is a dark, loamy sand, 10 cm thick and a B-horizon about 85 cm thick. The upper part of the B horizon is yellowish brown to dark brown and very friable, loamy sand. The lower part is yellowish brown, loose sand. Permeability is very rapid in the upper part of MtB soil and moderate in the lower part. The available water holding capacity of this series is described as moderate.



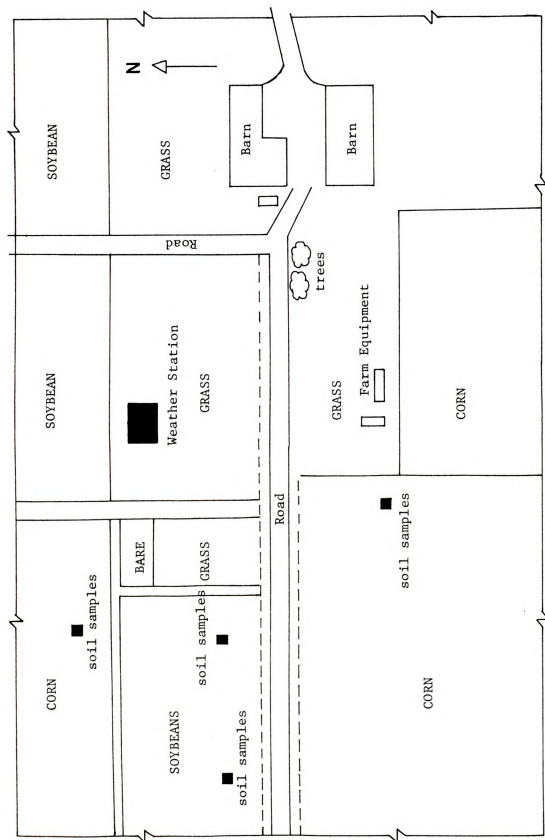


Figure 1. Schematic diagram of the experimental site on the MSU Soil Science Farm.

Michigan State University is located at East Lansing in the northwest corner of Ingham County and within the south central climatic division of Michigan. East Lansing's inland location substantially reduces the climatic influence of the Great Lakes. The prevailing local wind is generally from the southwest averaging about 5 m/s. The average mid-day relative humidity varies from 51% in May to 78% in December. Precipitation is well distributed throughout the year; the growing season, May-October, receives an average of 45 cm or 61% of the average annual total. Summer precipitation is mainly in the form of afternoon showers and thundershowers. Potential evapotranspiration, based on Class A pan observations, exceeds the average precipitation by 90% during the growing season (90).

#### Soil Measurements

Soil properties measured in this study were as follows: profiles of gravimetric moisture content, soil moisture-matric potential values, bulk density and the soil temperature profile. Soil samples of known volume were taken early in the morning and late in the afternoon during days with no rainfall from 5, 10, 20, 40, and 80 cm depths at three different locations, using a Veihmeyer tube-type sampler. The sampling sites were: (1) a "High Yield Corn Study" - treatment 5 (Zea maize, var. M5922) with 75-cm row spacing and population of 84,000 plants per hectare, (2) a non-irrigated section of an "Irrigation Management Study for Soybeans" - treatment 1 (Glycine max, var. Gnome with 45-cm row spacing and population

of 150,000 plants per hectare, and (3) the same as site 2, except the plots were irrigated at a matric potential of less than 50 centibars during the entire growing season. Additional soil moisture data for non-irrigated corn (*Zea mays* var. P-3780), 75-cm-row spacing and population of 60,000 plants per hectare were obtained through an exchange of information with Mr. V. Braults of Department of Agricultural Engineering.

Tensiometers were also used to monitor the soil moisture status and irrigation requirements of the soybean and corn crops. In the corn plots, 11 tensiometers were installed at depths of 25 cm, between the rows and at 25- and 40-cm depth in the planted row. In the soybean plots a total of 9 tensiometers were used at depths of 25 cm and 40 cm in and between the planted rows.

Tensiometer data were obtained from all plots in one- or two-day periods based on the weather conditions. During the cool, humid and less windy days, the data were obtained once every two days in the afternoon. In the hot, less humid and windy periods, tensiometers were read at the end of each day. Five composite, disturbed soil samples were taken from each level of all three sites and were analyzed in the laboratory for soil moisture retention according to Richards (72), see Figure 2.

Profiles of soil temperature were obtained at the experimental site by placing 22-gage copper-constantan thermocouples at 5, 10, 20, 40 and 80 cm below the soil surface. The soil temperature probe was constructed from a

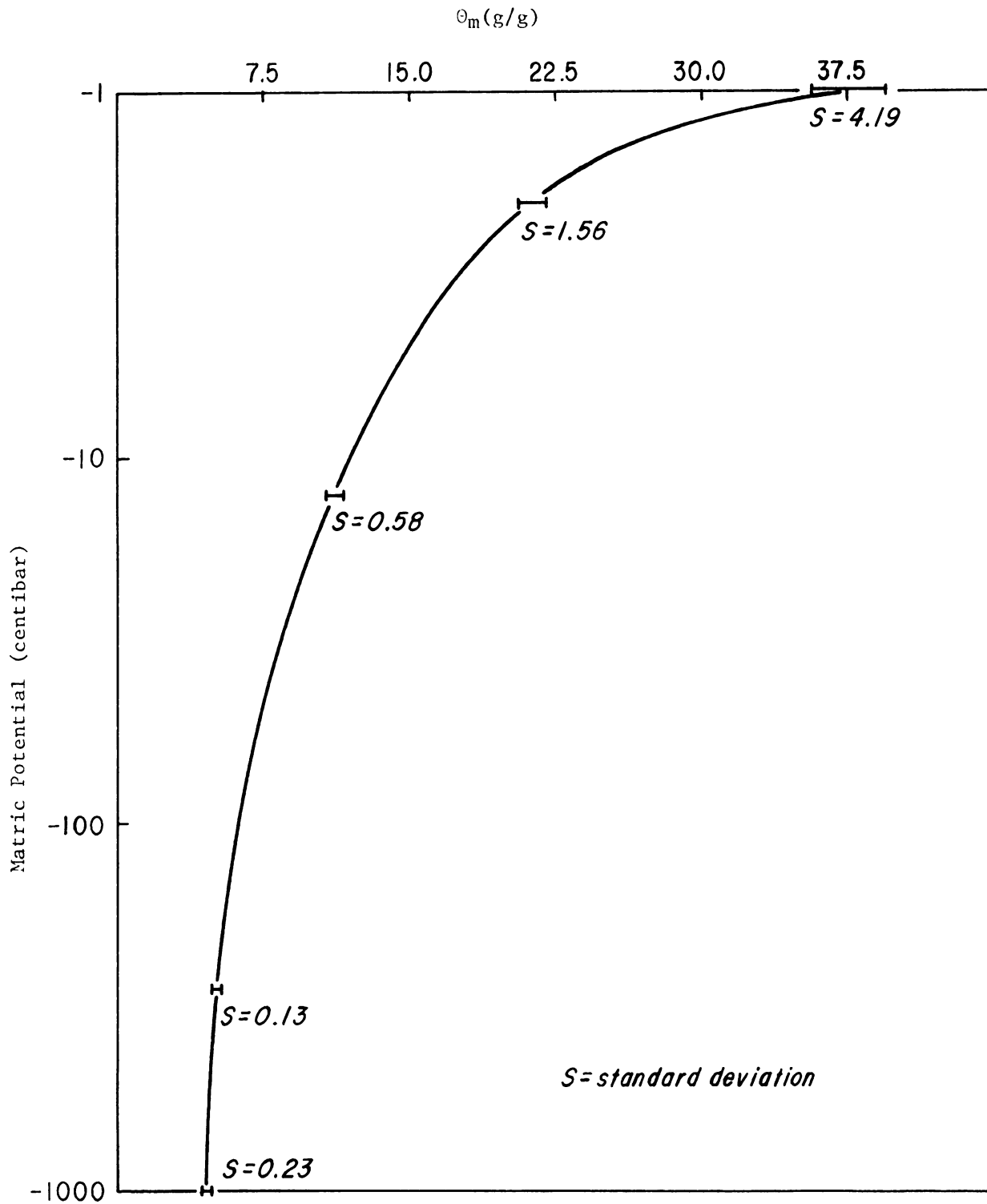


Figure 2. Soil moisture content-matric potential relationship for Metea loamy sand. Each point is the mean of 25 measurements - five measurements being taken at 5, 10, 20, 40 and 80 cm depths.





wooden stake, 6x3 cm and 150 cm long. Two small grooves were cut 5 mm deep, 4 mm wide and about 1 cm apart from each other in the oblong section of the stake. Thermocouple wires were placed inside the grooves. The assigned thermocouples were marked on the stake and fastened by masking tape. The soldered junction of thermocouples were insulated by an electrical insulating varnish to prevent any electrical conductance. Then the junctions were turned 180° such that they were lying flat on the taped section of the stake. Installation was completed by driving the stake into the ground. This approach had some inherent advantages over older excavation methods: (1) it eliminated the possibility of any loose contact between the soil and thermocouple, (2) reduced the labor and error of excavating and disturbing the soil and (3) consumed less time for installation. The signals, generated by the five thermocouples, were transmitted through a reference junction board and channel expander to the data acquisition system.

#### Evaporation Measurements from Class A Pan

A U.S. Class A evaporation pan was automated and used for monitoring evaporative losses continuously. The U.S. Class A pan, 121 cm in diameter, 25 cm deep and normally constructed of galvanized iron, was mounted on an open frame such that the pan base was 15 cm above the ground. The water level in the pan was monitored at 5 cm below the rim. In addition to measuring water losses electronically,

measurements of the water level were made daily by a fixed gage (41). Although one-day interval, Class A pan evaporation measurements have given reasonable estimates of potential evapotranspiration especially under humid conditions, its major limitation is the inaccuracy for which reasonable estimates of evaporation can be made for shorter time periods (62,85). One objective of this study was to design a monitoring assembly that when combined with a Class A pan experiment, would give an accurate, continuous assessment of water losses over short time periods.

A number of available systems which could be utilized for this purpose were assessed. All were complicated and costly (9,68). Some equipment which was applicable to our needs was insensitive and unstable over the load range of a Class A pan (7,30). After much deliberation and searching, a unique combination of the Wheatstone bridge circuit in conjunction with an elastic stress system was selected for monitoring the water losses. Considerable effort was put forth in selecting a set of strain gages (stress transducer sensors) and an appropriate Wheatstone bridge that would maximize the desired output. A change in electrical resistance of the wire gages as a result of a change in strain is the basic principle upon which this system works (67).

The selection of wire resistance-strain gages and strain transducer materials depends on the load, precision and accuracy required (101). Proper transmission of strain to

the gage requires the gage wire to be as thin as possible. However, wire thinness causes a higher gage resistance and thus a higher voltage output at a given gage current which, in turn, is limited by the amount of heat generated in the gage. A higher resistance gage can, of course, also be obtained with longer wires (53). The transducer materials should have a small length to radius ratio to ensure freedom from buckling (67). The precision with which strains can be measured also depends on hysteresis, creep and fatigue properties of transducer materials and the environment of the gage, especially temperature and humidity (54).

A basic device which can be used to measure all classes of strain is the Wheatstone bridge. Its function is to determine resistance with the required degree of precision. The amount by which resistance changes in relation to change in strain is an index of what is known as strain sensitivity of wire or "strain gage factor" (51). For a uniform straight wire this may be expressed as

$$GF = \frac{\Delta R/R}{\Delta L/L} \dots \dots \dots [1]$$

where GF = strain gage factor

R = resistance

$\Delta R$  = change in resistance

L = length

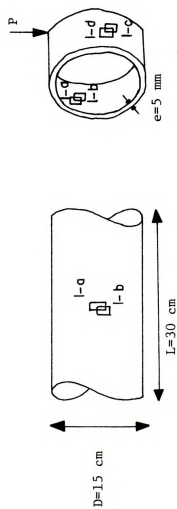
$\Delta L$  = change in length

The higher the gage factor, the more sensitive is the gage and the greater is its electrical output for indication and recording purposes (53).

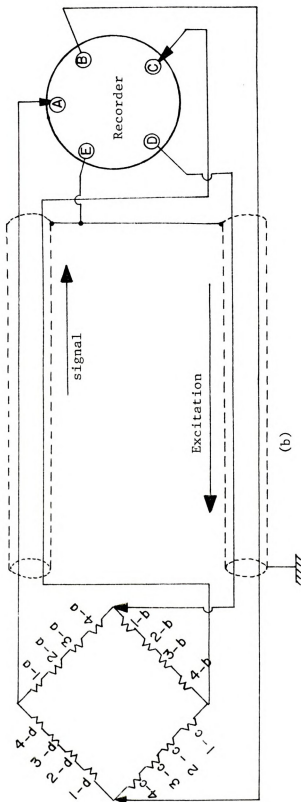
To automate the Class A evaporation pan, sixteen general purpose, self-temperature compensated, constantan strain gages, type CEA -13-250UW-120, were mounted on four metal cylinders (arms), these being the strain transducer materials. The arms were made of aluminum pipe, each 30 cm long, 15 cm in diameter and 5 mm thick. The low modulus of elasticity of aluminum (i.e.  $E_1 = 55-70 \times 10^9 \text{ N/m}^2$ ), increased the output voltage of the gages by increasing the strain per unit load (17). Figure 3-a shows the arrangement of gages on one arm. More information on surface preparation and application of strain gages is presented in "Micro-Measurement Catalog and Technical Data" published by Vishay Intertechnology, Inc. (51).

An important feature of this system was the spatial arrangement of the strain gages which were inherently temperature compensated. For a tension load applied on each arm, gages 1 and 3 were in compression and gages 2 and 4 were in tension. With the bridge arrangement shown in Figure 3-b, these effects were additive resulting in a larger output. To increase the sensitivity of the system and also protect the gages against the outdoor environment, all gages were covered with a special combination of three different coating materials, M-COATS B, D and G, obtained from "Micro-Measurement Inc." These were applied as follows: After installation of the gages on the supporting arms, M-COAT B was applied and cured for 24 hours, followed by a coating with M-COAT D. Another 24 hours later M-COAT G was applied and cured for a period of 48 hours. The combination of these three coating





(a)



(b)

Figure 3. Position of strain gages (a) on an active arm, and (b) their full bridge arrangement.

materials gave a good, short and long term stability to the gages and also protected them against the outdoor environment.

In order to level the arms under the pan and prevent any heat conduction between the arms and the pan, the arms were placed between two pieces of plywood, 120x120 cm and 1.25 cm thick. This enabled the system to meet the Weather Bureau requirement that the pan base be at least 10 cm above the ground. A Sanborn dual-channel, carrier amplifier recorder, Model 321, was used to record the output voltage generated by the strain gages. A full-bridge arrangement of strain gages with the recorder is shown in Figure 3-b. The relationship between the bridge output ( $E_B$ ), bridge supply voltage ( $V$ ), strain ( $\epsilon$ ), gage factor ( $GF$ ), and percent resistance change in the gages for a four active arm bridge is

$$\Delta E_B = \frac{V}{4} \left( \frac{\Delta R_1}{R_1} + \frac{\Delta R_2}{R_2} + \frac{\Delta R_3}{R_3} + \frac{\Delta R_4}{R_4} \right) \dots [36]$$

or

$$\Delta E_B = \frac{V}{4} (S_O \cdot GF) P \dots [37]$$

Equation [3] can be rearranged and expressed as

$$\frac{\Delta E_B}{V \cdot P} = \frac{\epsilon \cdot GF}{4} \dots [38]$$

where  $\epsilon = S_O$  = strain per kilogram load on the arm  
 $P$  = load applied, kilogram

The output of the system was in millivolts (mv) bridge output/volts bridge supply/kilogram axial load applied. A calibration curve (see Figure 4) was obtained for the system by adding and subtracting small aliquots of water (0.375 cm water/area of pan). Both the eye-fitted line and coefficient of determination

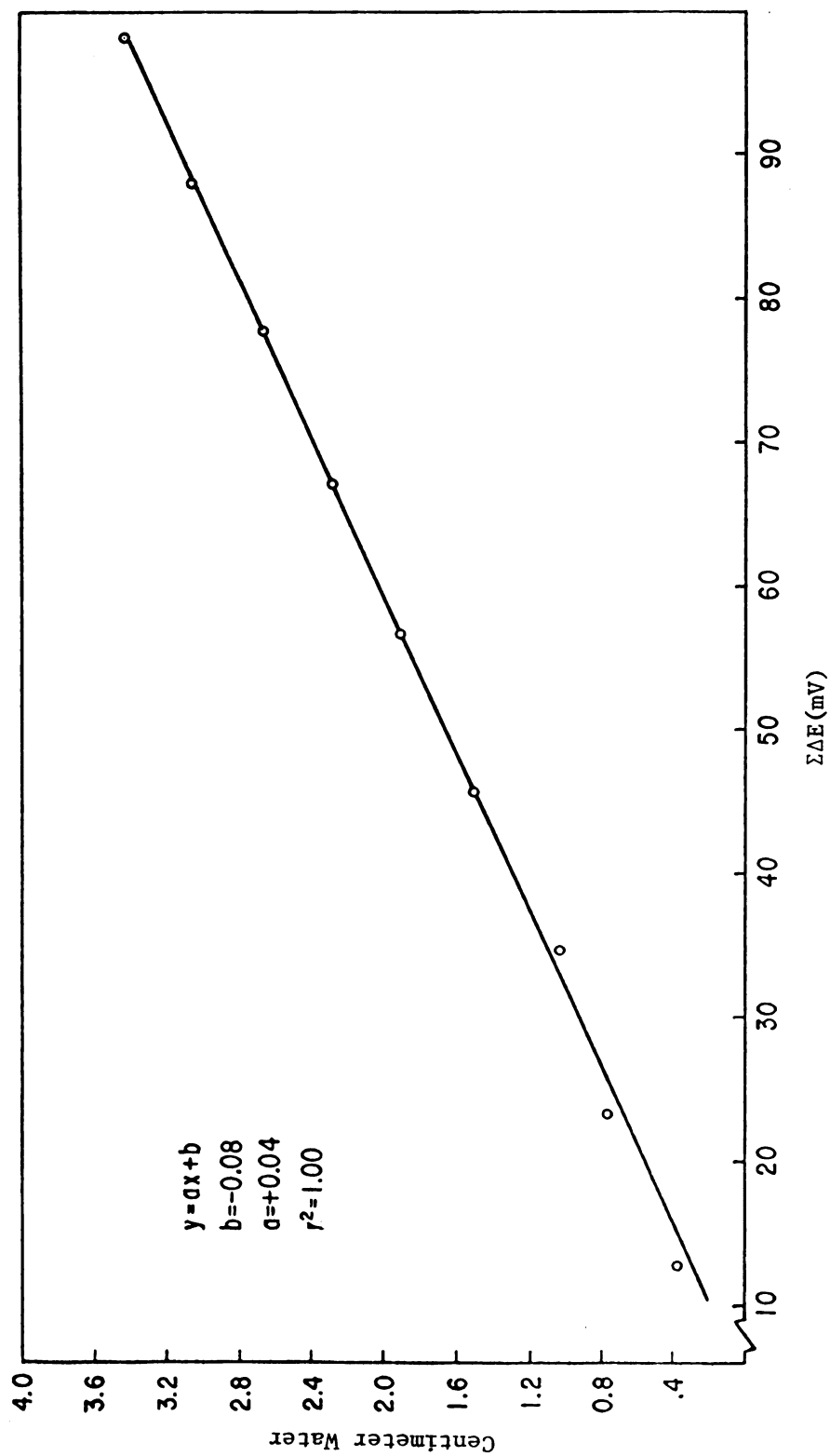


Figure 4. Calibration curve for pan assembly. Each value is the mean of 10 measurements.



( $r^2=0.99$ ) are indicative of linear response of the system to changes in water levels over a wide range.

The sensitivity of this system was estimated as

$$\text{Sensitivity} = \frac{\Delta(\overline{\text{cm of water}})}{\Delta(\overline{E_B})} \dots [39]$$

where

$\Delta(\overline{\text{cm of water}})$  = average quantity of water added to or subtracted from the pan, cm

$\Delta(\overline{E_B})$  = average change in bridge output for a given quantity of water added to or subtracted from the pan, mv.

Based on this relationship and data obtained from the calibration procedure, sensitivity of the system in predicting water loss was 0.034 mm water/0.1 mv bridge output. Since 0.1 mv was the smallest voltage change detectable, then 0.034 mm water was the smallest water loss that could be accounted for. Based on total weight, 1 g in 6000 g was detectable.

### Micrometeorological Measurements

Two atmospheric profile measurement masts were constructed from 10-m long, 7.5-cm diameter, aluminum, irrigation pipe, mounted on a tilt-up base staked to the ground. Arms for mounting instruments were constructed of 1.25-cm diameter, galvanized steel pipe and mounted on the masts with saddle-T risers.

Wind profiles were measured over two-minute intervals with 3-cup anemometers, Climet Model 011-1, mounted at 50, 100, 200, 400 and 800-cm levels on the first mast and 200- and 400-cm levels on the second mast. The digital signal from these



seven light-chopper-type anemometers were transmitted via wire to a Tachometer 555 circuit to fix the width and height of pulses, Figure 5. The conditioned pulses were then transmitted through a channel expander to specially modified channels of the data acquisition system.

Wind directions were measured over two-minute intervals with a Climet Anemovane. The calibration for this system was established by adjusting the pointer between zero and  $\pm 180$  mv output, corresponding to north and south, respectively. The range between these limits was divided into 8 equal quadrants for wind direction analyses. The output of this unit was also transmitted via the channel expander to the data acquisition system.

Temperature and humidity profiles were measured over two-minute periods at the 50-, 100-, 200-, 400-, and 800-cm levels on the first mast and at 100-, 200-, and 400-cm levels on the second mast, using aspirated, adjustable water level, radiation shielded psychrometers. The psychrometers were constructed out of dual bakelite tubes for radiation shielding (32), a squirrel cage fan for aspiration ( $300 \text{ cm sec}^{-1}$ ), plexiglas water reservoir and 22-27 gage copper-constantan thermocouple wires as dry and wet bulb sensing elements (56). Figures 6-a and 6-b show a schematic and a close-up view of one of these units. The thermocouples were calibrated in the laboratory by testing them in the ice and hot water baths at  $0^\circ\text{C}$  and  $100^\circ\text{C}$ , respectively. The millivolt analog signals from the psychrometers were transmitted via thermocouple wires to a 24-point reference

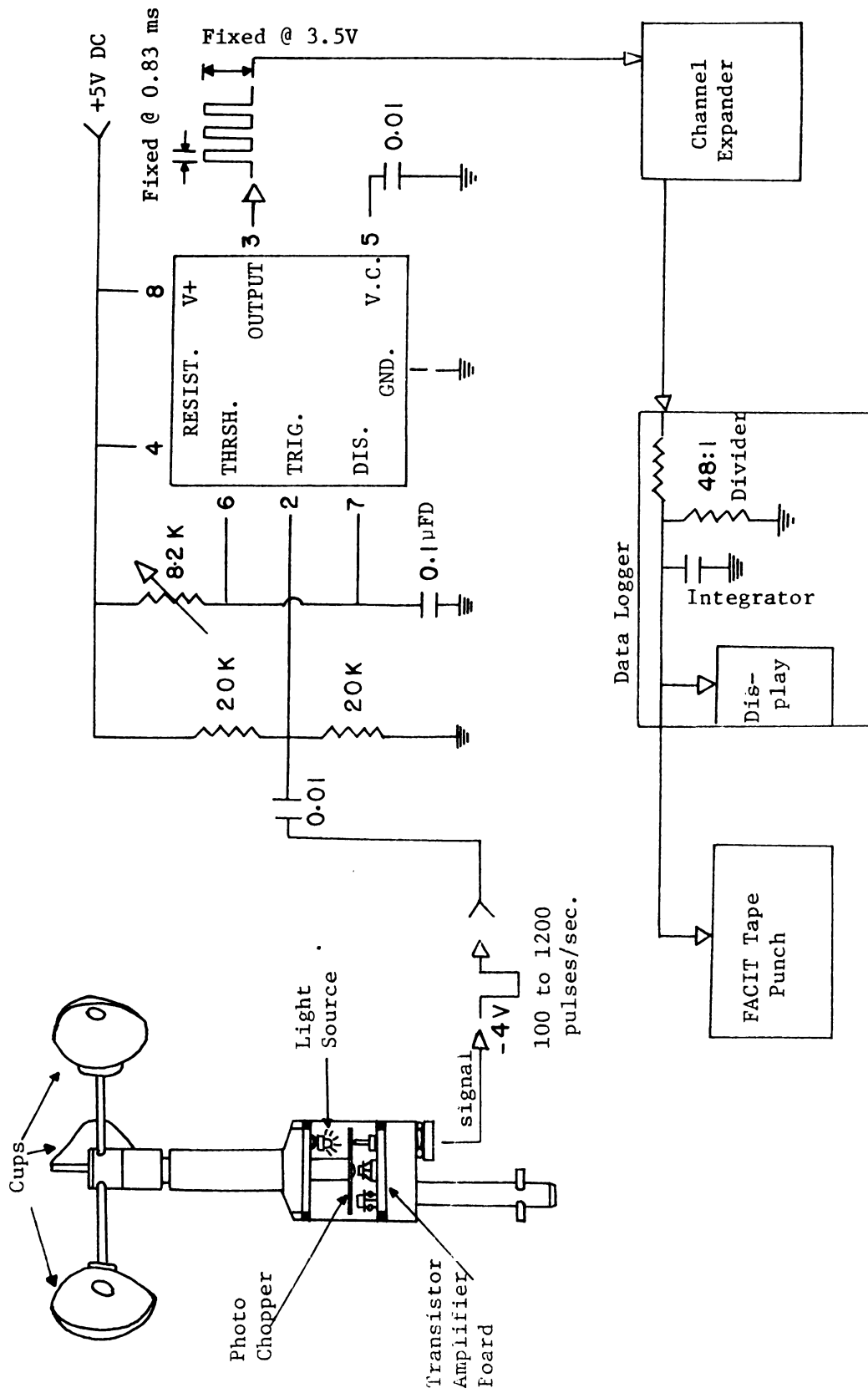


Figure 5. Tachometer-555 circuit for conditioning anemometer signals.



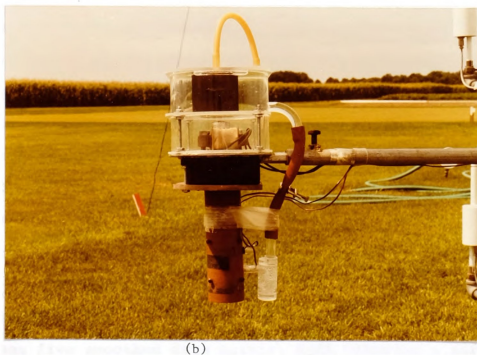
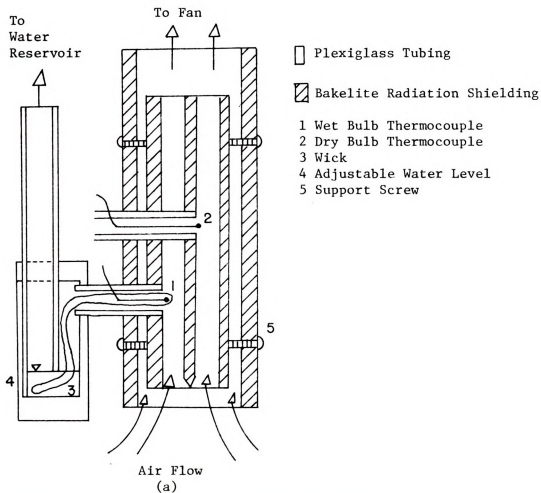


Figure 6. Cross sectional (a), and close-up (b) views of a psychrometer unit.

junction board and channel expander to the data acquisition system.

### Collecting and Analysis of Data

The data acquisition system for this study was an Esterline-Angus Recorder Model D-2020 combined with a Channel Expander and a FACIT paper tape recorder Model 4070. The combination of the expander and recorder provided up to 100 channels for recording. Only 54 of these channels were utilized in this study. All signals processed by the recorder were transmitted to the paper-tape unit and were recorded on the standardized, 8-channel, paper tape according to the American Standard Code for Information Interchange (ASCII), 1968 version, Figure 7.

The data on paper tapes were read using the University of Michigan computer facilities (MTS). The MERIT computer network was used to transfer the data from the University of Michigan computer to the Michigan State University computer system (CDC). A FORTRAN IV computer program was written to convert the millivolt analog signals to digital engineering units, Appendix A. Also, a FORTRAN Psychrometric Model written by Mr. Lloyd Lerew of the Department of Agricultural Engineering (46) was used to compute the atmospheric humidity based on the wet and dry-bulb temperatures.

A binomial scheme recommended by Bevington (2) involving three sequential measurements was used to smooth the data. Then five smoothed data points, each covering a period of

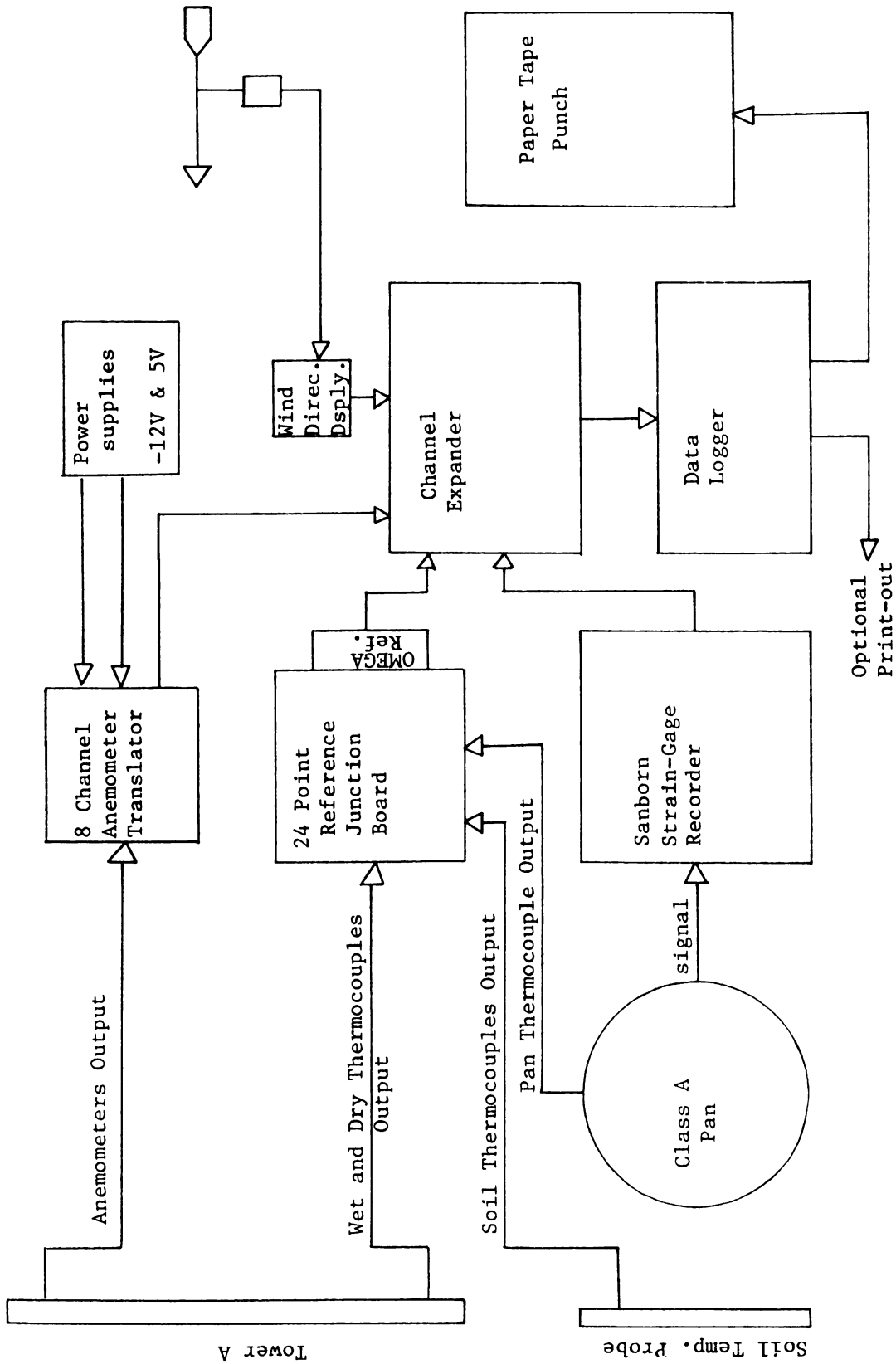


Figure 7. Schematic view of all sensors and data acquisition system.



two minutes, were combined and averaged to obtain a single reading for a period of ten minutes.



## RESULTS AND DISCUSSION

### I. Evapotranspiration from Soil

Soil moisture status was monitored daily at four different locations in the vicinity of the weather station both gravimetrically and by tensiometers during the course of the study, see Figure 1. The gravimetric moisture determinations for the period of this study are presented in Table 1. The results show changes in soil moisture content with time. The magnitude of changes are greater in non-irrigated areas than in the irrigated areas. This general pattern holds for the entire period of study. Hence, it was not possible to obtain a meaningful water loss relationship over short time periods in a given treatment. This difficulty was due to frequent changes in soil moisture content due to intermittent rainfall which was received during the course of this study.

The rainfall distribution and changes in soil moisture potential, measured by tensiometers, for irrigated corn and soybean treatments are presented in Figure 8. According to these data, the lowest soil moisture potentials for corn and soybeans were -44 and -39 centibars, respectively. These values were obtained in September 8, 1980 late in the growing season. Another record low potential was -38 centibars

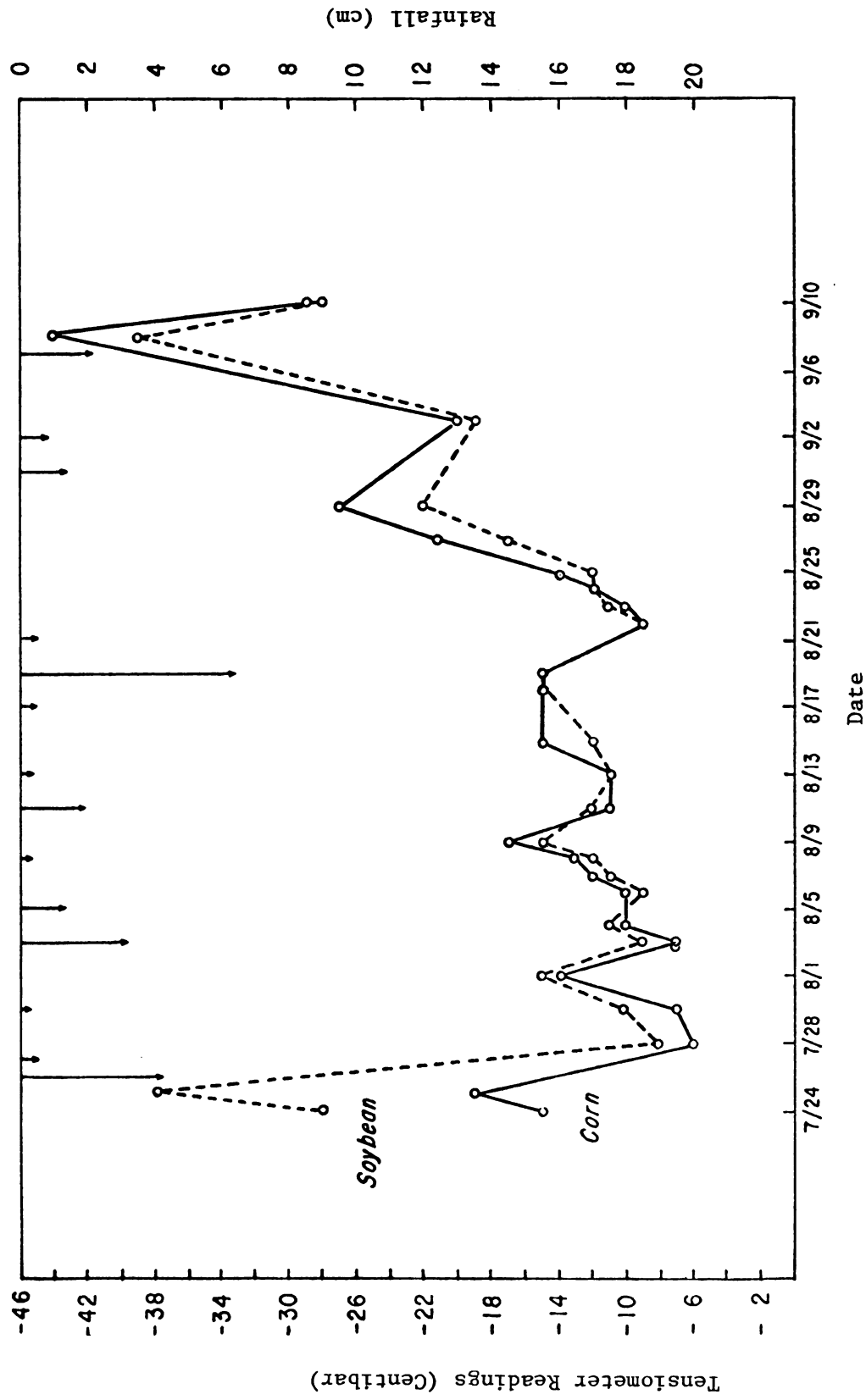


Figure 8. Rainfall distribution and soil moisture status during the growing season as indicated by tensiometers placed in irrigated corn and soybean plots.

Table 1. Soil moisture content influenced by irrigation, rainfall and type of crop during the experimental study. Each value represents the mean of 15 measurements-three measurements being taken at 5, 10, 20, 40 and 80 cm depths.

<u>Date</u>	<u>Moisture Content (%)</u>			
	<u>Corn</u>		<u>Soybean</u>	
	<u>Irrigated</u>	<u>Non-Irrigated</u>	<u>Irrigated</u>	<u>Non-Irrigated</u>
July 24	11.63	7.67	7.68	4.36
July 25	10.57	5.85	7.49	4.07
July 30	12.88	9.19	10.43	9.27
August 1	11.75	--	9.91	6.67
August 3	14.96	--	12.07	9.80
August 4	15.00	14.60	12.89	10.54
August 9	10.55	10.00	9.62	6.97
August 19	12.95	12.85	9.61	7.62
August 29	10.44	9.39	5.82	5.64

recorded for soybeans earlier in the growing season, July 25, 1980. In spite of these record lows, tensiometer data do not show potentials lower than -50 centibars at any time during the growing season. This limit is considered to be safe for the crops growing in medium textured soils used in this study (21). Hence, during the course of this study the soil moisture level did not impose any restriction on the rate of evapotranspiration from the irrigated treatments.

This supposition was supported by measuring the water holding capacity of the Metea loamy sand at different tension levels in the laboratory, Table 2. From the data in Table 1 and Figure 8, one can conclude that the soil moisture contents in the irrigated corn and soybean treatments were greater than the equivalent moisture content held in the soil at -33 centibars. Therefore, evapotranspiration from these treatments was at its potential rate during the entire season (16,97).

The rate of evapotranspiration under this condition is determined primarily by the available energy and indicated by weather parameters (73). However, this was not the case in non-irrigated treatments. Generally, in these treatments soil moisture contents varied between the equivalent moisture potentials held at -33 to -750 centibars, respectively, see Figure 2. On one occasion (July 24) the soil moisture content in a soybean area fell below the equivalent moisture content held at -1500 centibars, normally considered as the end-point for moisture availability to plants. Therefore, under the non-irrigated treatments, evapotranspiration was



Table 2. Bulk density and moisture holding capacity of metea loamy sand at different potential levels and sampling depths. Each value is the mean of 25 measurements.

Soil Depth (cm)	Bulk Density (gr/cm <sup>3</sup> )	CB <sup>†</sup>	Moisture Content (%)				
			0	6	33	100	1500
5	1.10		40.99	20.53	11.37	9.65	4.47
10	1.30		39.44	21.18	11.91	9.72	4.92
20	1.48		39.76	19.97	11.18	9.35	4.62
40	1.50		36.04	19.53	10.75	9.17	4.56
80	1.50		30.64	17.10	10.41	8.59	4.30
$\bar{x}$	1.38		37.37	19.66	11.12	9.30	4.57
S	0.16		4.19	1.56	0.58	0.45	0.23

<sup>†</sup> CB = Centi-Bar





controlled by the soil, and weather parameters were only of secondary importance (55,69).

## II. Evapotranspiration from Class A Pan

A specially modified U.S. Weather Bureau, Class A, Evaporation Pan was used to monitor quantities of water loss from the pan over short time periods. Two-minute intervals were selected for measuring the amount of water lost from the pan. However, during smoothing and processing, the data were combined and averaged over periods of ten minutes. The final results are presented, as mm of water loss from the pan in ten-minute intervals, in column 21 of Tables B-1 thru B-7 in Appendix B. These data can also be presented as linear regression equations for each date of measurement, Table 3. The good fit of these regression equations is indicated by the coefficients of determination,  $r^2$ . The changes in slopes and intercepts of these equations represent the variation in cumulative pan evaporation under different weather conditions on different dates. Generally, if cumulative evaporation started slowly early in the morning and increased gradually during the day, the regression equations had a small slope coefficient and a negative intercept (see regression equations for July 25 and 30). On the other hand, if cumulative evaporation increased uniformly with time, these equations had a larger slope coefficient and a positive intercept (see regression equation for July 24). Similar

Table 3. Regression equations representing cumulative Pan evaporation over short periods at different dates.

<u>Date</u>	<u>Number of Measurements</u>	<u>Regression Equation</u>	<u>r<sup>2</sup></u>
July 24	21	$Y=0.0760+0.0196X^a$	0.9964
July 25	59	$Y=-0.0252+0.0125X$	0.9876
July 30	26	$Y=-0.1567+0.0110X$	0.9888
August 1	30	$Y=-0.2161+0.0114X$	0.9976
August 4	50	$Y=0.0835+0.0097X$	0.9978
August 7	25	$Y=-0.2716+0.0098X$	0.9936
August 8	15	$Y=-0.2667+0.0110X$	0.9826
<hr/>			
All Dates, cumulatively	226	$Y=3.3310+0.0100X$	0.9962
All Dates, separately	226	$Y=0.1760+0.0101X$	0.9016

@

X = time, min.

Y = cumulative Pan evaporation, mm

expressions have been established and reported for seasonal cumulative pan evaporation based on daily or weekly observations (8,62). But, due to limited number of measurements and the variation of weather, the quality of such regression equations indicated by  $r^2$  is not as good as the ones obtained on the short time basis for daily observations in this study. This is also indicated by a decrease in the magnitude of  $r^2$  when cumulative pan evaporation from all dates in this study were used to obtain a regression fit, Table 3. In order to be able to use such equations more reliably in a given region, similar experiments should be conducted for more than one growing season to include all possible variations due to changes in weather (10,11,25,41).

Table 4 represents the simple correlation coefficients ( $r$ ), between pan evaporation rates, pan temperature, air temperature, relative humidity and wind speed on different dates. All correlation coefficients, with exception of the one between cumulative pan evaporation and relative humidity on August 7, were highly significant at the one percent level of probability. However, the strongest correlation was obtained between pan evaporation rates and pan temperature. The correlation coefficients obtained between pan evaporation and air temperature, measured at 50 cm above the ground surface, were generally smaller than the ones given for pan temperature. Hence, water temperature is more representative of water loss from the pan than air temperature at a given period, Figures 9, 10 and 11. These figures were prepared by choosing the

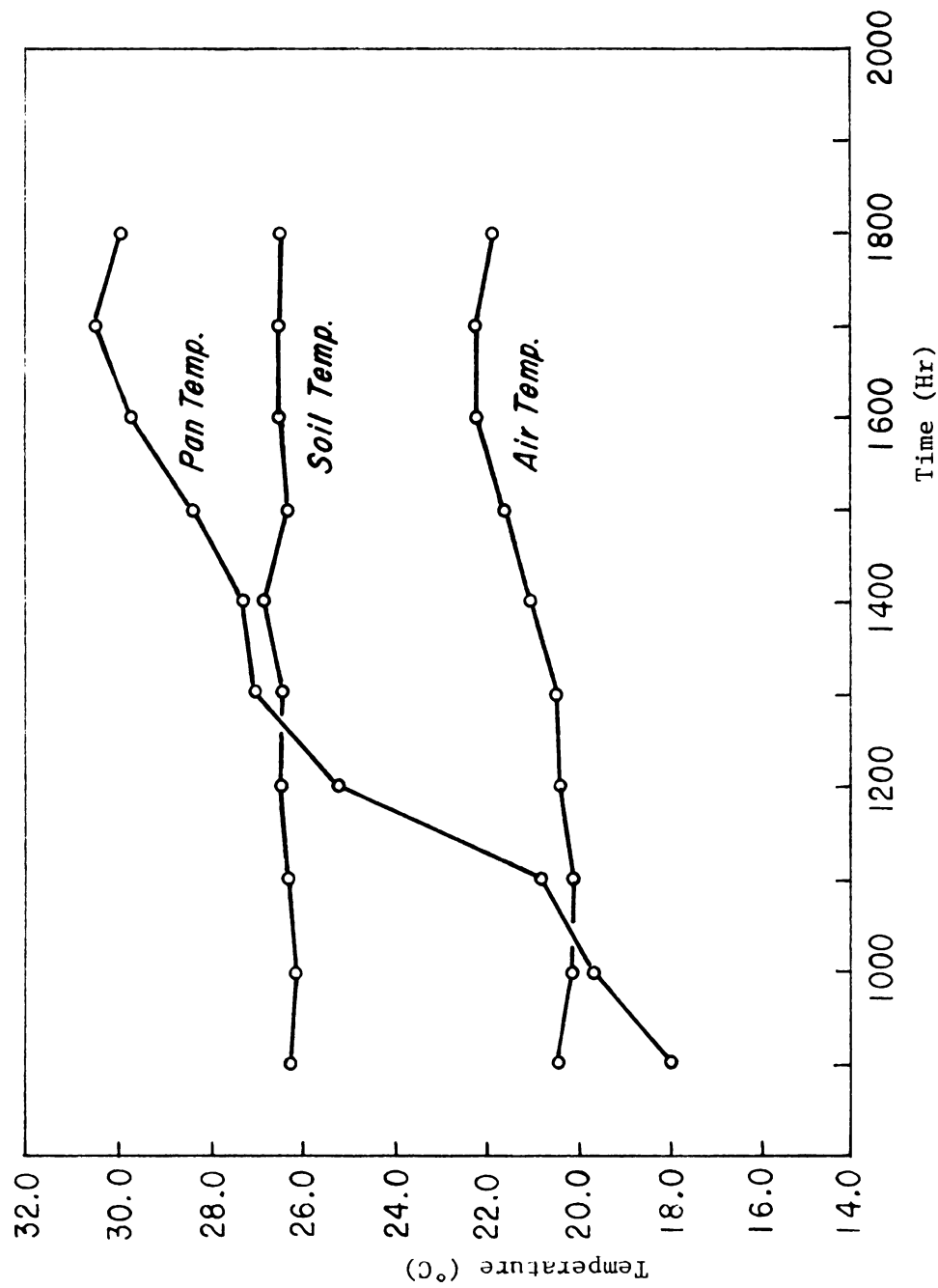


Figure 9. Air, soil and Class A pan temperature, averaged hourly, July 25, 1980. Air and soil temperature were measured at 50 cm above and 5 cm and 10 cm below a turfgrass cover, respectively.

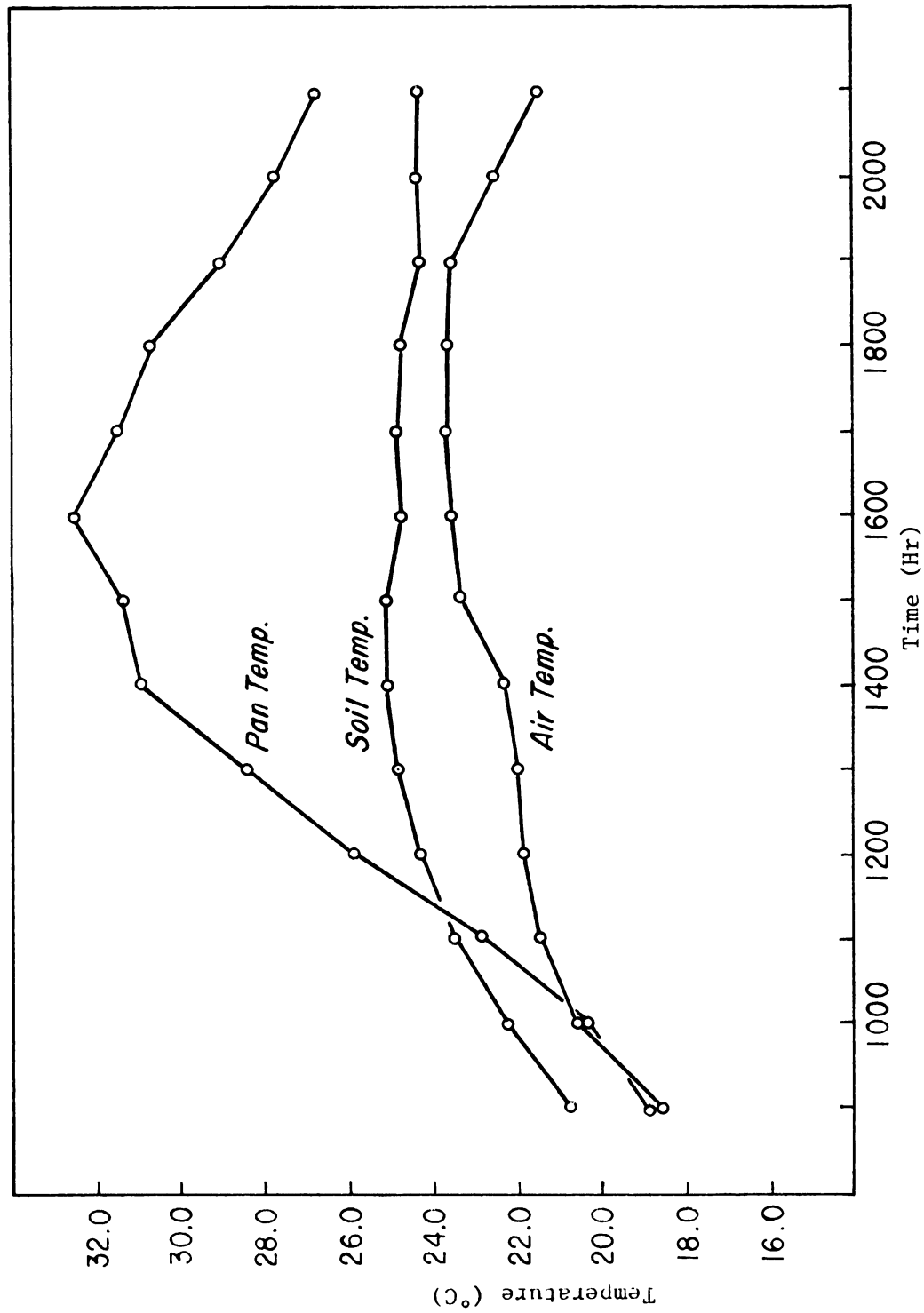


Figure 10. Air, soil and Class A pan temperature, averaged hourly, August 4, 1980. Air and soil temperature were measured at 50 cm above and 5 cm and 10 cm below a turfgrass cover, respectively.

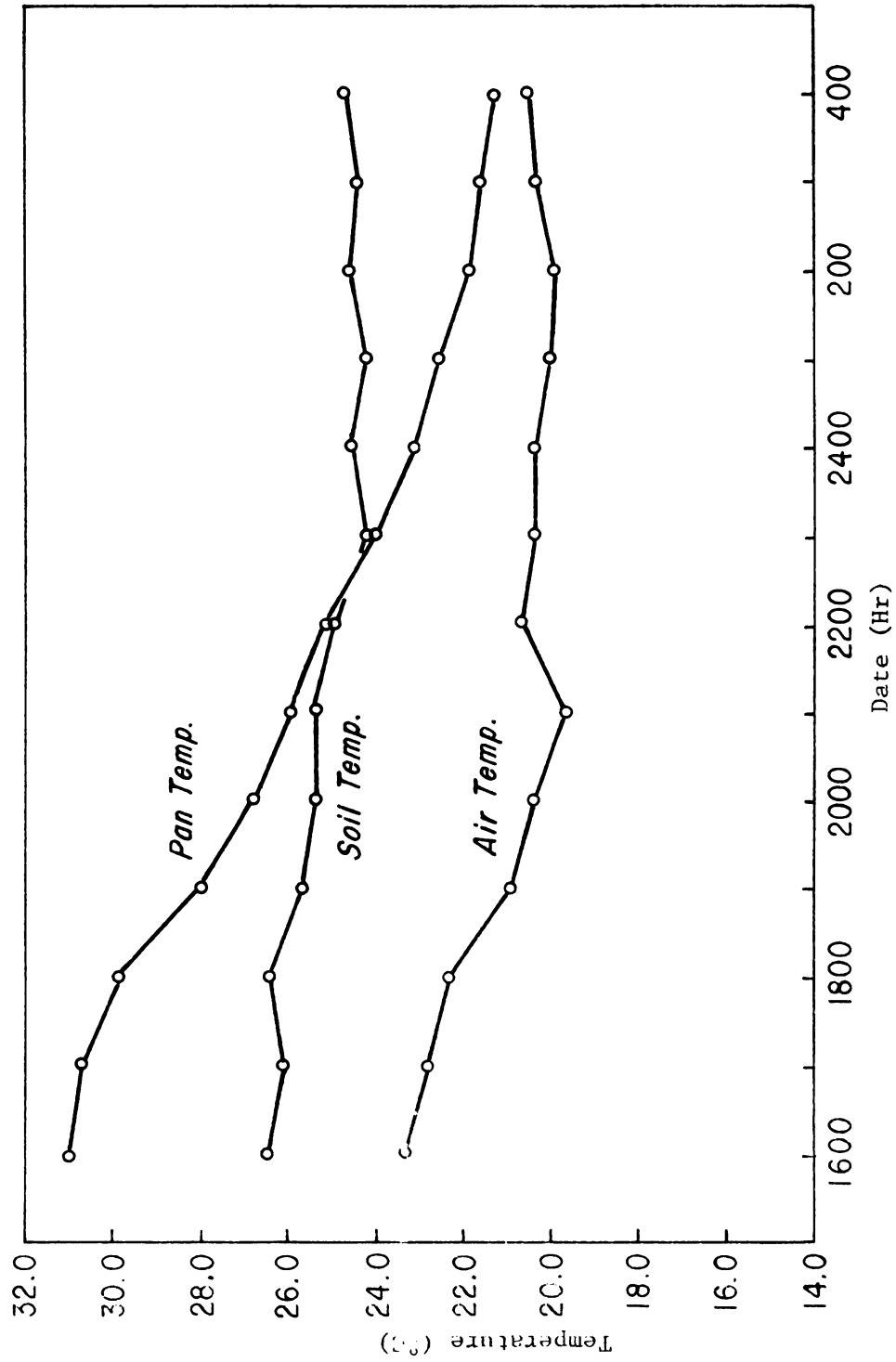


Figure 11. Air, soil and Class A pan temperature, averaged hourly, August 7, 1980. Air and soil temperature were measured at 50 cm above and 5 cm and 10 cm below a turfgrass cover, respectively.



Table 4. Simple correlation coefficients between cumulative pan evaporation, pan temperature and weather parameters for short duration measurements.

Cumulative Pan Evaporation	Number of Measurements	Time of Day	Correlation Coefficient (r)		
			$T_{\text{pan}}$	$(T_{\text{air}})_{50}$	(Humidity) <sub>50</sub> (Wind Speed) <sub>50</sub>
July 24	21	16:20-20:20	0.96**	+0.94**	-0.93** +0.57**
July 25	59	8:50-18:30	0.98**	+0.90**	-0.93** +0.66**
July 30	26	7:20-14:30	0.99**	+0.96**	-0.92** +0.92**
August 1	30	14:00-19:20	0.98**	+0.93**	-0.93** +0.63**
August 4	50	8:10-21:00	0.99**	+0.98**	-0.98** +0.86**
August 7	25	16:30-24:00	0.65**	-0.62**	-0.32 <sup>NS</sup> +0.59**

\*\* Significant at 1% level

NS Not significant

starting points of the curves at different hours of different days. They all show pan temperature increases more than air and soil temperature over the same period. This is related to the limited and discontinuous mass of water in the pan and the low reflection of solar radiation from the water surface (18). This increase in water temperature contributes to a greater loss of water from the pan and thereby causes an overestimation in pan evaporation as compared to potential evaporation from soil (41,100).

A comparison between profiles of air and soil temperature indicated that generally air temperature was lower than soil temperature during the course of this study, see Tables B-1 through B-7. This was caused by the replacement of normal, warm summer air as indicated by U.S. Weather Service data for the months of July and August, by a cool air front. For example, the cooler air temperature on July 24 was caused by lower than normal air temperature for that time of year. The data indicated an average July temperature of  $21.10^{\circ}\text{C}$  and the average temperature for July 24, 1980 was  $18.06^{\circ}\text{C}$ . The presence of a turfgrass cover acted as an insulating layer, which helped in maintaining the higher soil temperature (74,87).

The only non-significant correlation coefficient found between pan evaporation rate and relative humidity, measured at 50 cm above the ground surface, was for the data of August 7, 1980. These data were obtained during the night and early hours of the morning. Small quantities of water loss and mild changes in atmospheric humidity during these hours probably contributed to the weak correlation. The



rest of the coefficients indicate a very strong negative correlation between pan evaporation rates and relative humidity.

The coefficients between pan evaporation and wind-speed are also highly significant. However, the magnitude of these coefficients are smaller compared to the other positive relationships in the table. This is probably due to rapid changes in wind-speed during the day. If these changes had not been considered and accounted for, probably significant correlations would not have been obtained between pan evaporation and wind-speed (29). Such cases have been reported in the literature (39,42). In all of these reports, researchers were not able to establish any significant relationship between pan evaporation and wind-speed. This study indicates that the absence of such a relationship was caused by the use of a single daily averaged value for the wind-speed. Obviously, this cannot be the representative of the influence of wind-speed on pan evaporation over long periods.

In the process of relating pan evaporation ( $E_{pan}$ ) to reference evapotranspiration ( $ET_0$ ), the climate and environment of the pan should be considered. Such considerations are usually made by introducing a pan coefficient ( $K_p$ ). This coefficient is defined as the ratio of potential evapotranspiration ( $ET_p$ ) to pan evaporation ( $E_{pan}$ ). Unfortunately, it was not possible to establish a reliable pan coefficient for this study because of the uncertainties in the soil moisture data. However, values of this coefficient were obtained

Table 5. Pan coefficient ( $K_p$ ) for Class A Pan for different ground covers, relative humidity and wind speed (After Doorenbos and Pruitt, 1979).

Wind Speed (cm/sec)	Case A: Pan in short green cropped area				Case B: Pan in dry fallow area			
	Windward side distance of green crop (m)	Relative Humidity(%)			Windward side distance of dry fallow (m)	Relative Humidity(%)		
		Low <40	Medium 40-70	High >70		Low <40	Medium 40-70	High >70
Light <200	1	0.55	0.65	0.75	1	0.70	0.80	0.85
	10	0.65	0.75	0.85	10	0.60	0.70	0.80
	100	0.70	0.80	0.85	100	0.55	0.65	0.75
	1000	0.75	0.85	0.85	1000	0.50	0.60	0.70
Moderate 200-495	1	0.50	0.60	0.65	1	0.65	0.75	0.80
	10	0.60	0.70	0.75	10	0.55	0.65	0.70
	100	0.65	0.75	0.80	100	0.50	0.60	0.65
	1000	0.70	0.80	0.80	1000	0.45	0.55	0.60
Strong 495-815	1	0.45	0.50	0.60	1	0.60	0.65	0.70
	10	0.55	0.60	0.65	10	0.50	0.55	0.65
	100	0.60	0.65	0.70	100	0.45	0.50	0.60
	1000	0.65	0.70	0.75	1000	0.40	0.45	0.55
Very Strong >815	1	0.40	0.45	0.50	1	0.50	0.60	0.65
	10	0.45	0.55	0.60	10	0.45	0.50	0.55
	100	0.50	0.60	0.65	100	0.40	0.45	0.50
	1000	0.55	0.60	0.65	1000	0.35	0.40	0.45
Case A				Case B				
Dry Surface				wind				
50 m or more				Green Crop				
varies				Dry Surface				
varies				varies				



Table 6. Reference evapotranspiration ( $ET_0$ ), computed from cumulative pan evaporation ( $E_{pan}$ ) and pan coefficient ( $K_p$ ).

Date	Number of Measurements	Duration of Experiment (min)	Cumulative Pan Evaporation (mm)	Pan Coefficient	Cumulative Reference Evapotrans- piration (mm)
July 24	21	210	4.20	0.85	3.57
July 25	59	590	6.72	0.75	5.04
July 30	26	260	4.55	0.80	3.64
August 1	30	300	3.65	0.80	2.92
August 4	50	500	5.90	0.80	4.72
August 7	25	250	3.70	0.80	2.96





based on the wind-speed and relative humidity data and the recommended relations suggested by Doorenbos and Pruitt (81). These relations with minor modification in the unit of wind speed are given in Table 5. The measured pan losses and selected pan coefficients were multiplied to give computed reference evapotranspiration for different dates as shown in Table 6.

To obtain actual crop evapotranspiration, reference evapotranspiration values must be multiplied by a crop coefficient,  $K_c$ . This coefficient is dependent on the type of the crop and the stages of growth (19). Stages of growth is a primary variable that must be considered in computation of actual evapotranspiration. It is obvious that plants in rapid growth stages use water at a greater rate than early seedling stage. The relationship between crop coefficient and percent of growing season for three main crops under consideration in this study, namely corn, soybeans and turf-grass, are given in Figures 12, 13 and 14, respectively. These crop coefficients are presently recommended for the State of Michigan (96). The appropriate  $K_c$  values selected from Figures 11, 12 and 13 for the periods of interest give actual evapotranspiration when multiplied by the reference evapotranspiration. These are shown in Table 7. Generally, the variations in actual evapotranspiration throughout the growing season is greater for annual crops such as corn and soybeans than for perennial crops such as turfgrass (89,91).

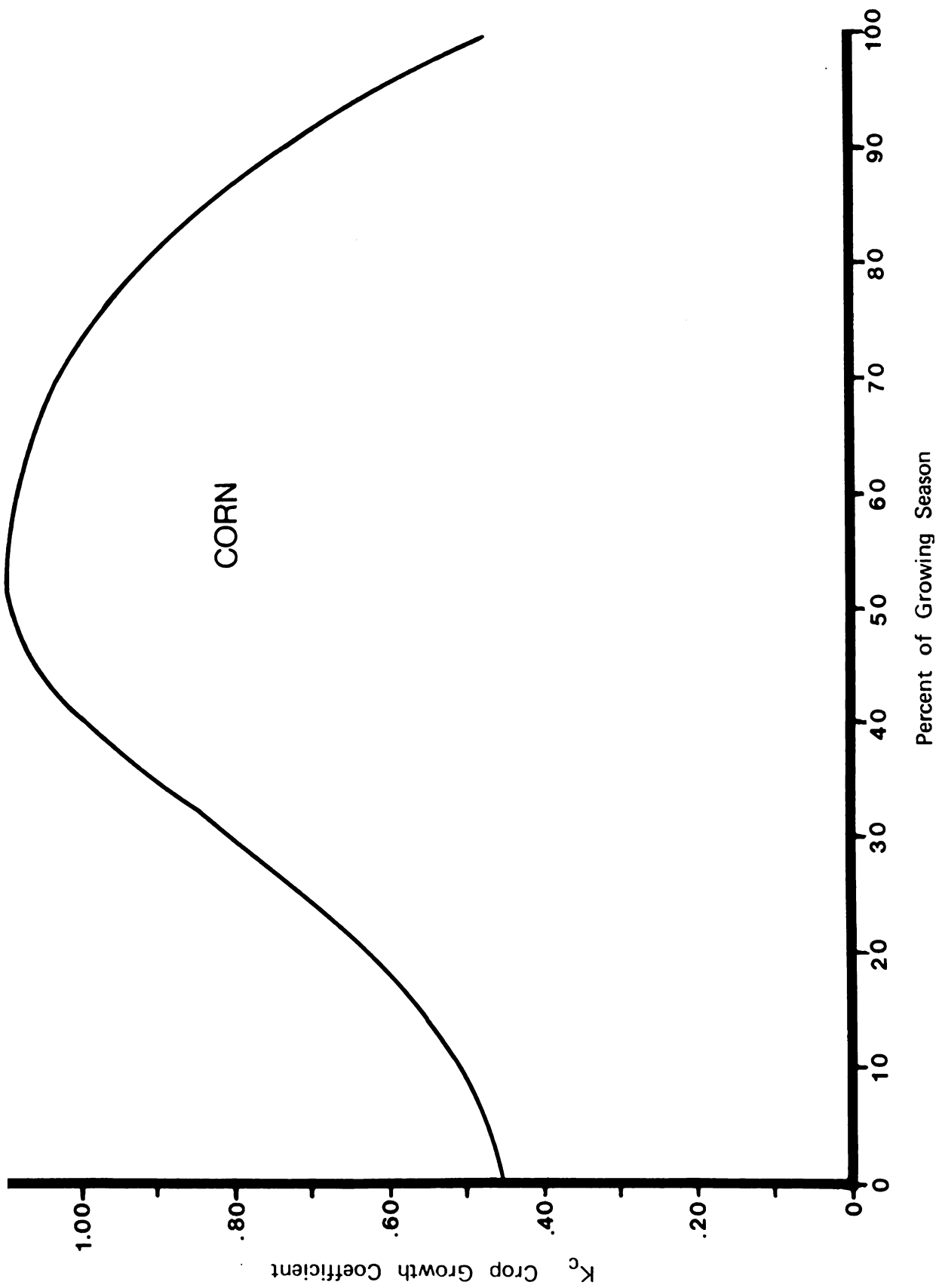


Figure 12. Crop coefficient as related to percent of growing season for Corn in Michigan (After Vitosh et. al. 1980).



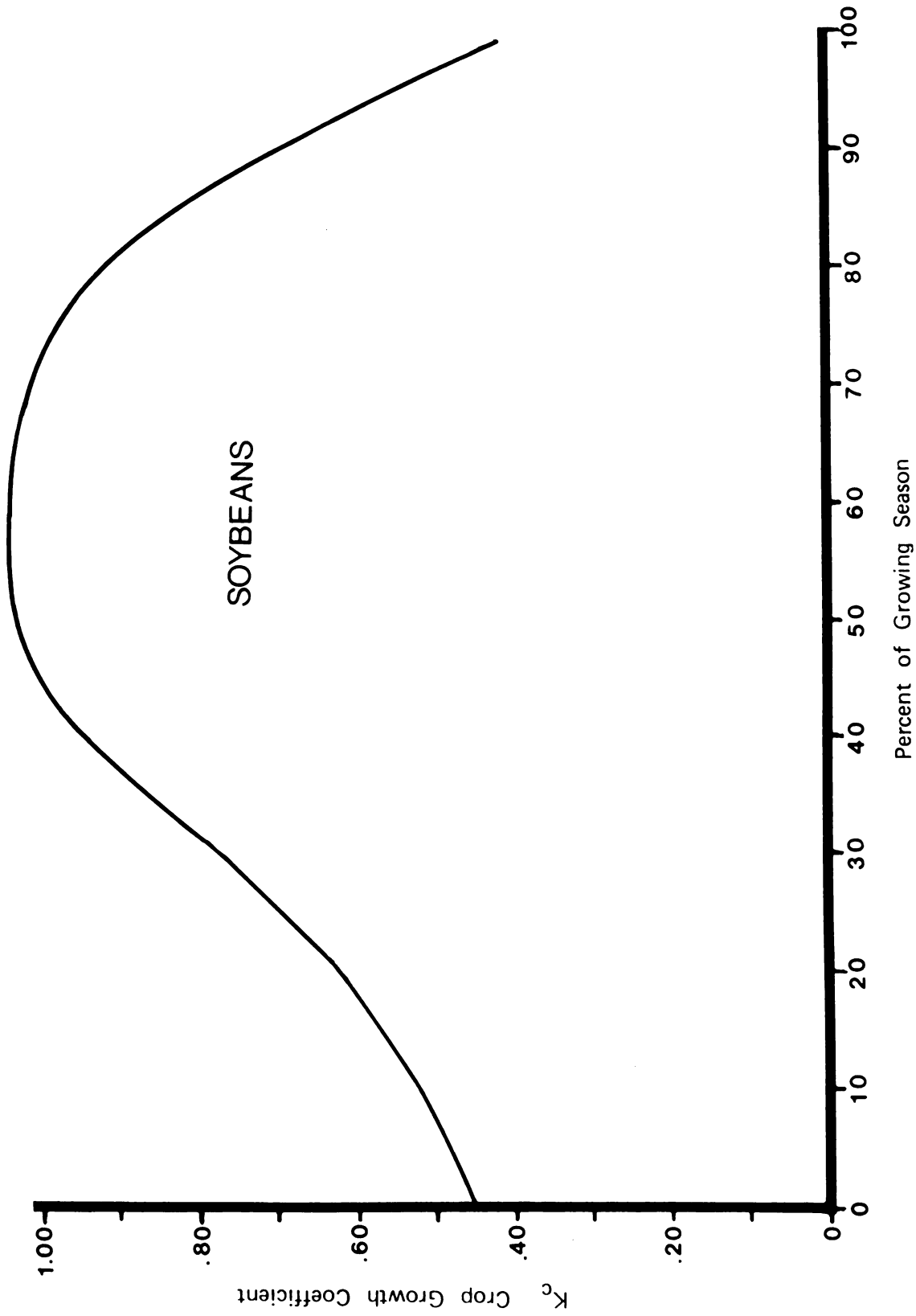


Figure 13. Crop coefficient as related to percent of growing season for Soybeans in Michigan (After Vitosh et. al. 1980).

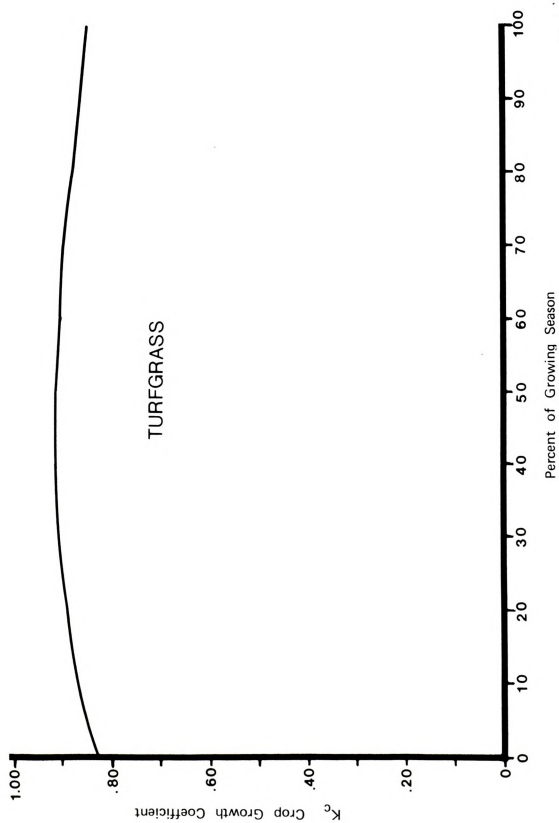


Figure 14. Crop coefficient as related to percent of growing season for Turfgrass in Michigan (After Vitosh et. al. 1980).

Table 7. Cumulative actual evapotranspiration (ET) for corn, soybean and turfgrass computed from reference evapotranspiration (ET<sub>o</sub>) and crop coefficient (KC).

Date	Cumulative Reference Evapotranspiration (mm)	Crop Coefficient (KC)			Actual Evapotranspiration (mm)		
		Corn	Soybean	Turfgrass	Corn	Soybean	Turfgrass
July 24	3.57	1.09	1.03	0.90	3.89	3.68	3.21
July 25	5.04	1.09	1.03	0.90	5.49	5.19	4.54
July 30	3.64	1.08	1.01	0.89	3.93	3.68	3.24
August 1	2.92	1.08	1.01	0.89	3.15	2.95	2.60
August 4	4.72	1.06	1.00	0.88	5.00	4.72	4.15
August 7	2.96	1.05	0.99	0.88	3.11	2.93	2.60

### III. Evaporation Estimated by Aerodynamic Models

The data reported herein were collected during the months of July and August, 1980. Data collection was conducted for seven days and was limited to days and times when the sky was clear and cloudless and wind movement was mostly out of the south to southwest. Because of the large volume of the data collected, only three days of data were selected for presentation in this section. Originally, measurements were taken and recorded every two minutes, but during smoothing and processing they were combined and averaged to represent ten minute periods (see Tables B-1 to B-7 in Appendix B).

The air temperature profiles, representative of three-hour intervals on July 25, August 4 and 7, are presented in Figures 15, 16 and 17, respectively. These figures show the variation of each profile with elevation from the ground surface and also the change in slope of the profiles with time for a given date. Generally, all three figures indicate at one time or another the presence of an unstable atmospheric condition ( $\partial T / \partial Z$  negative) particularly late at night and very early in the morning. This changes gradually to a more stable condition ( $\partial T / \partial Z$  positive) with an increase in air temperature. The absence of stable temperature profiles (i.e. inversion), in Figure 17 for 2400 and 200 hr, was due to high soil temperatures. This resulted in a reversal of

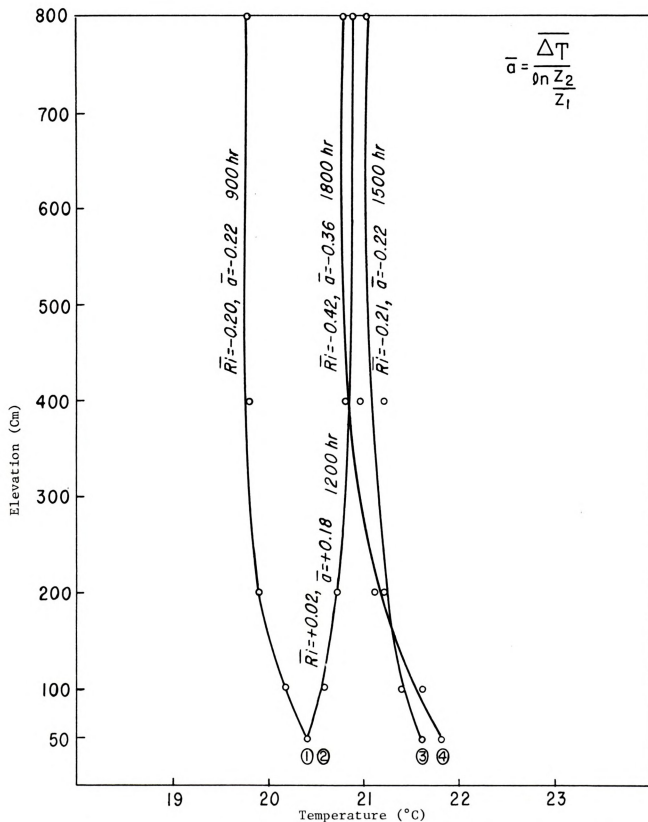


Figure 15. Air temperature profiles at different hours above a short turfgrass cover, July 25, 1980. Richardson numbers and  $\bar{a}$ 's are the average values for the entire profile.



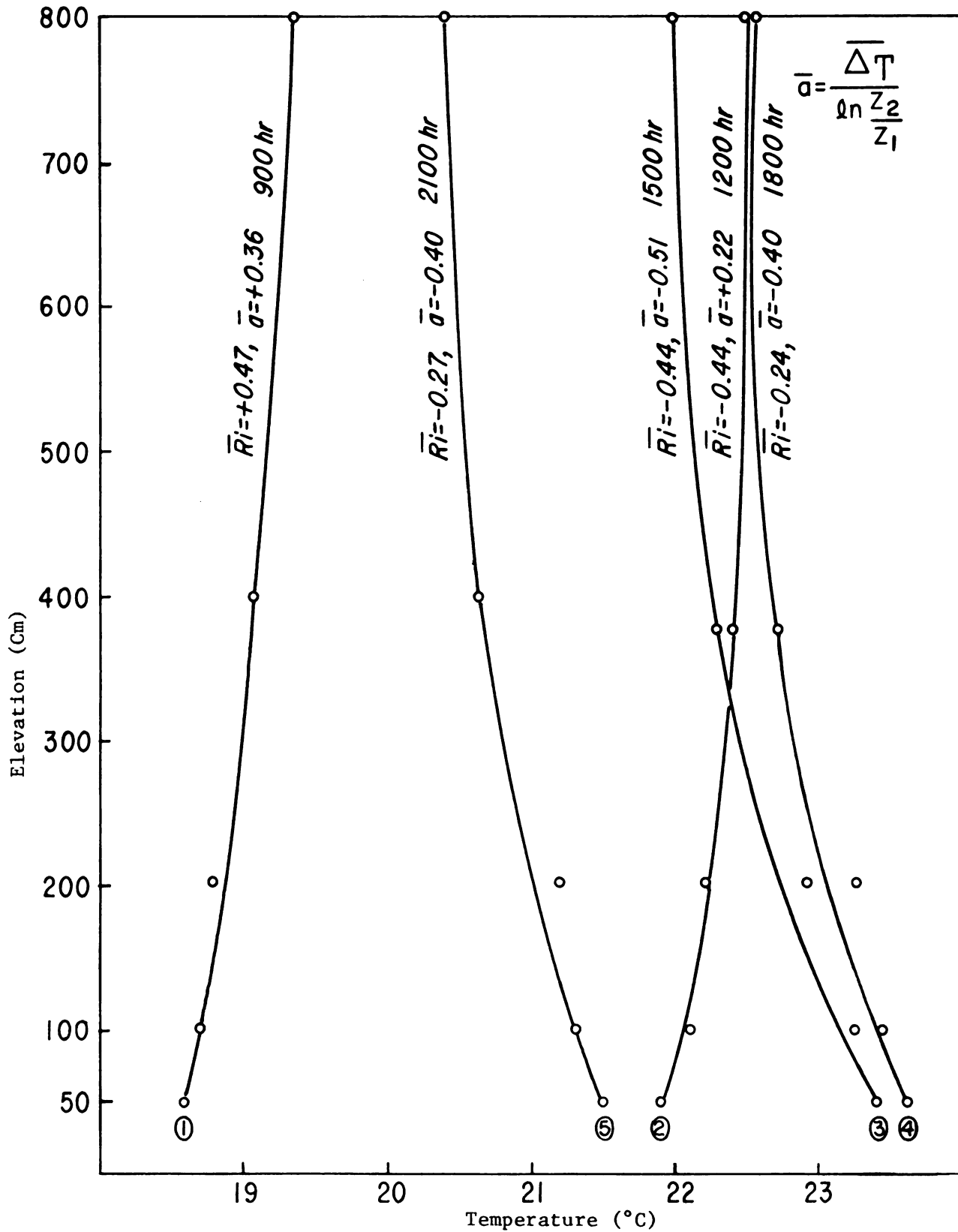


Figure 16. Air temperature profiles at different hours above a short turfgrass cover, August 4, 1980. Richardson numbers and  $\bar{a}$ 's are the average values for the entire profile.



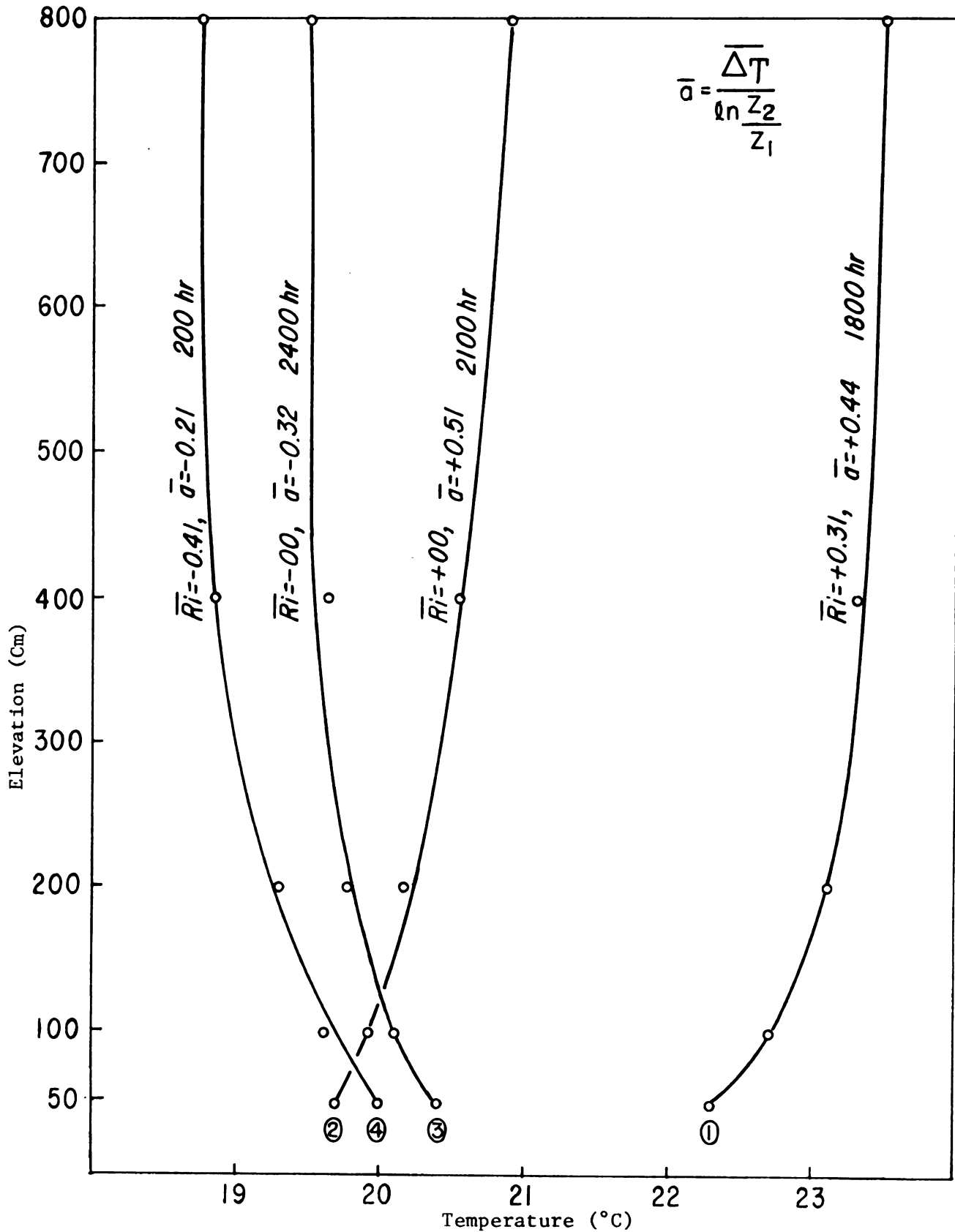


Figure 17. Air temperature profiles at different hours above a short turfgrass cover, August 7, 1980. Richardson numbers and  $\bar{a}$ 's are the average values for the entire profile.

the heat gradient causing heat to flow from the soil to the air layer above it, see Figure 11. This phenomenon was further intensified by exceptionally high wind speeds recorded during these specific hours, see Figure 20.

The changes in temperature gradient provide a thermal stratification in the atmosphere. The buoyancy caused by this gradient induces thermal turbulence and plays an important role in the mixing and transport of water vapor (58,59, 74). To include this phenomena in our theoretical development, we introduced the variable  $\bar{a}$  in the definition of stability parameter,  $S$  (see Equations [24] and [28]). The sign and magnitude of  $\bar{a}$  determine the role of the temperature gradient on the atmospheric stability and the extent of its departure from neutrality. The computed values of  $\bar{a}$  and Richardson number for temperature profiles are presented in Figures 15, 16 and 17. A comparison between these two parameters helps to understand the role of each in predicting the condition of the atmosphere. The parameter  $\bar{a}$  illustrates the influence of changes in air temperature on atmospheric stability. Richardson number is indicative of the combined influence of air temperature and wind speed on the stability of atmosphere.

The profiles of wind speed for July 25, August 4 and 7 are presented in Figures 18, 19 and 20, respectively. These figures show the formation of mechanically induced turbulent boundary layers (profiles) above the ground surface and also their changes with time for a given date. All three figures

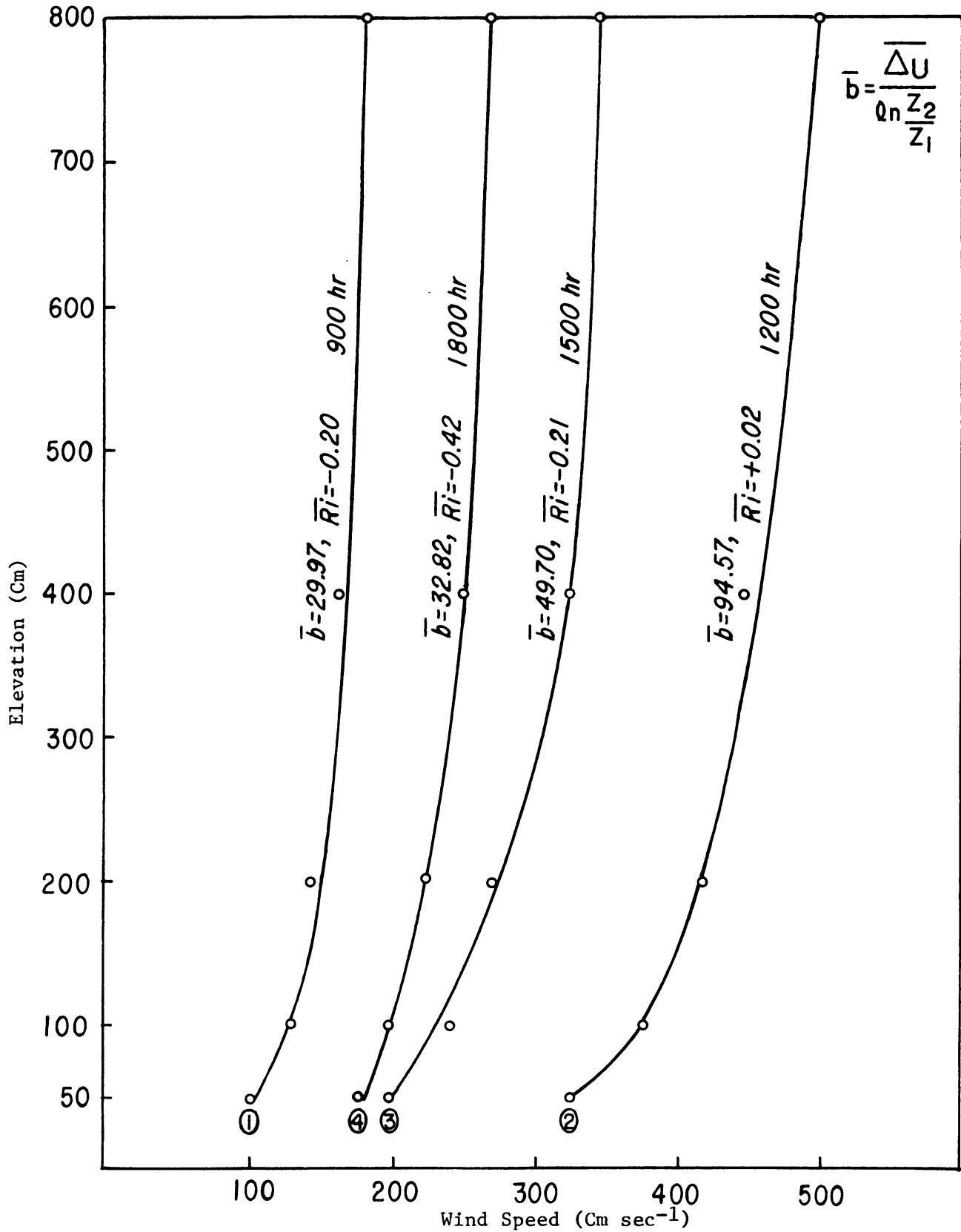


Figure 18. Wind speed profiles at different hours above a short turfgrass cover, July 25, 1980. Richardson numbers and  $\bar{b}$ 's are the average values for the entire profile.

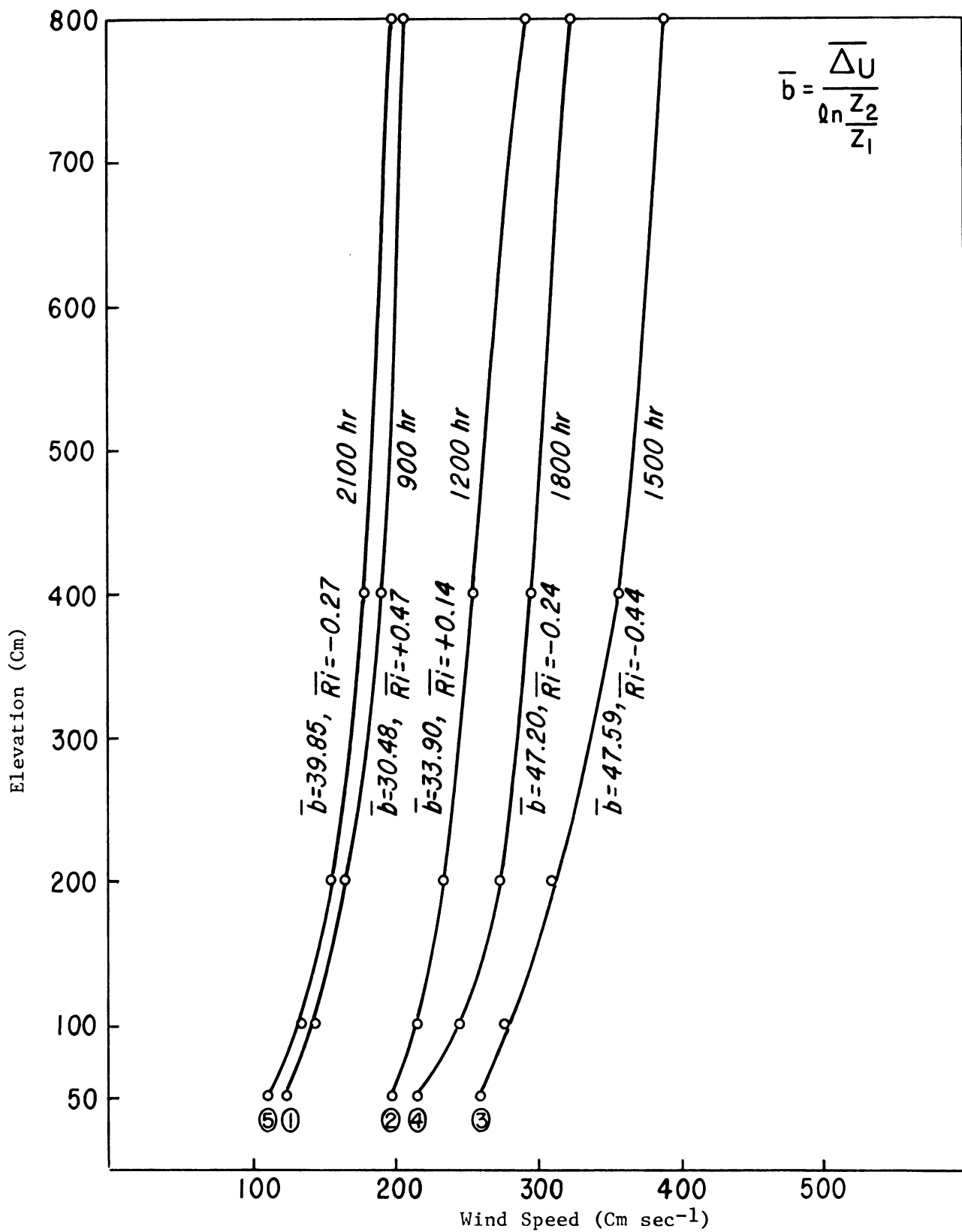


Figure 19. Wind speed profiles at different hours above a short turfgrass cover, August 4, 1980. Richardson numbers and  $\bar{b}$ 's are the average values for the entire profile.

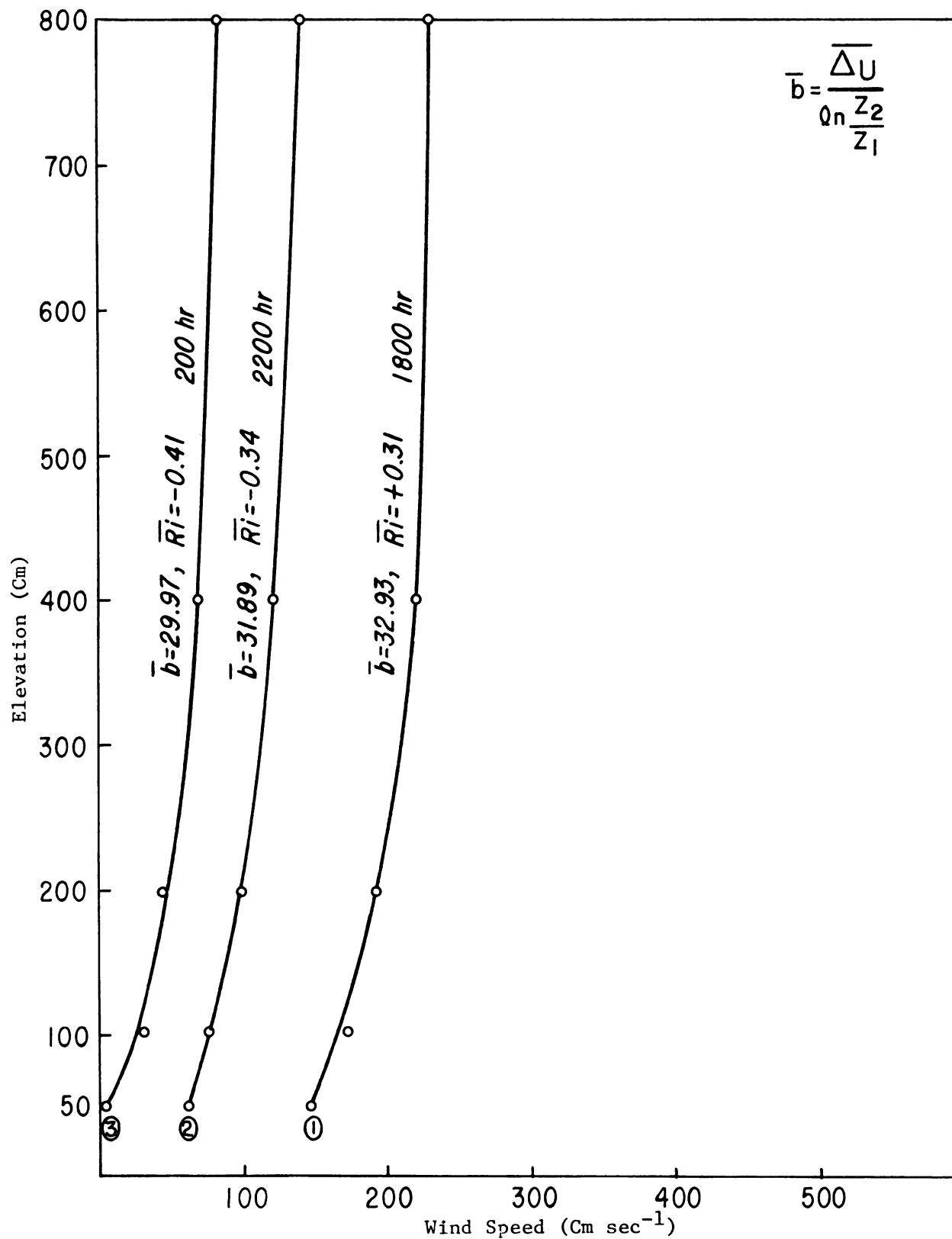


Figure 20. Wind speed profiles at different hours above a short turfgrass cover, August 7, 1980. Richardson numbers and  $\overline{b}$ 's are the average values for the entire profile.





indicate that the thickness of the boundary layers gradually increases, starting early in the morning until mid-day and then decreasing in the latter hours of the day. To include these changes in our theoretical developments, we introduced a variable,  $\bar{b}$ , into the definition of stability parameter  $S$  (see Equations [25] and [28]). The parameter  $\bar{b}$  does not have any influence on the sign of  $S$ . This is due to positive wind speed gradient above the ground surface at all times and also the squaring of  $\bar{b}$  in Equation [28]. However,  $\bar{b}$  strongly affects the magnitude of  $S$ . The computed  $\bar{b}$  values and Richardson numbers are shown in Figures 18, 19 and 20. As indicated by Equation [31], the parameter  $\bar{b}$  only illustrates the influence of mechanical forces of wind on the formation of a turbulent boundary layer and its stability under certain atmospheric condition. But, Richardson number represents the combined influence of mechanical forces of wind speed plus the buoyancy effects due to thermal gradient on atmospheric conditions. However, the changes in both of these parameters also represents the variation of the turbulent boundary layer (wind speed profiles). Under extremes of atmospheric conditions (i.e. very stable and/or very unstable), the logarithmic law applied to wind speed profiles needs to be modified to include the effects of air temperature (47,99).

A graphical procedure was used to obtain aerodynamic parameters such as displacement height( $d$ ), roughness coefficient( $Z_0$ ), frictional velocity( $U_*$ ) and shear stress( $\tau$ ) from the wind speed profiles (61,74). The results are given in

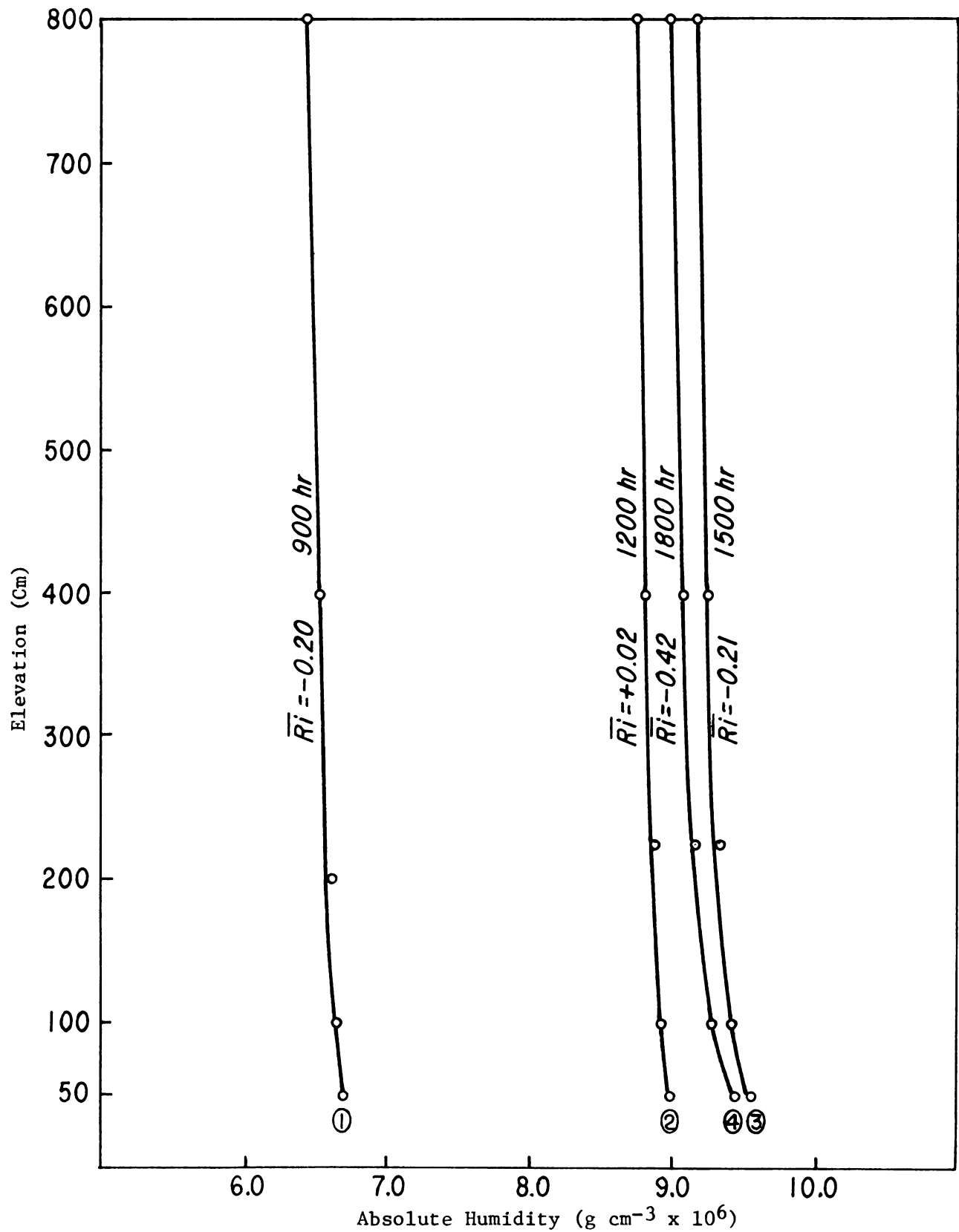


Figure 21. Absolute humidity profiles at different hours above a short turfgrass cover, July 25, 1980. Richardson numbers are the average values for the entire profile.



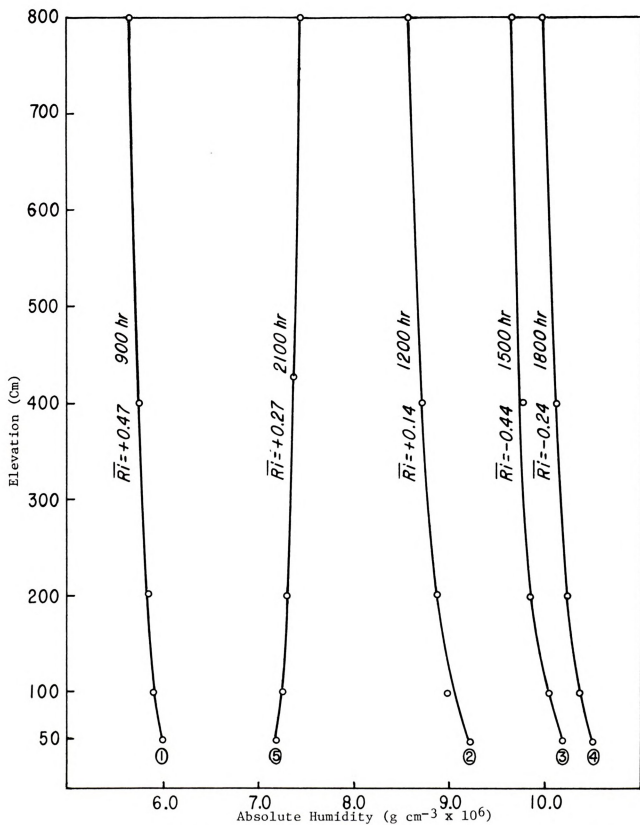


Figure 22. Absolute humidity profiles at different hours above a short turfgrass cover, August 4, 1980. Richardson numbers are the average values for the entire profile.



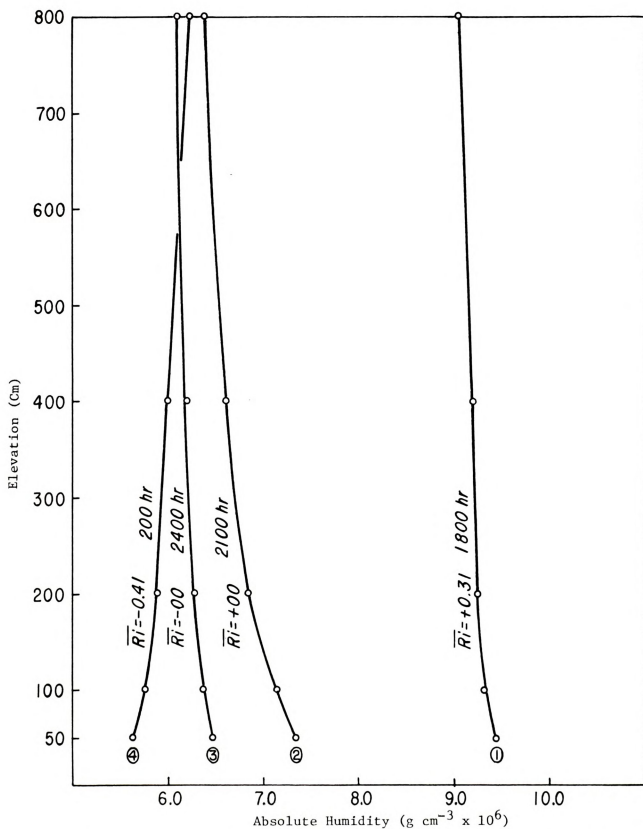


Figure 23. Absolute humidity profiles at different hours above a short turfgrass cover, August 7, 1980. Richardson numbers are the average values for the entire profile.

Table 8. According to these data, the magnitude of aerodynamic roughness coefficients and displacement height values were not large enough to significantly influence  $K_m$ , the coefficient of turbulent exchange, see Equations [6] and [9]. From Equation [17] the corresponding influence of  $K_m$  on  $E$ , the rate of water vapor transport, is readily apparent. The data obtained for these parameters fall within the range of values previously reported for short, green grass crops (76,80,81).

Profiles of absolute humidity for July 25, August 4 and 7 are presented in Figures 21, 22 and 23, respectively. The profiles in all three figures show a gradual decrease in humidity with elevation from the ground surface in a given day. However, this relation is reversed for late evening and early morning hours. For profiles with Richardson numbers of less than  $-0.1$  (very unstable atmosphere), the ratio of heat to water vapor diffusivity coefficients ( $K_h/K_w$ ) will depart smoothly from unity and become greater than one (12,49). This ratio also departs from unity for the Richardson numbers greater than  $+0.1$  (very stable atmosphere) and becomes less than one (98). The Richardson numbers at 2100 and 2400 hours on August 7 reach their absolute maximum and minimum values, respectively. In these cases the turbulence has vanished and the main mechanism for water vapor transport is probably molecular diffusion (59). This is supported by the fact that no air motion was detected at these hours (see Figure 20).

Table 8. Displacement height, roughness parameter, frictional velocity and shear stress determined from wind speed profiles.

Date	Number of Measurements	Displacement Height (cm)	Roughness Coefficient (cm)	Friction Velocity- $l$ (cm sec $^{-1}$ )	Shear Stress (dynes cm $^{-2}$ )
July 25	10	0.00	0.477	1.845	0.0041
August 4	12	0.00	0.539	1.833	0.0040
August 7	10	0.00	0.317	3.951	0.0024
Mean		0.00	0.444	2.543	0.0035





Previous discussion of temperature, wind speed and humidity profiles support the idea that equations of heat, momentum and water vapor transport should be modified such that they are representative of these phenomena under a wide range of atmospheric conditions (12,23,40,50). This suggestion prompted the derivation of a new equation describing the transport of water vapor in this study. The equation is an extension of an evaporation equation of Thornthwaite and Holzman (88). Their equation was modified for all conditions of atmospheric stability by introducing the stability parameter  $S$ , Equation [28]. This introduces a correction factor to the original equation of Thornthwaite-Holzman for the cases of unstable and stable atmospheric conditions as given in Equations [33] and [34]. Temperature, wind speed and humidity data of Appendix B were used to investigate the feasibility of  $S$  as a function of Richardson number. The results are shown in Figure 24. The linear, functional relationship between these two parameters show that  $S$  like the Richardson number can account for all the possible changes in temperature and wind speed profiles under a wide range of atmospheric conditions. It was not possible to use and manipulate the Richardson number in its defined form, Equation [10], as a stability criterion in the proposed analytical development. This difficulty was resolved by the use of the stability parameter  $S$ .

Table 9 shows a comparison between the evaporation rates measured by the automated Class A pan, the computed rates

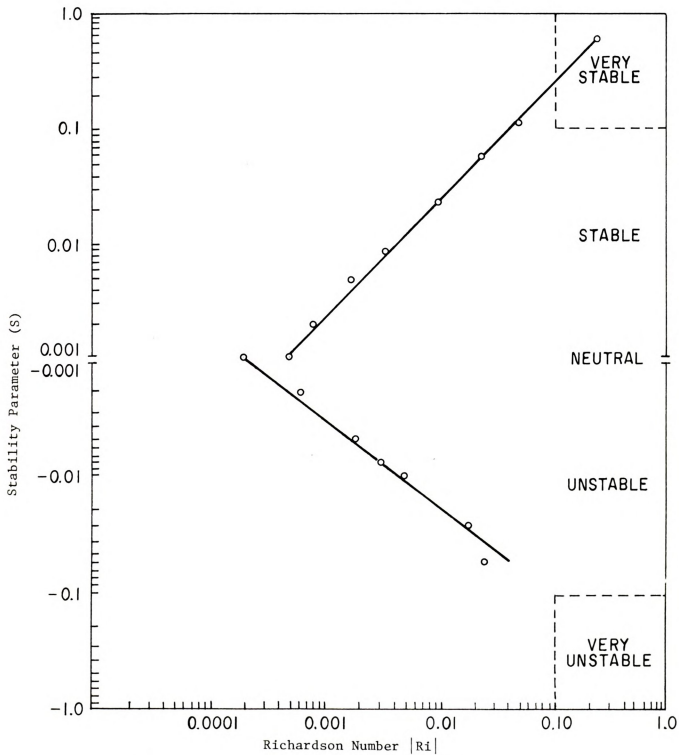


Figure 24. Functional relationship of stability parameter  $S$ , and Richardson number  $Ri$ , under different atmospheric conditions.

Table 9. Evaporation rates measured with an automated Class A pan and computed according to the Thornthwaite-Holzman and a modified Thornthwaite-Holzman from atmospheric profile data over short periods.

Date	Number of Measurements	Mean evaporation rate (mm/10 min)			
		Pan	Thornthwaite-Holzman <sup>†</sup>	Modified Thornthwaite-Holzman <sup>†</sup>	Error <sup>††</sup>
July 24	21	0.232	0.1000	-0.5690	0.0826
July 25	59	0.114	0.0669	-0.4132	0.0764
July 30	26	0.175	0.0299	-0.8291	0.0315
August 1	30	0.122	0.1181	-0.0320	0.1094
August 4	50	0.118	0.0843	-0.2865	0.0987
August 7	25	0.148	0.0587	-0.6034	0.0600
					-0.6440
					-0.3298
					-0.8200
					-0.1033
					-0.1636
					-0.5946

<sup>†</sup> Values obtained from profile data between levels of 50 cm and 100 cm

<sup>††</sup> Fractional values of error are computed according to Error =  $\frac{E_{\text{pan}} - E_{\text{aero}}}{E_{\text{pan}}}$

obtained from the original equation of Thornthwaite-Holzman, Equation [35], hereon referred to as TH, and the modified version, Equation [31], hereon referred to as MTH. The computed evaporation rates from both the TH and MTH equations are smaller than the measured pan evaporation rates. However, in general the MTH equation estimates pan losses better than the TH equation, see Table 9. The MTH equation approximates pan evaporation best under unstable atmospheric conditions when  $S$  and Richardson number are negative. Under these conditions the accuracy of approximation increases as the magnitude of  $S$  or  $Ri$  increases. The computed evaporation rate for July 25 is representative of this case. Detailed analysis of the profile data indicate that unstable atmospheric conditions prevailed most of the time during this date (see  $Ri$  values in Table B-2).

Under stable conditions, the MTH equation approximates pan evaporation best when  $S$  and Richardson number are positive in sign and small in magnitude; however, the degree of improvement in approximating pan evaporation under these conditions is not as good as under unstable atmospheric conditions. This may be observed by referring to computed evaporation rates for July 24 and 30, in Table 9. Detailed analysis of the profile data indicate that stable atmospheric conditions prevailed most of the time on these dates (see  $Ri$  values in Tables B-1 and B-3). Sample calculations for both stable and unstable atmospheric conditions are presented in Appendix D.

When a combination of both stable and unstable atmospheric conditions prevailed, the degree of improvement in

approximating pan evaporation based on MTH equation was about 7 to 12 percent better than the original TH equation. The data for August 1 and 4 indicate that both stable and unstable conditions prevailed on these dates (see  $R_i$  values in Tables B-4 and B-5). This improvement in calculating the pan evaporation from meteorological profile data is a definite advantage for the equation proposed in this study.

To illustrate the accuracy of the proposed model in estimating evapotranspiration rates, there was a need for measuring soil water losses over short periods. Generally, weighing lysimeters are used for this purpose. Since such a device was not available in the vicinity of the experimental site, the data of Morgan et. al. (52) were selected and used for analysis. Six days of data were selected randomly. These data included evapotranspiration rates measured by a 6.1-meter lysimeter, air temperature, wind speed and absolute humidity profiles recorded over 30 minute periods in 1966 at the University of California, Davis. Table 10 presents the evapotranspiration rates recorded by the lysimeter and rates computed according to the TH and MTH equations. The meteorological profile data selected for this analyses were obtained between 700 and 1900 hr at the 25 and 50 cm levels above a short grass cover.

Generally, both TH and MTH underestimated the evapotranspiration losses from the lysimeter when unstable atmospheric conditions prevailed. The error of estimate by MTH was about 4 to 17 percent smaller than TH for days with

Table 10. Evapotranspiration rates measured with lysimeter (after Morgan et. al.) and computed according to the Thornthwaite-Holzman and modified Thornthwaite-Holzman equations from atmospheric profile data.

Date	Number of Measurements	Mean evaporation rate (mm/60 min)			
		Lysimeter	Thornthwaite-Holzman <sup>†</sup>	Error <sup>††</sup>	Modified Thornthwaite-Holzman Error <sup>††</sup>
May 5	24	0.2213	0.1908	-0.1378	0.1988 -0.1016
June 2	24	0.4432	0.2088	-0.5289	0.2849 -0.3572
June 3	24	0.4698	0.2781	-0.4080	0.3234 -0.3161
July 13	24	0.4609	0.2829	-0.3862	0.3395 -0.2634
July 14	24	0.4792	0.2732	-0.4299	0.3539 -0.2641
September 29	24	0.3321	0.3953	+0.1903	0.3935 +0.1848

<sup>†</sup> Values obtained from profile data between the levels of 25 and 50 cm

<sup>††</sup> Fractional values of error are computed according to  $\text{Error} = \frac{\text{Elysim} - \text{Eaero}}{\text{Elysim}}$

unstable atmospheric conditions. The one exception, September 29 was for stable atmospheric conditions. For the profile data of September 29 both TH and MTH equations overestimated evapotranspiration losses recorded by the lysimeter.

The results of estimating evapotranspiration from a lysimeter and evaporation from a Class A pan using the MTH equation illustrate the degree of effectiveness of the S parameter and its related functions  $f(S)$  in adjusting for the influence of the changing atmospheric conditions in transport of water vapor. Based on these results it was found that the proposed MTH equation performed better in estimating water losses from a lysimeter than a Class A pan. This was probably due to less variation in meteorological conditions at Davis as compared to the conditions found in Michigan. However, in both cases the MTH equation performed the best under unstable atmospheric conditions.



## CONCLUSIONS

The following conclusions have been drawn from this investigation:

- (1) Under optimum soil moisture conditions evapotranspiration reaches its potential rate. As such, it is controlled primarily by weather parameters.
- (2) Cumulative pan evaporation measured over short periods increased linearly with time during each measurement period but changed significantly from one day to the next during the period of study.
- (3) Cumulative pan evaporation measured over short periods correlates best with pan temperature followed by air temperature and wind speed.
- (4) Simple correlation coefficient between cumulative pan evaporation and atmospheric humidity indicated a very significant negative correlation between these two parameters.
- (5) Detailed analysis of air temperature, wind speed and absolute humidity profiles obtained over short periods, indicated a need for the modification of heat, momentum and water vapor transfer equations to better represent these processes under a wide range of atmospheric conditions.

- (6) A proposed stability parameter  $S$  proved to be more effective than Richardson number in taking into account all possible changes in atmospheric conditions, but unlike Richardson number  $S$  is very easy to use in the analytical development of the proposed evaporation model.
- (7) The modified version of the Thornthwaite-Holzman equation proposed in this study proved to be more effective than the original form in estimating evapotranspiration rates from a lysimeter and evaporation rates from a Class A pan over short periods.
- (8) The proposed model developed in this study will work for all conditions of atmospheric stability, but it approximates evapotranspiration from lysimeter and pan evaporation best under unstable atmospheric conditions.

## APPENDICES

## APPENDIX A

FORTRAN IV PROGRAM FOR DATA PROCESSING AND DATA CONVERSION

The following FORTRAN IV program was used to read the analog, digitized data from paper tapes and convert it to digital forms with appropriate engineering units by means of specified calibration curves and/or functional relationships. The program consisted of the main program GAWTHR; subroutines PAUXCYBER, GETDAT and SMOOTH; and function FNR.

The main program in addition to converting the analog data into useful digital numbers also computed certain parameters such as water vapor flux, Richardson numbers and stability functions based on the atmospheric profile data.

Subroutine PAUXCYBER was written by Mr. Lloyd Lerew of the Department of Agricultural Engineering at Michigan State University (46). This subroutine was called in the main program to compute the moisture concentration in the air from dry and wet-bulb temperatures.

Subroutine GETDAT read the converted digitized data into common blocks. This subroutine also checked for bad or missing data points during processing.

Subroutine SMOOTH used a binomial distribution procedure (2), to smooth the data over  $\underline{n}$  data points. The magnitude of  $\underline{n}$  could vary between 3 to 9.

Function FNR converted the wet and dry bulb air temperatures from degrees Centigrade to degrees Fahrenheit for use in subroutine PAUXCYBER.

```

      PROGRAM GAWTHR(OUTPUT,TAPE2=/182,REPORT,TAPE6=REPORT,TAPE1,
      *REPT2,TAPE7=REPT2)
C ANDERS G JOHANSON AUGUST 1980
C FOR C1050 GHASEM ASRAR
C TO READ ANALOG DIGITIZED TAPE OUTPUT(INPUT TO THIS PROGRAM)
C AND PRODUCE CUSTOM REPORT AND POSSIBLY CONVERTED DATA FILE OUTPUT
C
      COMMON /PRESS/ PATH
      COMMON /PRESET/ XMD,STAR
      COMMON /THEDATA/ JDATE(2),JTIME(2),CHNL(100),IEOF
      COMMON /RESULTS/NWIND,TEMP(10),HUM(5),WINDV(5),EVAPF,SOILT(5),PANT
      DIMENSION IWINDV(5),ITEMP(10)
      * ,HGT(5),RN(5),EAERO(4),PSOILT(5)
      DIMENSION PTEMP(10),PWINDV(5)
      DIMENSION IERRX(6)
      REAL KA
      DATA IERRX/0,-0,-0,0,-0,-0/
      DATA ITEMP /5,6,7,8,9,12,13,14,25,26/, NTEMP/10/
      DATA IWINDV /100,1,2,3,20/, NWINDV /5/
      DATA IEOF /0/,WINDV/5*999.9/,SOILT/5*99.99/,PSOILT/5*99.99/
      DATA NLINES /90/,HUM/5*999.9/,TEMP/10*999.9/
      DATA HGT /50.,100.,200.,400.,900./
      DATA XMD/0.9999/, STAR/8.8868/,ISMMOOTH/1H /
      DATA PANT,3V/5*999.9/,PTEMP/10*999.9/,PANT/99.99/
      DATA PPANT/99.99/,EVAPF/999.9/,PEVAPF/999.9/
C JDATE(1) = MONTH, (2) = DAY
C JTIME (1) = HOUR, (2) = MINUTE
C CHNL (1) CONTAINS VALUE FOR CHANNEL 1, I=1,99 I=0 AS 100
C IEOF = 1 WHEN END-FILE READ TIL THEN ZERO
C
C INITIALIZE
C
      CALL SYSTEMC(78,IERRX)
C NVALS = NUMBER OF POINTS TO USE IN SMOOTHING
      NVALS= 5
      PATH = 14.696
C MUST IGNORE *****
      WHAT = 1.0
C *** FOR SPECIAL 10MIN AVG DATA FILE
      IEOF = 1
      NVALS = 10
      ISMOOTH = 2HND
      GO TO 890
C
100 CALL GETDAT
   IF (IEOF.EQ.1) GO TO 900
C PROCESS WIND VELOCITY
   DO 250 I = 1,NWINDV
     J = IWINDV (I)
     IF (CHNL(J).LT.0) GO TO 230
     IF (CHNL(J).GT.50) GO TO 220
     VALUE = (CHNL(J) - (0.01 * CHNL(J) - 2.27)) * 19.51 - 42.26
     GO TO 240
C > 50
220 VALUE = PWINDV (I)
     GO TO 240
C < 0
230 VALUE = 0
240 WINDV (I) = VALUE
250 CONTINUE
C EVAPORATION

```

```

C CHANNEL 11
  EVAPO = ABS((CHNL(11) - (0.01 * CHNL(11) - 2.27))) * 0.35 - 0.08
  EVAPF = PEVAPF - EVAPO
C WIND DIRECTION CHANNEL 10
  CHNL(10) = CHNL(10) * 100.
  IVALUE = 2HN
  IF (CHNL(10).LT.22.5 .AND. CHNL(10).GT.-22.5) GO TO 300
  IVALUE = 2HNW
  IF (CHNL(10).LT.67.5 .AND. CHNL(10).GE.+22.5) GO TO 300
  IVALUE = 2HW
  IF (CHNL(10).LT.102.5 .AND. CHNL(10).GE.+67.5) GO TO 300
  IVALUE = 2HSW
  IF (CHNL(10).LT.157.5 .AND. CHNL(10).GE.+102.5) GO TO 300
  IVALUE = 2HS
  IF (CHNL(10).GE.157.5 .OR. CHNL(10).LT.-157.5) GO TO 300
  IVALUE = 2HNE
  IF (CHNL(10).LE.-22.5 .AND. CHNL(10).GT.-67.5) GO TO 300
  IVALUE = 2HE
  IF (CHNL(10).LE.-67.5 .AND. CHNL(10).GT.-102.5) GO TO 300
  IVALUE = 2HSE
300 NWIND = IVALUE
C TEMPERATURE
  DO 350 I = 1,NTEMP
    J = ITMP(I)
    IF (CHNL(J).LT.0) GO TO 330
    IF (CHNL(J).EQ.STAR) GO TO 330
    IF (ABS(CHNL(J)).GE.2.99) GO TO 330
    VALUE = -0.0951 * 26.0544 * CHNL(J) - 0.6801 * (CHNL(J)*CHNL(J))
    GO TO 340
330 VALUE = TEMPI(I)
340 TEMP(I) = VALUE
350 CONTINUE
C HUMIDITY
  N = NTEMP / 2
  DO 450 I = 1,N
    J = 2 * I - 1
    DB = FNR(TEMP(J))
    WB = FNR(TEMP(J+1))
    PV = PVDBWB(DB,WB)
    HUM(I) = (HAPV(PV) * 0.001137) * 1000000.
    IF (LEGVAR(HUM(I)).NE.0) HUM(I) = 0.0
450 CONTINUE
C SOIL TEMP - CHANNELS 45 - 49
  DO 500 I=1,5
    J=I + 44
    IF(CHNL(J).LT.0)GO TO 480
    IF(CHNL(J).EQ.STAR)GO TO 480
    IF(ABS(CHNL(J)).GE.2.99)GO TO 480
    VALUE = -0.0951 * 26.0544 * CHNL(J) - 0.6801 * (CHNL(J)*CHNL(J))
    GO TO 490
480 VALUE = PSOILT(I)
490 SOILT(I) = VALUE
500 CONTINUE
C PAN TEMP CHANNEL 52
  IF(CHNL(52).LT.0)GO TO 510
  IF(CHNL(52).EQ.STAR)GO TO 510
  IF(ABS(CHNL(52)).GE.2.99)GO TO 510
  VALUE = -0.0951 * 26.0544 * CHNL(52) - 0.6801 *
    + (CHNL(52)*CHNL(52))
  GO TO 520
510 VALUE = PSOPAN

```

```

520  PANT = VALUE
C
C ABOVE READS RAW DATA
C
525  CONTINUE
C
C ENTER HERE WHEN READING& PROCESSING SMOOTHED DATA
C AS FOLLOWING PERFORMS ALL CALCULATIONS AND PRINTS RESULTS
C
C RICHARDSON NUMBER
      KI = 1
      DO 550 I = 1,4
C 546  BELOW FOR ABS TEMP
      X1 = 1960. / ((TEMP(KI)+TEMP(KI+2)) + 546.)
      DELT = TEMP(KI+2) - TEMP(KI)
      DELU = (WINDV(I+1) - WINDV(I))
      DELZ = HGT(I+1) - HGT(I)
      RN(I) = (X1*DELT/DELZ) / ((DELU*DELU)/(DELZ*DELZ))
      KI = KI + 2
550  CONTINUE
C EAERO
      KI = 1
      DO 590 I=1,4
      KI = KI + 2
      DELT = TEMP(KI+2) - TEMP(KI)
      DELU = (WINDV(I+1) - WINDV(I))
      AYE = DELT / ALOG(HGT(I+1)/HGT(I))
      BEE = DELU / ALOG(HGT(I+1)/HGT(I))
      TAVG = (TEMP(KI) + TEMP(KI+2)) / 2.0
      IF (ABS(BEE).LT.0.00001) GO TO 560
      ESS = (19.0+991.0*AYE) / (BEE*REF+TAVG)
      IF (ESS.EQ.0) GO TO 560
      IF (ESS.GT.0) GO TO 555
      SUM1 = SQRT(1.0-(ESS * HGT(I+1)))-1.0
      SUM2 = SQRT(1.0-(ESS * HGT(I+1)))+1.0
      SUM3 = SQRT(1.0-(ESS * HGT(I)))-1.0
      SUM4 = SQRT(1.0-(ESS * HGT(I)))+1.0
      GO TO 559
555  CONTINUE
      SUM1 = SQRT(1.0+(ESS * HGT(I+1)))-1.0
      SUM2 = SQRT(1.0+(ESS * HGT(I+1)))+1.0
      SUM3 = SQRT(1.0+(ESS * HGT(I)))-1.0
      SUM4 = SQRT(1.0+(ESS * HGT(I)))+1.0
559  CONTINUE
      COEFF = ALOG(ABS((SUM1/SUM2) * (SUM3/SUM4)))
      IF (ESS.GT.0) COEFF =
      + 2.0 * ALOG(ABS((SUM1+1.0)/(SUM3+1.0))) + COEFF
      COEFF = 1.0 / COEFF
      GO TO 570
560  COEFF = 1.0
570  DELQ = HUM(I) - HUM(I+1)
C ADJUST FOR HUM*1000000
      DELQ = DELQ / 1000000.
      RHO = 0.0012
      KAY = 0.41
      EAERO(I)=(RHO * (KAY**2.0) * DELQ * DELU)/ALOG(HGT(I+1)/HGT(I))
      + * COEFF
      GO TO 590
580  EACPO(I) = 0.99999
C SET TO PHONY VALUE IF RN(I) ILLEGAL
590  CONTINUE

```



```

      IF(ISMOOTH .NE. 1H )GO TO 605
C
C SET TO PREVIOUS VALUES
C
      PEVAPF = EVAPO
      DO 600 I = 1,NTEMP
600    PTEMP(I) = TEMP(I)
      DO 601 I = 1,NWINDV
601    PWINDV(I) = WINDV(I)
      PPANT=PANT
      DO 602 I=1,5
      PSOILT(I) = SOILT(I)
602    CONTINUE
C WRITE OUT CONVERTED DATA
C
      WRITE(2,2) JDATE,JTIME,NWIND,TEMP,HUM,WINDV,EVAPF,SOILT,PANT
2      FORMAT(4I2,A2,10F5.1,5F10.3,5F6.1,F6.2,5F6.2,F6.3)
C
C OUTPUT
605    IF(JDATE(2).NE.LDATE)NLINES=90
      LDATE=JDATE(2)
C
      IF (NLINES.LT.50) GO TO 650
      NLINES = 0
      WRITE(6,20)ISMOOTH
20      FORMAT(1H1,A10)
      WRITE(6,8)
8      FORMAT(1X,"TIME",12X,"TEMPERATURE",32X,"ABSOLUTE HUMIDITY",33X,
+ "WIND SPEED")
      WRITE(6,9)
9      FORMAT(18X,"DEGREES C",30X,"GRAMS PER CUBIC CM*10**6",29X,
+ "CM PER SEC")
      WRITE(6,10)JDATE
10     FORMAT(1X,I2,1H/,I2,4X,"50      100      200      400      800",10X,
+ "50      100      200      400      800",6X,
+ "50      100      200      400      800")
      WRITE(6,11)
11     FORMAT(1H ,132("-"))
      WRITE(6,19)
19     FORMAT(1H )
      WRITE(7,20)ISMOOTH
      WRITE(7,13)
13     FORMAT(6X,"RICHARDSON NUMBER",9X,"EVAPORATION",12X,"EAERO *10**6"
+ ,18X, "SOIL TEMPERATURE",18X,"PAN",5X,"WIND")
      WRITE(7,14)
14     FORMAT(4X,"FOR INTERVALS",33X,"FOR INTERVALS",21X,"DEGREES C",
+ 21X,"TEMP",4X,"DIR")
      WRITE(7,15)
15     FORMAT(1X,"50-100 100-200 200-400 400-800",13X,
+ "50-100 100-200 200-400 400-800",5X,
+ , "5      10      20      40      80",6X"DEG C")
      WRITE(7,16)
16     FORMAT(1H ,132("-"))
      WRITE(7,18)
18     FORMAT(1H )
C ***BELOW TO ELIMINATE BAD DATA AT START OF A PARTICULAR TAPE
C *** DATE & TIME MUST CHANGE FOR EACH TAPE PROCESSED
650    IF (JDATE(1).EQ.7 .AND. JDATE(2).EQ.24 .AND. JTIME(1).EQ.16
+ .AND. JTIME(2).LT.11) GO TO 655
      NLINES = NLINES + 1
      WRITE(6,4) JTIME,(TEMP(I),I=1,9,2),HUM,WINDV

```



```

6      FORMAT(1X,I2,1H:,I2.2,2X,5(F5.2,2X),1X,5(F10.3,1X),1X,
+5(F5.1,2X))
      WRITE(7,17)(RN(I),I=1,4),EVAPF,EAERO,SOILT,PANT,NWIND
17     FORMAT(1X,4F8.3,F8.2,3X,4F8.5,5F8.2,2X,F6.2,
+ 3X,A2)
655    CONTINUE
      IF (IEOF.EQ.0) GO TO 100
C I.E. IF RAW DATA GO BACK AND READ NEXT RAW OBS
C ELSE SMOOTH NEXT DATA ELEMENT FIRST
890    CALL SMOOTH(NVALS)
      IF (IEOF.EQ.2) GO TO 990
      GO TO 523
C THEN GO TO CALC & PRINT ROUTINES
C
C HERE WHEN RAW DATA AT EOF
C
900    WRITE(6,7)
      WRITE(7,7)
7      FORMAT(1H1)
      ENCODE (10,901,ISMOOTH) NVALS
901    FORMAT(8HSMOOTHED,I2)
      NLINES = 90
C RESET FOR PAGE HEADINGS TO START SMOOTHING
      REWIND 2
      REWIND 6
      REWIND 7
      GO TO 890
990    CONTINUE
      IF (NVALS.GT.3) GO TO 995
      REWIND 7
      NVALS = 5
      GO TO 900
995    CONTINUE
      WRITE(6,7)
      WRITE(7,7)
      END
      SUBROUTINE GETDAT
C READS DIGITIZED DATA TAPE INTO COMMON BLOCK
      COMMON /PRESET/ XMD,STAR
      COMMON /THEDATA/ JDATE(2),JTIME(2),CHNL(100),IEOF
      DIMENSION IN(4),IN2(5),ITIME(2),IDATE(2)
      DATA IFIRST/0/
      DATA ICT/0/,KCT/0/
      DO 10 I = 1,100
10     CHNL(I) = XMD
      JDATE (1) = -1
      KCT = KCT + 1
C     IF (KCT.GT.100) GO TO 900
      IF (IFIRST.EQ.1) GO TO 100
      IF (IFIRST.EQ.2) GO TO 900
      IFIRST = 1
C ONLY FIRST TIME CALLED
C ELSE SKIP READ AS DATA ALREADY IN
50     READ(1,1) IN
1      FORMAT(3R1,A8)
      IF (EOF(1)) 790,100
100    ICT = ICT + 1
C     IF (ICT.GT.1000) GO TO 900
      IF (IN(1).EQ.1RC) GO TO 200
C IGNORE DATA LINES WITH SPACE AT BEGINNING
      IF (IN(1).EQ.1R ) GO TO 50

```

```

C CHK TO MAKE SURE WE HAVE HR RECORD
  K = IN(4).AND.7777000000B
C ASSUMES 1 DIGIT MONTH
  K = SHIFT(K,-18)
  IF (K.EQ.2RHR) GO TO 55
  PRINT 51,KCT,ICT,IN
51  FORMAT(" BAD RECORD",2I5," REC-",3R1,A8)
  GO TO 50
55  CONTINUE
C
C
C MUST BE TIME MDDHH:MMHR
C SET FOR 1 DIGIT MONTH ONLY
  IDATE (1) = IN(1) - 33B
  IDATE (2) = (IN(2)-33B)*10 + (IN(3)-33B)
  DECODE(5,105,IN(4)) IN2
105  FORMAT(5P1)
  ITIME (1) = ((IN2(1)-33B)*10) + (IN2(2)-33B)
  ITIME (2) = ((IN2(4)-33B)*10) + (IN2(5)-33B)
C ITIME(2) NE JTIME(2) CAUSES ALL 3 OBS FOR SAME TIME PER
C   TO BE ACCEPTED AS ONE OBS
  IF(JDATE(1).NE.-1.AND.ITIME(2).NE.JTIME(2))RETURN
  JTIME(1) = ITIME(1)
  JTIME(2) = ITIME(2)
  JDATE(1) = IDATE(1)
  JDATE(2) = IDATE(2)
  GO TO 50
200  IF (JDATE(1).EQ.-1) GO TO 780
C CHANNEL DATA, CONVERT
  ICHNL = (IN(2)-33B)*10 + (IN(3)-33B)
  IF (ICHNL.EQ.0) ICHNL = 100
  IF (ICHNL.LT.1 .OR. ICHNL.GT.100) GO TO 770
  K = SHIFT(IN(4),6).AND.77B
  IF (K.EQ.1R+) GO TO 290
  IF (K.EQ.1R-) GO TO 260
C POSITIVE VALUE
  DECODE(5,245,IN(4)) VALUE
245  FORMAT(F5.0)
  GO TO 300
C NEGATIVE VALUE
260  DECODE(6,261,IN(4)) VALUE
261  FORMAT(F6.0)
  GO TO 300
290  VALUE = STAR
300  CHNL(ICHNL) = VALUE
  GO TO 50
C
770  PRINT 771,KCT,ICT,IN
771  FORMAT(2I6," ILLEGAL CHANNEL-",3R1,A10)
  GO TO 50
780  PRINT 781,KCT,ICT,IN
781  FORMAT(2I6," NO DATE YET-",3R1,A10)
  GO TO 50
790  IFIRST = 2
C EOF HAS OCCURRED, SET IFIRST INDICATOR
C THEN CHECK IF ANY DATA PRESENT
  IF (IDATE(1).EQ.-1) GO TO 900
C YES , SEND DATA BEFORE EOF INDICATON
  RETURN
C
900  IEOF = 1

```

```

      RETURN
      END
      FUNCTION FNR(T)
C CONVERT FROM CEL TO FAREN REL
      FN = 1.8 * T + 32.
      FNR = FN + 459.67
      RETURN
      END
      SUBROUTINE SMOOTH(NVALS)
      COMMON /THEDATA/JDATE(2),JTIME(2),CHNL(100),IEOF
      COMMON /RESULTS/NWIND,TEMP(10),HUM(5),WINDV(5),EVAPF,SOILT(5),PANT
C REAL FLG ONLY TO FAKE COMPILER INTO NOT CONVERTING FROM REAL-INTEG
      REAL JDATE,JTIME,NWIND
      DIMENSION SMDAT(7,32)
      DATA IFIRST/0/,ISET/3/

C
C FIRST TIME ONLY TO SET BEGINNING ARRAY CONFIGURATION
C TO BEGIN, READ THE FIRST RECORD OF DATA
C
      IF (NVALS.NE.10) GO TO 104
      READ(2,100) JDATE,JTIME,NWIND,TEMP,HUM,WINDV,EVAPF,SOILT,PANT
      IF (EOF(2)) 101,102
101  IEOF = 2
102  RETURN
104  CONTINUE
      IF(IFIRST.NE. 0)GO TO 4
      IFIRST = 1
C ADD 1 TO ISET AS THIS VALUE GETS SHIFTED DOWN
      ISET = ISET + 1
      READ(2,100)(SMDAT(1,J),J=1,32)
100  FORMAT(4I2,A2,10F5.1,5F10.3,5F6.1,F6.4,6F6.1)
C
C DUPLICATE THE FIRST OBSERVATION IN THE CORRECT NUMBER OF
C LINES OF THE ARRAY +1 SO AS TO ALLOW THE MAIN LOOP TO
C SHIFT AND READ ON THE FIRST PASS
C
      DO 3 I=2,ISET
      DO 2 J=1,32
      SMDAT(I,J) = SMDAT(1,J)
2      CONTINUE
3      CONTINUE
C
C FILL THE REMAINING ROWS OF THE ARRAY WITH THE NEXT
C
1003 K = NVALS - ISET
      IF (K.LE.0) GO TO 1004
      ISET = ISET + 1
      READ (2,100) (SMDAT(ISET,J),J=1,32)
      GO TO 1003
1004 ISET = (NVALS+1) / 2
C
C END INITIALIZATION, BEGIN REGULAR PROCESSING
C
4      CONTINUE
C
C MAIN LOOP BEGINS HERE
C FIRST SHIFT 2, 4, OR 6 ROWS OF THE ARRAY
C TO MAKE ROOM FOR A NEW OBSERVATION
C
      NLines = NVALS - 1
      DO 6 I=1,NLines

```

```

      DO 5 J=1,32
      K=I + 1
      SMDAT(I,J) = SMDAT(K,J)
5      CONTINUE
6      CONTINUE
C
C NOW READ IN THE NEXT OBSERVATION POINT
C INTO THE CORRECT ROW OF THE ARRAY USING NVALS
C CHECK FOR END OF FILE AT THIS POINT
C
      READ(2,100)(SMDAT(NVALS,J),J=1,32)
      IF(EOF(2) .NE. 0)GO TO 25
C
C THIS NEXT PART SMOOTHS THE DATA
C
      IF(NVALS .EQ. 5)GO TO 10
      IF(NVALS .EQ. 7)GO TO 14
C
C THIS IS FOR NVALS = 3
C
      DO 7 J=6,32
      SMDAT(1,J) = (0.25*SMDAT(1,J))+(0.5*SMDAT(2,J))+
      + (0.25*SMDAT(3,J))
7      CONTINUE
      GO TO 17
C
C NOW FOR NVALS = 5
C
10     CONTINUE
      DO 11 J=6,32
      SMDAT(1,J) = (0.0625*SMDAT(1,J))+(0.25*SMDAT(2,J))+
      + (0.375*SMDAT(3,J))+(0.25*SMDAT(4,J))+
      + (0.0625*SMDAT(5,J))
11     CONTINUE
C
      GO TO 17
C
C LAST FOR NVALS = 7
C
14     CONTINUE
      DO 15 J=6,32
      SMDAT(1,J) = (-----)+
      + (-----)+
      +
      +
C
C 15 CONTINUE
C 16 CONTINUE
C
17     CONTINUE
C
C NOW MOVE THE DATE AND TIME INTO THE
C FIRST ROW OF THE ARRAY WITH THE SMOOTHED VALUES
C THE FIRST ROW IS USED AS IT IS SHIFTED OUT ON THE
C NEXT PASS
C
      DO 9 K=1,5
      SMDAT(1,K) = SMDAT(ISET,K)
9      CONTINUE
C
C LAST, REPLACE THE SMOOTHED DATA IN THE
C COMMON BLOCK ARRAYS AND RETURN TO THE MAIN

```

## C ROUTINE

C

```

      DO 18 I=1,2
      J = I + 2
      JDATE(I) = SMDAT(1,I)
      JTIME(I) = SMDAT(1,J)
18    CONTINUE
      NWIND = SMDAT(1,5)
      EVAPF = SMDAT(1,26)
      PANT = SMDAT(1,32)
      DO 19 I=1,5
      J = I + 15
      K = I + 20
      L = I + 26
      HUM(I) = SMDAT(1,J)
      WINDV(I) = SMDAT(1,K)
      SOILT(I) = SMDAT(1,L)
19    CONTINUE
      DO 20 I=1,10
      J = I + 5
      TEMP(I) = SMDAT(1,J)
20    CONTINUE
      RETURN

```

C

C LAST NVALS/2 POINTS ARE LOST AND NOT SMOOTHED

C IF THIS IS NOT DESIRED,MUST CHANGE

C

```

25    IEOF = 2
      RETURN
      END
      PROGRAM CNVRT(TAPE1,TAPE2=/182,OUTPUT)
C AGJ 12/80 FOR 1050 G.A.
C TO CONVERT KEYED 10 MIN AVG DATA TO PROGRAM FORMAT
      DIMENSION IN(4),XN(27)
      DATA ICT /0/
      REWIND 1
      REWIND 2
10    READ(1,1) IN,XN,IWIND
1    FORMAT(I1,1X,I2,1X,I2,1X,I2,1X,5(F5.2,F1.0),F5.2,4F6.2,F7.2/
      * F6.2,3F7.2,F5.2,5F6.2,F6.2,1X,A2)
      IF(EOF(1)) 99,20
20    ICT = ICT + 1
      DO 25 I = 11,15
25    XN(I) = XN(I) / 3.0
      IF(IN(1).NE.0) GO TO 30
      IN(1)=IMON
      IN(2) = IDAY
30    WRITE(2,2) IN,IWIND,XN
2    FORMAT(4I2,A2,10F5.1,5F10.3,5F6.1,F6.2,5F6.2,F6.3)
      IDAY = IN(2)
      IMON = IN(1)
      GO TO 10
99    PRINT 100,ICT
100   FORMAT(" RECS CONVERTED = ",I6)
      END

```





APPENDIX B  
SMOOTHED AND AVERAGED FIELD DATA

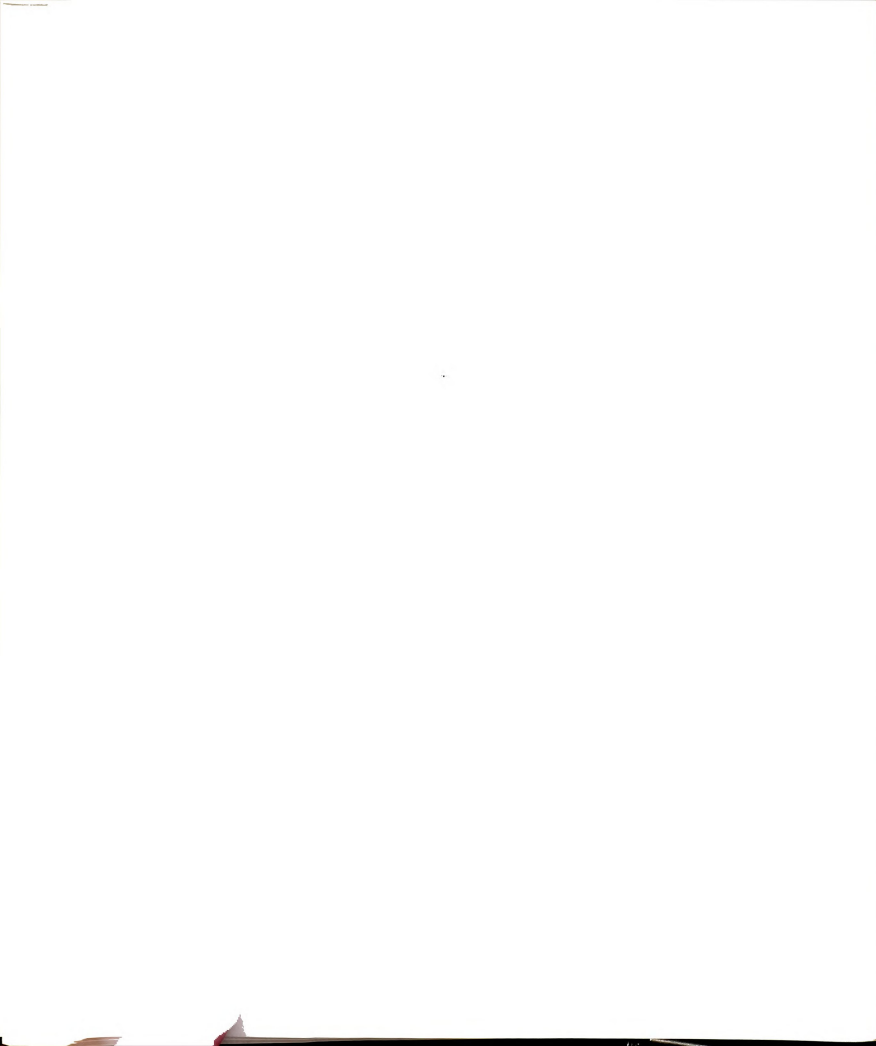
The raw data which were gathered over two-minute periods during this field study were processed and smoothed by computer into ten-minute mean values. The results are presented in Tables B-1 to B-9 in the following pages. Each table contains 32 columns which are printed on two separate pages. The first column on the first page shows the sampling time. The next five columns present the dry-bulb air temperatures, expressed in degrees Centigrade and measured at five different elevations above the ground surface. These elevations are .5, 1, 2, 4 and 8 m. Absolute humidities, expressed in grams moisture per cubic centimeter of dry air based on the measured dry and wet-bulb temperatures at five elevations are presented in columns 6 to 10. Wind speeds at five indicated elevations are given in columns 11 to 16. Richardson numbers were computed for four different elevation intervals based on measured dry air temperature and wind speeds. Computed Richardson numbers are given in columns 17 to 20 starting on the second page of each table. The water loss from the automated Class A pan is presented as millimeters of water per ten minute period in column 21. Columns 22 to 25 of these tables show the computed water vapor flux based on the modified version of Thornthwaite-Holzman equation for four different elevation intervals. These fluxes have the dimensions of gram per square centimeter per second. Soil

temperatures were measured in degrees Centigrade and are presented in columns 26 to 30. Column 31 shows the water temperature for the Class A pan in degrees Centigrade. Recorded wind directions are presented in the last column of each table.





[illegible]



[illegible]

























[illegible]



Table B-6. Smoothed atmospheric and soil data averaged over ten-minute periods, August 7, 1980.

[illegible]









APPENDIX C  
INTEGRATION OF EQUATION [29]



The integration of Equation [29] was performed by the following steps. First, consider the case of an unstable atmospheric condition. The exponent  $\underline{n}$  in Equation [29] is positive and the equation becomes

$$\frac{\partial q}{\partial z} = - \frac{1}{\rho_{ak} z^2 b} \cdot \frac{1}{Z(1+|SZ|)^{+\frac{1}{2}}} \dots \dots \dots [C1]$$

Separating variables gives

$$\partial q = - \frac{1}{\rho_{ak} z^2 b} \cdot \frac{\partial z}{Z(1+|SZ|)^{+\frac{1}{2}}} \dots \dots \dots [C2]$$

Writing the partial differentials as total differentials and integrating between the corresponding limits of  $q_1$  to  $q_2$  and  $z_1$  to  $z_2$  we have

$$q_1 \int^{q_2} dq = - \frac{E}{\rho_{ak} z^2 b} \int_{z_1}^{z_2} \frac{dz}{Z(1+|SZ|)^{+\frac{1}{2}}} \dots [C3]$$

The integration of the left-hand side is straightforward and gives

$$q_1 - q_2 = - \frac{E}{\rho_{ak} z^2 b} \int_{z_1}^{z_2} \frac{dz}{Z(1+|SZ|)^{+\frac{1}{2}}} \dots [C4]$$

To integrate the right-hand side term we use formula 192.11 of Dwight (22) and obtain

$$q_2 - q_1 = - \frac{E}{\rho_{ak} z^2 b} \left\{ \ln \left| \frac{(1+SZ_2)^{\frac{1}{2}-1}}{(1+SZ_2)^{\frac{1}{2}+1}} \right| - \ln \left| \frac{(1+SZ_1)^{\frac{1}{2}-1}}{(1+SZ_1)^{\frac{1}{2}+1}} \right| \right\} \dots [C5]$$

for  $a=1$  and  $(1+SZ) > 0$ .

According to logarithmic properties, Equation [C5] can be rearranged as

$$q_2 - q_1 = - \frac{E}{\rho_{ak} z^2 b} \left\{ \ln \left| \frac{\sqrt{1+SZ_2}-1}{\sqrt{1+SZ_2}+1} \cdot \frac{\sqrt{1+SZ_1}+1}{\sqrt{1+SZ_1}-1} \right| \right\} \dots \dots \dots [C6]$$

or

$$q_1 - q_2 = + \frac{E}{\rho_{ak}^2 b} \left\{ \ln \left| \frac{\sqrt{1+SZ_2}-1}{\sqrt{1+SZ_2}+1} \cdot \frac{\sqrt{1+SZ_1}+1}{\sqrt{1+SZ_1}-1} \right| \right\} \dots \dots \dots [C7]$$

From Equation [31] we have

$$b = \frac{U_2 - U_1}{\ln \left( \frac{Z_2}{Z_1} \right)} = \frac{\Delta U}{\ln \left( \frac{Z_2}{Z_1} \right)} \dots \dots \dots [C8]$$

Substituting for  $\bar{b}$  in Equation [C7] and solving for E gives

$$E = \frac{\rho_{ak}^2 (q_1 - q_2) (U_2 - U_1)}{\ln \left( \frac{Z_2}{Z_1} \right)} \cdot \frac{1}{\left\{ \ln \left| \frac{\sqrt{1+SZ_2}-1}{\sqrt{1+SZ_2}+1} \cdot \frac{\sqrt{1+SZ_1}+1}{\sqrt{1+SZ_1}-1} \right| \right\}} \dots \dots [C9]$$

Rewriting Equation [C9] by expressing the changes in humidity and wind speed in finite difference notation results in

$$E = \frac{\rho_{ak}^2 \Delta q \Delta U}{\ln \left( \frac{Z_2}{Z_1} \right)} \cdot f(S) \dots \dots \dots [C10]$$

where

$$f(S) = \frac{1}{\left\{ \ln \left| \frac{\sqrt{1+SZ_2}-1}{\sqrt{1+SZ_2}+1} \cdot \frac{\sqrt{1+SZ_1}+1}{\sqrt{1+SZ_1}-1} \right| \right\}} \dots \dots \dots [C11]$$

Equation [C10] and [C11] are Equations [32] and [33], respectively.

Second, we consider the stable atmospheric conditions when  $n$  is negative and Equation [29] becomes

$$\frac{\partial q}{\partial z} = - \frac{1}{\rho_{ak}^2 b} \cdot \frac{E}{Z(1+|SZ|)^{-\frac{1}{2}}} \dots \dots \dots [C12]$$

or

$$\frac{\partial q}{\partial z} = - \frac{E}{\rho_{ak}^2 b} \cdot \frac{(1+|SZ|)^{+\frac{1}{2}}}{Z} \dots \dots \dots [C13]$$

Separating the terms and writing the integrals as total differentials we obtain

$$\int_{q_1}^{q_2} dq = - \frac{E}{\rho_{ak} z \bar{b}} \int_{z_1}^{z_2} \frac{(1+|SZ_2|)^{\frac{1}{2}}}{z} dz \dots \dots \dots [C14]$$

The solution of the left-hand side integral is the same as the previous case. To integrate the right-hand side term, we use Formula 194.11 of Dwight (22) and obtain

$$q_2 - q_1 = - \frac{E}{\rho_{ak} z \bar{b}} \left\{ 2[(1+|SZ_2|)^{\frac{1}{2}} - (1+|SZ_1|)^{\frac{1}{2}}] + \int_{z_1}^{z_2} \frac{dz}{2(1+|SZ|)^{\frac{1}{2}}} \right\} \cdot [C15]$$

The solution of the integral term on the right-hand side is the same as the one obtained for the unstable case. Rearranging Equation [C15], substituting for  $\bar{b}$  and solving for E, we obtain

$$E = \frac{\rho_{ak}^2 \Delta U \Delta q}{\ln\left(\frac{z_2}{z_1}\right)} \cdot f(S) \dots \dots \dots [C16]$$

where

$$f(S) = \frac{1}{\{2[(\sqrt{1+SZ_2}) - (\sqrt{1+SZ_1})] + \ln \left| \frac{\sqrt{1+SZ_2}-1}{\sqrt{1+SZ_1}+1} \cdot \frac{\sqrt{1+SZ_1}+1}{\sqrt{1+SZ_2}-1} \right| \}} \cdot [C17]$$

and the function needed in Equations [32] and [34].

#### APPENDIX D

ILLUSTRATIVE EXAMPLES FOR COMPUTING EVAPORATION  
RATES FROM EQUATIONS [32] and [35]

The following examples illustrate computational procedures used in calculating evaporation rates from TH and MTH equations under the same atmospheric conditions. Both stable and unstable atmospheric conditions are considered.

First, we consider a case of stable atmospheric conditions. For this case we use data obtained for the 50 and 100-cm elevations at 1930 hr on July 24, 1980 (see Table B-1). To evaluate the parameter S from Equation [28], we must first compute  $\bar{a}$  and  $\bar{b}$  from Equations [30] and [31].

Thus,

$$\bar{a} = \frac{\Delta T}{\ln\left(\frac{Z_2}{Z_1}\right)} = \frac{T_2 - T_1}{\ln\left(\frac{Z_2}{Z_1}\right)} = \frac{290.6 - 290.5}{\ln\left(\frac{100}{50}\right)} = +0.14$$

$$\bar{b} = \frac{\Delta U}{\ln\left(\frac{Z_2}{Z_1}\right)} = \frac{U_2 - U_1}{\ln\left(\frac{Z_2}{Z_1}\right)} = \frac{120.2 - 117.5}{\ln\left(\frac{100}{50}\right)} = +3.90$$

$$T_{\text{avg.}} = \frac{T_1 + T_2}{2} = \frac{290.6 + 290.5}{2} = 290.55$$

Assuming a value of 18 for B, (52), 981 cm sec<sup>-2</sup> for g and compute S to find

$$S = \frac{Bg^{\bar{a}}}{b^{\bar{b}}T} = \frac{(18)(981)(0.14)}{(3.9)(3.9)(290.55)} = +0.56$$

For this value of S and from Equation [34] we find f(S) to be 0.225.

To evaluate the evaporation rate from Equation [35], the TH equation, assume a value of 0.41 for  $k$ ,  $0.0012 \text{ g cm}^{-3}$  for  $\rho_a$  and Table data for  $q$ ,  $U$  and  $Z$  to get

$$\begin{aligned}
 E &= \frac{\rho_a k^2 \Delta q \Delta U}{[\ln(\frac{Z_2}{Z_1})]^2} \\
 &= \frac{\rho_a k^2 (q_1 - q_2) (U_2 - U_1)}{[\ln(\frac{Z_2}{Z_1})]^2} \\
 &= \frac{(0.41)(0.41)(0.12)(2.7)}{[\ln(\frac{100}{50})]^2} \\
 &= 1.13 \times 10^{-4} \text{ g cm}^{-2} \text{ sec}^{-1} \\
 &= 1.13 \times 10^{-4} \text{ cm sec}^{-1}
 \end{aligned}$$

Since all data are based on 10 minute intervals, we multiply by 6000 (600 sec equal 10 min and 10 mm equal 1 cm) to obtain 0.068mm/10 min. Then the corresponding evaporation rate from MTH was computed according to Equation [32] as

$$\begin{aligned}
 E &= \frac{\rho_a k^2 \Delta q \Delta U}{[\ln(\frac{Z_2}{Z_1})]} \cdot f(S) \\
 &= \frac{(0.41)(0.41)(0.12)(2.70)}{\ln(\frac{100}{50})} \cdot (0.225) \\
 &= 0.177 \times 10^{-4} \text{ g cm}^{-2} \text{ sec}^{-1} \\
 &= 0.177 \times 10^{-4} \text{ cm sec}^{-1} \\
 &= 0.011\text{mm}/10 \text{ min}
 \end{aligned}$$

A similar procedure is used to compute the evaporation rates from these equations under unstable atmospheric conditions. For this case, we consider the data obtained for the 50 and 100-cm elevations at 1650 hr on July 25, 1980 (see





Table B-2). The  $\bar{a}$ ,  $\bar{b}$  and  $S$  parameters for this date are -0.29, 29.58 and -0.02, respectively. Using the value calculated for  $S$  and Equation [33], we find  $f(S)$  to be 0.448. The next step is to compute evaporation rates from Equations [32] and [35]. The computed rates according to these equations are 0.002 and 0.005mm/10 min, respectively.



LIST OF REFERENCES

# LIST OF REFERENCES

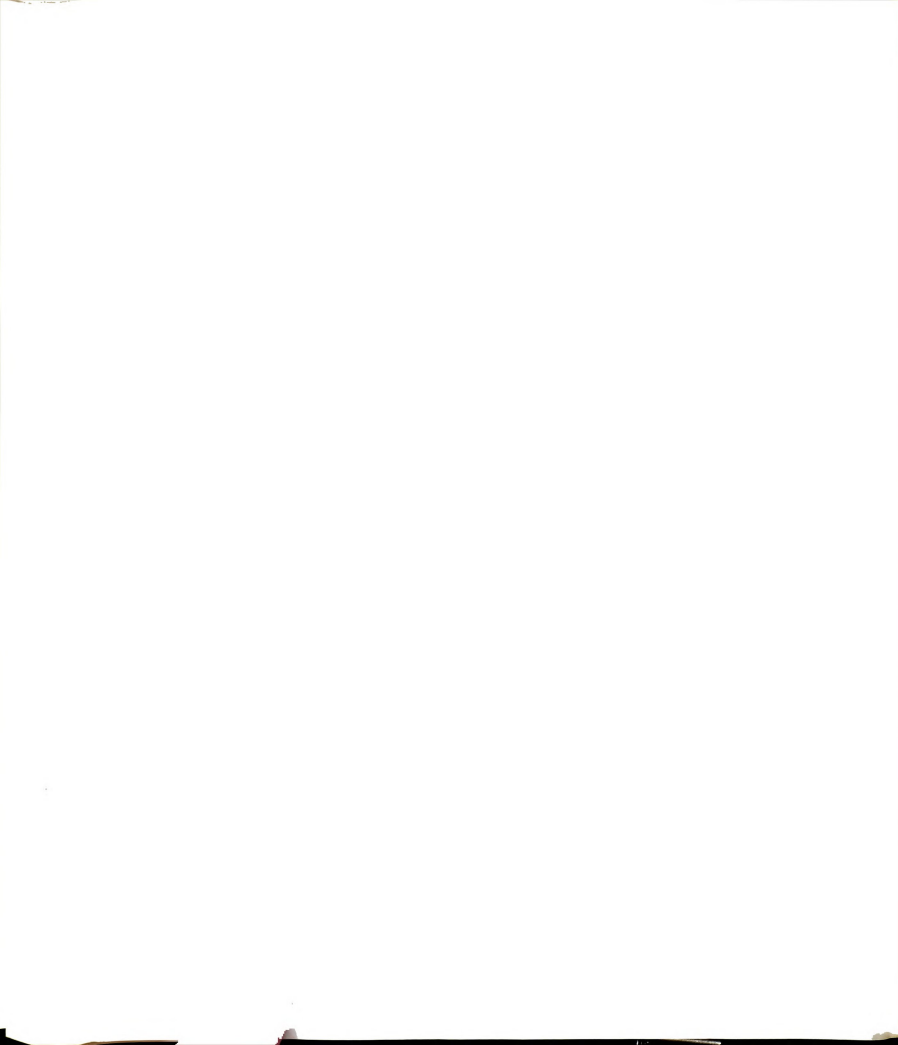
1. Bedell, D.J. and R.L. VanTil. 1979. Irrigation in Michigan 1977. Water Mang. Div., Dept. Natural Resources, Michigan State University, East Lansing, Michigan, 43 pp.
2. Bevington, P.R. 1969. Data reduction and error analysis for physical sciences. McGraw-Hill Book Co., New York, pp. 255-259.
3. Blaney, H.F. 1958. Evaporation from free water surfaces at high latitudes. Trans. ASAE, 123:385-404.
4. Blaney, H.F. and K.V. Morin. 1942. Evaporation and consumption use of water formulae. Part I: Trans. Amer. Geophy. Union, 23:76-83.
5. Brutsaert, W. 1965. Evaluation of some practical methods of estimating evapotranspiration in arid climates in low latitudes. Water Resource Res. 1:187-191.
6. Budyko, M.I. 1963. Evaporation under natural conditions. Translated from Russian by Israel Program for Scientific Translation, Published by NSF, Washington, D.C., pp. 16-61.
7. Burch, G.J. 1978. A weighing system for freely exposed loads. Agric. Meteorol. 20:489-490.
8. Cackett, H.E. and R.R. Metelerkamp. 1963. The relationship between evapotranspiration and development of the field beans. Rhodesian Jour. Agric. Res. 1:18-21.
9. Cheek, A.W. and C.F. Lambert. 1978. Automatic evaporation measurement system (AUTOVAP) development report. NOAA Tech. Memo. NWS-EDL-17, Equipment Development Lab., Silver Spring, MD 15 pp.
10. Christiansen, J.E. 1968. Pan evaporation and evapotranspiration from climatic data. Jour. Irrig. Drain. Div., Proc. ASCE, 94:243-265.
11. Christiansen, J.E. and G.H. Hargreaves. 1969. Irrigation requirements from evaporation. Trans. 7th Congr. Int. Comm. Irrig. Drain. 111:23.569-23.596.

12. Crawford, T.V. 1965. Moisture transfer in free and forced convection. *Quart. Jour. Roy. Meteorol. Soc.* 91:18-27.
13. Criddle, W.D. 1958. Methods of computing consumptive use of water. *Jour. Irrig. Drain. Div., Proc. ASCE*, 84:1-27.
14. Dalton, J. 1978. Experimental essay on the condition of mixed gases; on the force of steam from water and other liquids in different temperatures. *Mem. Manchester Lit. and Phil. Soc.* 5:535-602.
15. Deardorf, J.W. 1961. Evaporation reduction by natural films. *Jour. Geophys. Res.* 66:3613-3614.
16. Denmand, O.T. and R.H. Shaw. 1962. Availability of soil water to plants as affected by soil moisture contents and meteorological conditions. *Agron. Jour.* 45:385-390.
17. Doebelin, E.Q. 1975. Measurement systems; application and design. McGraw-Hill Book Co., New York, pp 225-232.
18. Doorenbos, J. and W.O. Pruitt. 1975. Crop water requirements. *Irrig. Drain. Paper No. 24*, FAO, Rome, Italy, 144 pp.
19. Doorenbos, J. and A.H. Kassem. 1979. Yield response to water. *Irrig. Drain. Paper No. 33*, FAO, Rome, Italy, 193 pp.
20. Doss, B.D. et. al. 1962. Evapotranspiration by irrigated corn. *Agron. Jour.* 54:497-498.
21. Dubetz, S. and L.G. Sonmore. 1964. Comparison of gravimetric, tensiometer and neutron methods of measuring soil moisture. *Cand. Agric. Eng.* 1:32-34.
22. Dwight, H.E. 1971. Tables of integrals and other mathematical data. The McMillan Co., New York, pp. 44-49.
23. Dyer, A.J. 1967. The turbulent transport of heat and water vapor in unstable atmosphere. *Quart. Jour. Roy. Meteorol. Soc.* 93:501-508.
24. Dyer, A.J. and B.B. Hicks. 1970. Flux gradient relationship in the constant flux layer. *Quart. Jour. Roy. Meteorol. Soc.* 96:715-721.
25. Dylla, A.S. et. al. 1980. Estimating water use by irrigated corn in west central Minnesota. *Soil Sci. Soc. Amer. Jour.* 44:823-827.

26. Eagleman, J.R. and W.L. Decker. 1965. The role of soil moisture in evapotranspiration. *Agron. Jour.* 57:626-629.
27. Ellison, T.H. 1957. Turbulent transport of heat and momentum from an infinite rough plane. *Jour. Fluid Mech.* 2:456-466.
28. Evans, N.A. 1962. Methods of estimating evapotranspiration of water by crops; In: Water Requirements of Crops. ASAE Special Publication SP-SW-0162, pp. 2-10.
29. Fitzpatrick, E.A. 1963. Estimates of pan evaporation from mean maximum temperature and vapor pressure. *Jour. Appl. Meteorol.* 2:789-792.
30. Frecks, G.A. et. al. 1973. Instrumentation for monitoring small weight changes. *Trans. ASAE*, 16:728-730.
31. Fritschen, L.J. and R.M. Shaw. 1961. Evapotranspiration for corn as related to pan evaporation. *Agron. Jour.* 53:149-150.
32. Fuchs, M. and G. Stanhill. 1963. The use of Class A evaporation data to estimate irrigation requirements of cotton crop. *Israel Jour. Agric. Res.* 13:63-79.
33. Fuchs, M. and C.B. Tanner. 1965. Radiation shields for air temperature thermometers. *Jour. Appl. Meteorol.* 6:852-857.
34. Goldberg, S.D. et. al. 1967. Relation between water consumption of peanuts and Class A pan evaporation during growing season. *Soil Sci.* 104:289-296.
35. Grant, D.R. 1975. Comparison of evaporation measurements using different methods. *Quart. Jour. Roy. Meteorol. Soc.* 101:289-296.
36. Hagen, L.J. and E.L. Skidmore. 1974. Reducing turbulence transfer to increase water use efficiency. *Agric. Meteorol.* 14:153-168.
37. Hargreaves, G.H. 1956. Irrigation data based on climatic data. *Jour. Irrig. Drain Div., Proc. ASCE*, 89:43-50.
38. Hargreaves, G.H. 1968. Consumptive use derived from evaporation pan data. *Jour. Irrig. Drain. Div., Proc. ASCE*, 94:97-105.
39. Hobbs, E.H. and K.K. Krogman. 1966. Evapotranspiration from alfalfa as related to evaporation and other meteorological variables. *Cand. Jour. Plant Sci.* 46:271-277.

40. Holzman, B. 1943. The influence of stability on evaporation. *Annals. N.Y. Acad. Sci.* 44:13-18.
41. Hounam, C.E. 1973. Comparison between pan and lake evaporation. *Tech. Note No. 126, World Meteorol. Organization, Geneva, Switzerland*, 52 pp.
42. Iruthayaraj, M.R. and Y.B. Morachan. 1978. Relationship between evaporation from different evaporimeters and meteorological parameters. *Agric. Meteorol.* 19:101-111.
43. Jensen, M.E. and A.R. Haise. 1963. Estimating evapotranspiration from solar radiation. *Jour. Irrig. Drain. Div., Proc. ASCE*, 89:15-41.
44. Jensen, M.E. et. al. 1971. Estimating soil moisture depletion from climate, crop and soil data. *Trans. ASAE*, 14:954-959.
45. Krishna, A. and R.S. Kushwaka. 1973. A multiple regression analysis of evaporation during the growing season on vegetation in arid zones of India. *Agric. Meteorol.* 12:297-307.
46. Lerew, L.E. 1972. A FORTRAN psychrometric model. M.S. Thesis, Dept. of Agric. Eng., Mich. State Univ., East Lansing, MI 44 pp.
47. Lumely, J.L. and H.A. Panofsky. 1964. The profile of temperature and wind close to the ground; In: The Structures of Atmospheric Turbulence. Interscience Publishers, New York, pp. 99-117.
48. Makink, G.F. and H.D.J. VanHeemst. 1956. The actual evapotranspiration as a function of potential evapotranspiration and soil moisture tension. *Neth. Jour. Agric. Sci.* 4:67-72.
49. McVehil, G.E. Jr. 1962. Wind distribution in diabatic boundary layer. Ph.D. Thesis, Pennsylvania State Univ., Pennsylvania, 130 pp.
50. McVehil, G.E. Jr. 1964. Wind and temperature profiles near the ground in stable stratification. *Quart. Jour. Roy. Meteorol. Soc.* 90:136-146.
51. Micro-Measurements. 1978. Catalog and technical data binder. Vishay Intertechnology Inc., Romulus, MI, 7 chapters.
52. Morgan, D.L. et. al. 1971. Analysis of energy, momentum and mass transfers above vegetative surfaces. *Res. Develop. Tech. Report ECOM-68-G10-F*, Dept. Soil and Water Eng., Univ. California, Davis, CA, 128 pp.





53. Murray, W.M. and P.K. Stein. 1956. Strain gage techniques. Volumes I and II, Massachusetts Institute of Technology, Cambridge, Mass., 588 pp.
54. Neubert, H.K.P. 1967. Strain gages; kinds and uses. St. Martin's Press, New York, pp. 28-69.
55. Norero, A.L. 1969. A formula to express evapotranspiration as a function of soil moisture and evaporative demand of atmosphere. Ph.D. Thesis, Utah State Univ., Logan, Utah, 145 pp.
56. Nurnberger, F.V. 1972. Microenvironmental modification by small water droplet evaporation. Ph.D. Thesis, Michigan State Univ., East Lansing, MI 178 pp.
57. Nurnberger, F.V. 1976. Summary of evaporation in Michigan. Weather Service, Mich. Dept. Agric., 1407 Harrison Rd., East Lansing, MI 21 pp.
58. Okamoto, M. and E.K. Webb. 1970. The temperature fluctuation in stable stratification. Quart. Jour. Roy. Meteorol. Soc., 96:591-600.
59. Oke, T.R. 1970. Turbulent transport near the ground in stable conditions. Jour. Appl. Meteorol. 9:778-786.
60. Panofsky, H.A. et. al. 1960. The diabatic wind profile. Quart. Jour. Roy. Meteorol. Soc., 86:390-398.
61. Panofsky, H.A. 1963. Determination of stress from wind and temperature measurements. Quart. Jour. Roy. Meteorol. Soc., 89:85-94.
62. Parmele, L.H. and J.L. McGuiness. 1974. Comparison of measured and estimated potential evapotranspiration in humid regions. Jour. Hydrol., 22:239-251.
63. Patel, A.C. and G.E. Christiansen. 1963. Comparison of four methods of computing evaporation. University Res. Proj. U-143, College of Eng., Utah State Univ., Logan, Utah.
64. Pelton, W.L. and H.C. Kroven. 1969. Evapotranspiration estimated in a semi-arid climate. Cand. Agric. Eng., 2:50-61.
65. Pennman, H.L. 1949. Evaporation in nature. London Physical Soc. Rep. Prof. in Physics. 2:366-388.
66. Pennman, H.L. et. al. 1967. Microclimate factors affecting evaporation and transpiration; In: Irrigation of Agricultural Lands. Monograph No. 11, Amer. Soc. Agron., Madison, Wisconsin, pp. 483-505.



67. Perry, C.C. and H.R. Lissner. 1955. The strain gage primer. McGraw-Hill Book Co., New York, 280 pp.
68. Phene, C.J. and R.B. Campbell. 1975. Automating pan evaporation measurements for irrigation control. Agric. Meteorol. 15:181-191.
69. Power, J.F. and D.D. Evans. 1962. Influence of soil factors on the water requirements of crops; In: Water Requirements of Crops. ASAE Special Publication SP-SW-0162.
70. Priestly, C.H.B. 1959. Turbulent transfer in the lower atmosphere. The University of Chicago Press, Chicago, 130 pp.
71. Pruitt, W.O. 1960. Relation of consumptive use of water to climate. Trans. ASAE, 125:9-14.
72. Richards, L.A. 1965. Physical conditions of water in soil; In: Methods of Soil Analysis. Agronomy No. 9, Part I; Physical and Mineralogical Properties, Including Statistics of Measurement and Sampling. Amer. Soc. Agron., Madison, Wisconsin, pp. 128-152.
73. Richardson, C.W. and J.T. Ritchie. 1973. Soil water balance for small watersheds. Trans. ASAE, 16:72-77.
74. Rosenberg, N.J. 1974. Microclimate; the biological environment. John Wiley & Sons, New York, pp. 100-205.
75. Rossby, C.G. and R.B. Montgomery. 1935. The layer of frictional influence in wind and ocean currents. Paper in Phys. Ocean & Meteorol., Vol. 3, No. 3.
76. Slabbers, P.J. 1977. Surface roughness of crops and potential evapotranspiration. Jour. Hydrol., 34:181-191.
77. Slatyer, R.O. 1956. Evapotranspiration in relation to soil moisture. Neth. Jour. Agric. Sci., 4:73-76.
78. Stanhill, G. et. al. 1961. A comparison of methods of calculating potential evapotranspiration from climatic data. Israel Jour. Agric. Res., 11:159-171.
79. Stanhill, G. 1962. The control of field irrigation practice from measurements of evapotranspiration. Israel Jour. Agric. Res., 12:51-62.
80. Stearns, C.R. 1970. Determining surface roughness and displacement height. Boundary Layer Meteorol., 1:102-111.



81. Stone, J.F. 1978. Evapotranspiration control on agricultural lands. A Symposium; New Developments in Soil and Crop Science. Crop and Soil Sci. Soc. Florida, 37:1-11.
82. Sutton, O.G. 1953. Diffusion and evaporation; In: Micrometeorology. McGraw-Hill Book Co., New York, pp. 273-323.
83. Swinbank, W.C. 1951. The measurements of vertical transfer of heat and water vapor by eddies in the lower atmosphere. Jour. Meteorol. 8:135-145.
84. Szeicz, G. et. al. 1969. Aerodynamic and surface factors in evaporation. Water Resources Res. 5:380-394.
85. Tanner, C.B. 1967. Measurement of evapotranspiration; In: Irrigation of Agricultural Lands. Monograph No. 11, American Soc. Agron., Madison, Wisconsin, pp. 534-574.
86. Taylor, S.A. 1962. Estimating future water requirements of crops; In: Water Requirements of Crops. ASAE Special Publication SP-SW-0162, pp. 10-23.
87. Taylor, S.A. and G.L. Ashcroft. 1972. Evapotranspiration; In: Physical Edaphology. W.H. Freeman and Co., San Francisco, pp. 45-84.
88. Thornthwaite, C.W. and B. Holzman. 1942. Evaporation from land and water surfaces. U.S. Dept. Agric. Tech. Release No. 21, 83 pp.
89. U.S. Department of Agriculture. 1970. Irrigation water requirements. Eng. Div., Soil Conservation Serv., Indiana, 88 pp.
90. U.S. Department of Agriculture. 1971. Climate of Michigan by station. Weather Service, Mich. Dept., Agric. 1405 Harrison Rd., East Lansing, MI.
91. U.S. Department of Agriculture. 1977. Irrigation guide for Indiana. Soil Conserv. Serv., Indiana, 254 pp.
92. U.S. Department of Agriculture. 1979. Soil survey of Ingham County, Michigan. Soil Conserv. Serv., Mich. Agric. Expt. Station, East Lansing, MI, 142 pp.
93. VanBavel, C.H.M. 1966. Potential evapotranspiration; The combination concept and its verification. Water Resource res. 2:455-467.
94. VanWijk, W.R. and D.A. DeVries. 1954. Evapotranspiration. Neth. Jour. Agric. Sci. 2:105-119.



95. Verma, S.B. et. al. 1978. Turbulent exchange coefficient for sensible heat and water vapor under advective conditions. Jour. Appl. Meteorol. 17:330-338.
96. Vitosh, M.L. et. al. 1980. Impact evaluation of increased water use by agriculture in Michigan: Section I; water demand present and future. Dept. Crop and Soil Sci., Michigan State Univ., East Lansing, MI 47 pp.
97. Ward, R.C. 1971. Measuring evapotranspiration: A Review. Jour. Hydrol. 13:1-21.
98. Warhaft, Z. 1976. Heat and moisture flux in stratified boundary layer. Quart. Jour. Roy. Meteorol. Soc. 102:703-704.
99. Webb, E.K. 1970. Profile relationship; the log-linear range and extension to strong stability. Quart. Jour. Roy. Meteorol. Soc. 95:67-90.
100. Wilcox, J.C. and H.C. Kroven. 1964. Some problems encountered in the use of evaporimeters for scheduling of irrigation. Canad. Agric. Eng. 1:29-31,45.
101. Zachary, A.H. ed. 1975. Instrumentation and measurements for environmental sciences. Amer. Soc. Agric. Eng., St. Joseph, MI, pp. 2.1-2.11.







MICHIGAN STATE UNIV. LIBRARIES



31293104153881